A NOVEL CONTROL STRATEGY FOR MITIGATION OF SSR EMPLOYING SVC AUXILIARY CONTROLLERS

by
YACHIKA GUPTA

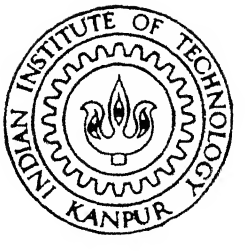

DEPARTMENT OF ELECTRICAL ENGINEERING
INDIAN INSTITUTE OF TECHNOLOGY KANPUR
APRIL, 1998

A NOVEL CONTROL STRATEGY FOR MITIGATION OF SSR EMPLOYING SVC AUXILIARY CONTROLLERS

A Thesis Submitted
In Partial Fulfillment of the Requirements
for the Degree of
MASTER OF TECHNOLOGY

by

YACHIKA GUPTA

to the
Department of Electrical Engineering
Indian Institute of Technology , Kanpur
April 1998

CERTIFICATE

It is certified that this M. Tech. thesis work entitled **A NOVEL CONTROL STRATEGY FOR MITIGATION OF SSR EMPLOYING SVC AUXILIARY CONTROLLERS** *by* **Yachika Gupta** *has been carried out under my supervision and this work has not been submitted elsewhere for a degree.*

(Dr. Rajiv K. Varma)
Associate Professor
Department of Electrical Engineering
Indian Institute of Technology Kanpur
INDIA.

20 April 1998

DEDICATED TO

MY MOTHER

ACKNOWLEDGEMENTS

I feel happy in expressing my deep gratitude and sincere thanks to my thesis supervisor Dr. Rajiv K. Varma, for his invaluable guidance, inspiration and constant encouragement throughout the course of this work. His rich experience, exemplary patience, concern and understanding has resulted in completion of this thesis to my full satisfaction.

I also wish to thank my friends and well wishers for their cooperation.

I am extremely grateful to Shri V. N. Verma and Smt. Meera Verma, for their blessings, affection and moral support.

It gives me a great pleasure to acknowledge the prayers and sacrifices of my parents in periods of trials, to see me get through. I offer my humble and profound gratitude to my elder brother Dr. R. K. Gupta and bhabhiji.

Last, but not the least, goes my gratitude to Vinay.

ABSTRACT

Static var compensators (SVC) are traditionally placed at the generator terminals to mitigate subsynchronous oscillations (SSO) in series compensated electric power transmission systems. An auxiliary control [14] of the SVC employing generator rotor frequency feedback is shown to be adequate for damping SSO.

It has been reported [15] that an SVC located at the midpoint of a series compensated line can be utilized for dual purposes of damping SSO and stability enhancement. Controllers of these SVCs have been designed based on a combination of line current signal and computed value of generator internal frequency (CIF). Both these signals utilize local measurements, as the current trend in power systems practice is to use local signals for the sake of reliability.

In this thesis an altogether new concept of SVC control employing a remote generator frequency signal transmitted over a telecom line, is presented for damping of SSO in series compensated transmission systems.

The IEEE First SSR Benchmark System is suitably modified to include an SVC at the midpoint of transmission line. Auxiliary controllers are designed for various signals such as line current, computed internal frequency (CIF) and remote frequency signal. Their effectiveness is then investigated for damping all the torsional modes at all critical levels of series compensation. Eigenvalue analysis is utilized to examine the system stability in each case.

It is concluded in this thesis that this remote rotor frequency signal together with line current signal can be successfully applied for damping all the torsional modes at all the critical levels of series compensation. The performance of remote rotor frequency signal is much better than the computed internal frequency signal. This remote frequency signal is observed to be efficient over a reasonable range of telecom delays.

This concept of remotely transmitted signal is being investigated for the first time in the control of static var compensators to damp subsynchronous oscillations.

CONTENTS

LIST OF FIGURES

LIST OF TABLES

LIST OF SYMBOLS

B	Susceptance
D	Damping constant
E,e	Source voltage
f_0	Nominal system frequency
G	Conductance
I,i	Current
j	$\sqrt{(-1)}$
K	Spring constant
K_p	Proportional gain of SVC voltage controller
K_I	Integral gain of SVC voltage controller
K_B	Gain of SVC auxiliary controller
K_D	Slope of SVC control characterisitic
L	Inductance
M	Inertia constant
P	Real power
Q	Reactive power
R,r	Resistance
S	Complex power
s	Complex frequency
T_e	Electrical torque
T_m	Mechanical torque
T	Time constant
T_{TD}	Telecom time delay
t	Time in seconds
u	Input variable
V,v	Voltage
x,X	State variable and the corresponding transformed variable in s domain
X,x	Reactance
Y,y	Admittance
y	Output variable
Z,z	Impedance
δ	Generator rotor angle
Ψ	Flux
λ	Eigenvalue
ϕ	Power factor angle
θ	Angle
ω	Angular velocity (rad/sec)

Prefix

Δ	Incremental change

Superscript

t	Transpose
*	Complex conjugation

Chapter 1

INTRODUCTION

1.1 General

The generation and consumption of electrical energy has been increasing at a tremendous rate throughout the world during the past many decades. The increasing need of transmitting greater and greater amounts of power has led to an increase in the transmission voltages at EHV and UHV levels. Series compensation is a powerful tool to improve the performance of EHV lines. It consists of capacitors connected in series with the line at suitable locations.

1.2 Advantages of Series Compensation

The use of series compensation leads to a number of advantages as regards power transfer capability, voltage regulation, etc.

(a) Increase in Transmission Capacity

The power transfer P_1 over a line is given by

$$P_1 = \frac{|E_1||E_2|\sin\delta}{X_e} \tag{1.1}$$

where $E_1\angle\delta$ = sending end voltage
$E_2\angle 0$ = receiving end voltage
X_e = line reactance
δ = phase angle between E_1 and E_2

If a series capacitor having capacitance X_c is inserted, the net series reactance becomes $X_e - X_c$ and the power transfer P_2 is given by

$$P_2 = \frac{|E_1||E_2|\sin\delta}{X_e - X_c} \tag{1.2}$$

From eqns.(1.1) and (1.2), it is seen that for the same magnitude of E_1, E_2 and δ, P_2 is higher than P_1. The increase in power transfer is given by

$$\frac{P_2}{P_1} = \frac{X_e}{X_e - X_c} = \frac{1}{1-k} \tag{1.3}$$

The factor k equals $\frac{X_c}{X_e}$ and is known as the degree of series compensation. Studies on transmission systems have revealed that in view of stable system operation, protection and economics, the practical degree of series compensation is chosen in the range of 40 % to 70 %.

(b) Improvement of System Stability

From eqns. (1.1) and (1.2), it is seen that for the same amount of power transfer and the same values of E_1 and E_2, the phase angle δ in the case of series compensated line is less than that for the uncompensated line. It is established from equal area criterion [17] that a lower angle δ implies better system stability. Some other methods for improvement of system stability are also used. These include reducing the reactance of generators and transformers, use of bundled conductors and increasing the number of circuits in parallel. Series compensation generally offers the most economic solution with respect to both the steady state and the transient stability.

(c) Load Division between Parallel Circuits

The reduction of series reactance by series compensation makes it a useful tool to balance the loading in parallel circuits. When a system is to be strengthened by the addition of a new line or when one of the existing circuits is to be adjusted for parallel operation in order to achieve maximum power transfer and minimize losses, series compensation can be used to a great advantage. It has been reported [18], that in Sweden, the cost of the first series compensation in the 420 kV system was entirely recovered due to the decreased losses in the 220 kV system operating in parallel with the 420 kV system.

1.3 Problems Associated with Series Compensation

The use of series compensation introduces a few problems too . Some of these are :

(a) Subsynchronous Resonance

The series capacitor introduces a sub-synchronous frequency (proportional to the square root of the compensation) in the system. In some cases this frequency may interact with weak steam-turbine generator shafts and give rise to high

torsional stresses. In hydro-turbine generators the risk of subsynchronous resonance is small because its natural frequency is lower than the range of frequencies in which subsynchronous torque is induced due to practical levels of series compensation.

(b) ***Ferroresonance***

When an unloaded or a lightly loaded transformer is energized through a series compensated line, ferroresonance may occur. The frequency of oscillation is an integral multiple of the system frequency [18] This can be suppressed by using shunt resistors across the capacitors or by short circuiting the capacitor temporarily through an isolator or a bypass breaker.

(b) Line Protection

Series compensation can lead to mal-operation of the distance relays of the line protection if the degree of compensation and capacitor location is not proper. To ensure correct operation of the distance protection the series compensation is limited to about 40 % (when the installation is located at the middle of the line) and 30 % per bank (when the installations are located at one-third and two-third distances along the line)

(d) High Recovery Voltage

Series capacitors produce high recovery voltages across the circuit breaker contacts.

Inspite of the above problems series compensation is very widely used for EHV systems in the 400-500 kV range in many countries of the world.

1.4 Subsynchronous Resonance and its Control

The subsynchronous resonance (SSR) phenomena is usually associated with synchronous machines connected to series compensated transmission networks . It has been defined by IEEE SSR task force [1] as follows :

"*Subsynchronous resonance* is an electric power system condition where the electric network exchanges energy with the turbine-generator at one or more of the natural frequencies of the combined system below the synchronous frequency of the system."

The definition includes any system condition that provides the opportunity for an exchange of energy at a given subsynchronous frequency. This includes what might be considered "natural" modes of oscillation that are due to the

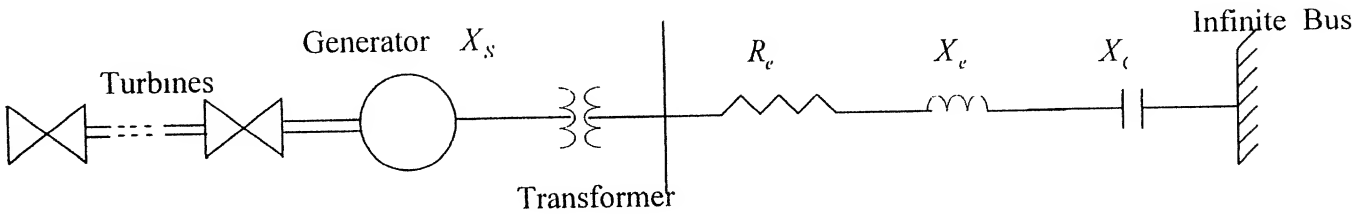

FIG . 1.1 TURBINE – GENERATOR FEEDING INFINITE BUS THROUGH SERIES COMPENSATED TRANSMISSION LINE

inherent system characteristics, as well as "forced" modes of oscillation that are driven by a particular device or control system. The first SSR problem was experienced on December 9, 1970 resulting in the failure of a turbine generator shaft at the Mohave plant in southern California [12]. It was not until a second shaft failure occurred on October 26, 1971 that the real cause of the failure was recognized as subsynchronous resonance.

The SSR phenomena is known to occur in two different forms:

(a) Self excited or steady state SSR resulting from the following two mechanisms

(i) induction generator action
(ii) torsional interaction

(b) Transient SSR

To understand these different aspects let us consider a simple radial system consisting of a synchronous generator connected to an infinity bus through a series compensated transmission line, as shown in Fig. 1.1.

The series resonant frequency f_e of the electrical network is given by

$$f_e = f_0\sqrt{\frac{X_c}{X_L'}} = \frac{f_0}{\sqrt{(\frac{1}{k} + \frac{X_s}{kX_e})}} \tag{1.3}$$

where

X_s = reactance of generator and transformer

X_e = line reactance

X_c = reactance of series capacitor

X_L' = total inductive reactance = $X_S + X_e$

k = degree of series compensation = $\frac{X_c}{X_e}$

f_0 = nominal system frequency

It is to be noted that $f_e < f_0$ since $k < 1$.

(a) Steady State SSR

Electrical subsynchronous currents of frequency f_e flowing in the armature induce subsynchronous torques and currents in the rotor circuit having frequency f_r given as

$$f_r = f_o - f_e \tag{1.4}$$

These rotor currents result in subsynchronous armature voltage components which may sustain or enhance the subsynchronous armature currents to produce the 'self-excitation' effect or steady state SSR. Self excitation can be divided into two categories, one involving electrical system dynamics alone and the other involving both the electrical system and mechanical system (turbine-generator) dynamics.

Induction Generator Action

The induction generator effect relates only to the electrical system dynamics. This results from the apparent negative resistance characteristic of generators at frequencies below the system synchronous frequency At the system resonant frequency f_e, if this apparent negative resistance exceeds the sum of the armature and network resistances, the subsynchronous armature currents may be negatively damped.

Torsional Interaction

This form of self excitation involves both the electrical and mechanical system dynamics. Torsional interaction problems may occur when the electrical resonant frequency f_e is near the complement of a torsional resonant frequency f_n of the turbine-generator (T-G) shaft system. In this context, the word 'complement' implies the difference between synchronous frequency and the torsional natural frequency. Under these conditions, a small voltage induced in the generator armature by rotor oscillations can result in a large subsynchronous current. When the net circuit resistance is positive, this current will produce a rotor torque which is phased to sustain or enhance the rotor oscillations. If the component of subsynchronous torque in phase with rotor velocity deviation equals or exceeds the inherent damping torque of the rotating system, the coupled electromechanical system will experience growing oscillations.

It is important to note that the induction generator effect and torsional interaction are not mutually exclusive but will co-exist. They are treated separately for ease in analysis.

(b) Transient SSR

Transient SSR generally refers to transient torques on segments of the T-G shaft resulting from subsynchronous oscillating currents in the network caused by faults or switching operations.

This usually occurs when the complement of the electrical network resonant frequency gets closely aligned with one of the torsional natural frequencies. Although, these transient torques decay with time their magnitudes are large and have the potential to cause serious damage to the T-G unit.

Infact, even if torques such as those produced by steady state subsynchronous currents may be limited in magnitude and result in stresses within the elastic limit, failure of a shaft can be caused due to cyclic fatigue stress, which is cumulative.

The phenomena of subsynchronous oscillations (SSO) is not restricted to series compensated systems alone. SSO has been reported to result on account of adverse interaction between the turbine-generator torsional system and HVDC control [19-21], dc converter loads and power system stabilizers [21]. An SSR condition can be created with shunt capacitor compensated systems if it is attempted to operate a long distance transmission system at a power angle in excess of 180° .

1.4.1 General Countermeasures to SSR Problems :

A wide variety of methods have been proposed in the literature [5] for counteracting SSR. These may be broadly classified as follows:

(a) ***Static filter*** : This can take the form of a blocking filter (parallel-resonance type) in series with the generator, or damping circuits in parallel with the series capacitors.

(b) ***Dynamic filter*** : This is an active device placed in series with the generator . It picks up a signal derived from rotor motion and produces a voltage in phase opposition so as to compensate for or even exceed the subsynchronous voltage generated in the armature.

(c) ***Dynamic Stabilizer***. This consists of thyristor modulated shunt reactors connected to the generator terminal Control of subsynchronous oscillations is achieved by modulating the thyristor switch firing angles, using signals derived from the generator shaft speed.

(d) ***Excitation system damper***: Generator excitation control is modulated by using a signal derived from the shaft speed so as to provide increased damping of torsional oscillations.

(e) ***Protective relays***: The SSR condition is detected by a relay and the affected units are tripped. The relay may take several forms : detection of excessive torsional motion by sensing rotor speed or detection of SSR condition by sensing the armature current.

(f) ***NGH scheme***: This consists of a linear resistor in series with back-to-back thyristors connected across the series capacitor. The presence of SSR components in the capacitor voltage is detected and reduced by the action of the resistor discharge circuit.

1.4.2 Control of SSR by SVC

Static var compensators (SVCs) are shunt connected static reactive power generators and/or absorbers whose outputs are adjusted to exchange capacitive or inductive current in a continuous manner. This is done to maintain or control specific parameters of the electrical power system, typically bus voltage. The term "static" is used to indicate that SVCs, unlike synchronous compensators, have no moving or rotating main components. Thus an SVC consists of static var generator (SVG) or absorber devices and a suitable control device.

A static var system (SVS) is a combination of different static and mechanically-switched var compensators whose outputs are coordinated.

Static var compensators have been in use since the early 1960s. The SVC began being applied for transmission system voltage control in the late 1970s. Since that time, many SVCs have been applied worldwide for voltage control and, in some cases stability enhancement. The dynamic range of SVC is typically from 60 MVAr to 600 MVAr.

An SVC installed at the midpoint of a long transmission line can be utilized for damping of torsional oscillations in addition to voltage control [4]. Different auxiliary control signals such as line current, computed internal frequency (CIF) of the generator [15], remote frequency signal and a suitable combination of them can be utilized to improve the damping of torsional oscillations significantly .

1.4.3 Analytical Methods to study SSR

Torsional interaction effects involve energy interchange between the generator shaft system and the inductances / capacitances of the network Therefore, the analysis of SSR problems requires representation of both the electromechanical dynamics of the generating units and the electromagnetic dynamics of the transmission network.

Several methods have been used for the study of SSR [1,5]. A brief description of these methods is given below·

1.4.3.1 Eigenvalue (modal) Analysis

Eigenvalue analysis uses the standard linear, state-space form of system equations and provides an appropriate tool for evaluating system conditions for the study of SSR, particularly for induction generator and torsional interaction effects.

1.4.3.2 Frequency Scanning

This technique computes the equivalent impedance as seen from the internal buses of generators looking into the network, for different values of frequency. It gives information about the natural frequencies of the system and the tendency towards self-excitation and SSR. This approach is particularly suited for preliminary analysis of SSR problems.

1.4.3.3 Frequency response analysis of full system

The stability of the subsynchronous oscillations is analyzed by using the multidimensional Nyquist criterion. This approach can handle detailed models and large systems.

1.4.3.4 Approximate frequency-domain analysis

This method analyzes the stability of individual torsional modes. It is limited to approximate detection of SSR.

1.4.3.5 Time domain analysis

The electromagnetic transient program (EMTP) may be used to compute the transient time response. It allows very detailed representation of equipment, including nonlinear effects It is particularly suited for analyzing transient shaft torque due to SSR. However, this method is limited to the analysis of small systems.

In this thesis, eigenvalue analysis is employed for the study of SSR, as this technique offers the following advantages :

- Uses the state-space equations, making it possible to utilize many other analytical tools which can be applied in the same equation form
- Computes all the exact modes of system oscillation in a single computation.
- Can be arranged to perform a convenient parameter variation to study parameter sensitivities.
- Can be used to plot root loci of eigenvalue movement in response to many different types of changes.

1.5 Objectives and Scope of the Thesis

The purpose of this thesis is to study the effect of SVC auxiliary controllers in damping all the torsional modes in the IEEE First SSR Benchmark System for all the critical levels of series compensation.

While all auxiliary controllers reported in the literature [15,23] are based on locally available signals, in this thesis for the first time a new auxiliary signal is studied which is transmitted on telecom channels from a remote location. This signal is the frequency of the synchronous generator, and is termed remote frequency (RF) signal.

In brief, the different objectives of this thesis are as follows :

- To develop different component models of IEEE First SSR Benchmark system [2] for the study of SSR.

- To study the effect of a mid point located static var compensator (SVC) with voltage control alone on damping of torsional oscillations.
- To examine the effectiveness of various local auxiliary control signals such as line current, computed internal frequency (CIF), remote generator frequency (RF) signal and a combination of them with respect to their ability to stabilize all the torsional modes.
- To study the effect of telecom delays associated with remote frequency signal on the damping of torsional modes, rotor mode and electrical mode.
- To study the effectiveness of auxiliary signals when SVC is placed at the generator end .

1.6 Organization of Chapters

Chapter 2 describes the development of models for the synchronous generator and its torsional system and the network for the IEEE First Benchmark Model for SSR analysis. The system eigenvalues with network tuned to different torsional modes are also presented .

Chapter 3 presents the modeling of network, SVC voltage controller and auxiliary controller for IEEE First SSR Benchmark Model when SVC is placed at the mid point of transmission line.

Chapter 4 studies the effect of different auxiliary signals such as line current, CIF, remote frequency (RF) signal and their combinations with respect to their ability to stabilize all the torsional modes. The effectiveness of auxiliary signals is examined at all the four critical series compensation levels for IEEE First SSR Benchmark system, i.e. 35.6 %, 54.8 %, 73 % and 90.8 %, when mode 4, mode 3, mode 2 and mode 1 respectively are critically destabilized.

Chapter 5 studies the effect of telecom delays associated with the transmission of RF signal on the damping of various critical modes Effectiveness of auxiliary signals is also studied when SVC is placed at the generator end.

A brief review of the various contributions of this thesis and the scope for future work has been consolidated in the sixth chapter.

Chapter 2

SYSTEM MODELING

2.1 Introduction

This chapter presents a detailed formulation of the synchronous generator model, the multi-mass turbine system model and the network model for IEEE First Benchmark Model for SSR analysis. The overall model of the system is obtained by appropriately combining the above component models. The system model thus obtained is nonlinear in nature.

2.2 Study System

The study system is the IEEE First Benchmark Model for SSR analysis, depicted in Fig. 2.1. An 892.4 MVA synchronous generator is connected to an infinity bus via a highly compensated 500 kV transmission line. The mechanical system consists of a four stages steam turbine, the generator and a rotating exciter.

The generator was represented by a Type – 59 synchronous machine source component. Two damper windings were provided in the q axis while at the d axis one damper and a field winding were considered. The mechanical system was represented by a multi mass spring dash pot system, with six lumped masses coupled by shaft sections of known torsional elasticity. Mechanical damping was assumed to be zero, to represent the worst damping condition

2.3 Generator Model

The mathematical model of the synchronous generator used here is as proposed in [6]. The schematic of the synchronous generator is shown in Fig 2.2. This shows three identical armature windings a, b, c and four rotor windings f, h, g and k. 'f' coil represents the rotor field winding. The fictitious 'g' coil represents the effect of eddy currents which circulate in the solid steel of rotor. The 'h' and 'k' coils represent the damper winding along d and q axis respectively. All windings except the field winding are short circuited as they are not connected to voltage sources. The additional dummy coil ' c ' has been introduced to handle transient saliency. The dummy coil is considered to be closed through a very high resistance and is assumed to have no mutual damping with other rotor coils.

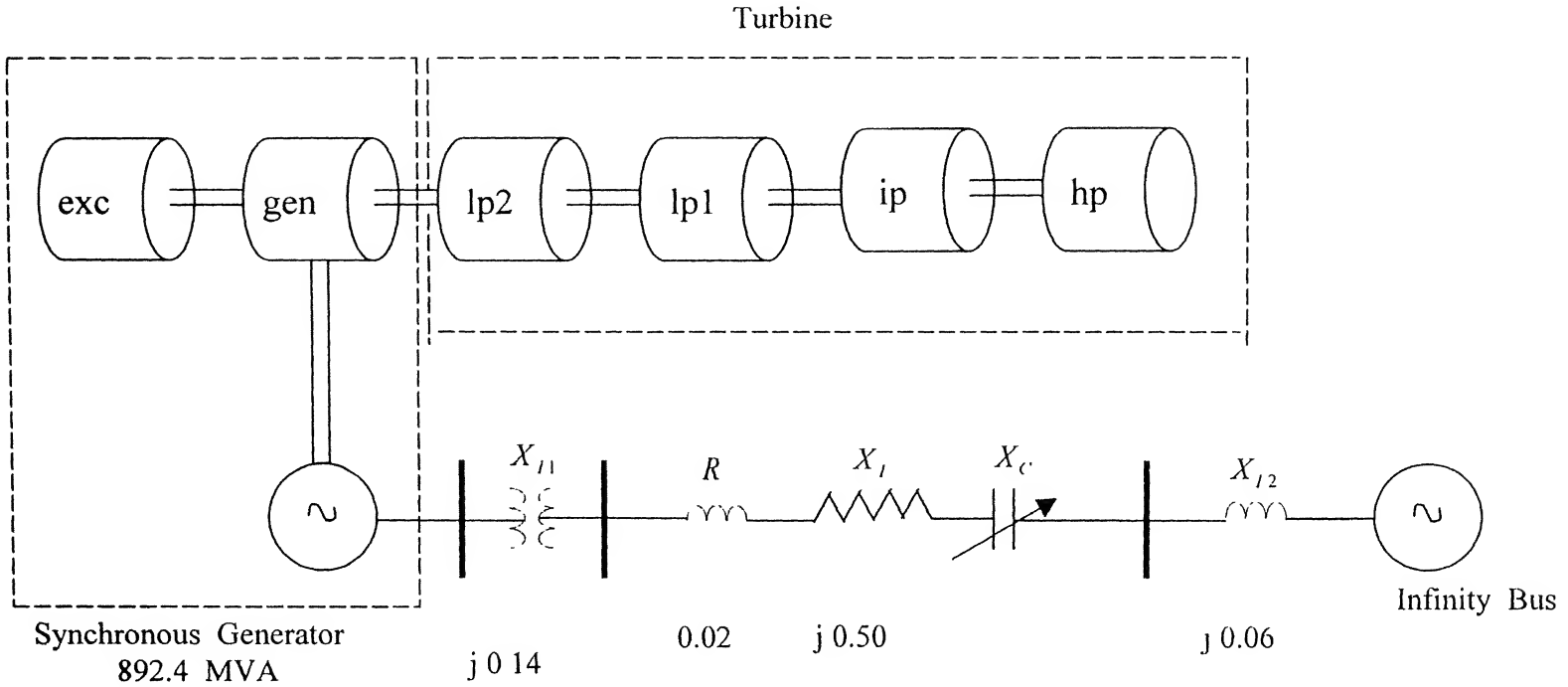

FIG. 2.1 STUDY SYSTEM (IEEE FIRST SSR BENCHMARK SYSTEM)

hp : high pressure turbine
ip : intermediate pressure turbine
lp1 : low pressure turbine A
lp2 : low pressure turbine B

The following assumptions are made :

(i) Fundamental frequency mmf distribution is considered in the air gap .
(ii) Saturation is ignored .

Assumption (ii) can be relaxed but is generally used to simplify the analysis. The effects of machine damping and prime mover dynamics are small and can also be neglected for simplicity. Such a model is considered to be sufficiently accurate for the purpose of studying torsional interaction.

The generator model described here can be further subdivided into :

(a) stator circuits
(b) rotor circuits
(c) mechanical system

2.3.1 Stator Circuits

In this model, the stator of synchronous generator is represented by a dependent current source I_S in parallel with an inductance L_S'' as shown in Fig.2.3. The dependent current source replaces the time varying coupling between the rotor windings and stator windings. It may be noted that I_S is a (3 × 1) vector and L_S'' is a (3 × 3) matrix. These are expressed as

$$I_S = [I_a \quad I_b \quad I_c]' = I_d\, c + I_q\, s \tag{2.1}$$

where

$$c' = \sqrt{(2/3)} \quad [\cos\theta \quad \cos(\theta - 2\pi/3) \quad \cos(\theta + 2\pi/3)]$$
$$s' = \sqrt{(2/3)} \quad [\sin\theta \quad \sin(\theta - 2\pi/3) \quad \sin(\theta + 2\pi/3)]$$

I_d , I_q are components of dependent current source along the d and q axis , respectively. θ is the rotor angle. Subscript t indicates transpose .

$$L_S'' = \frac{L_0}{3}\begin{bmatrix} 1 & 1 & 1 \\ 1 & 1 & 1 \\ 1 & 1 & 1 \end{bmatrix} + \frac{2L_d''}{3}\begin{bmatrix} 1 & -\frac{1}{2} & -\frac{1}{2} \\ -\frac{1}{2} & 1 & -\frac{1}{2} \\ -\frac{1}{2} & -\frac{1}{2} & 1 \end{bmatrix} \tag{2.2}$$

Such a representation of machine can handle both the symmetrical and unsymmetrical networks equally well. If the external network connected to machine terminals is symmetrical, as considered in this case, a, b, c components

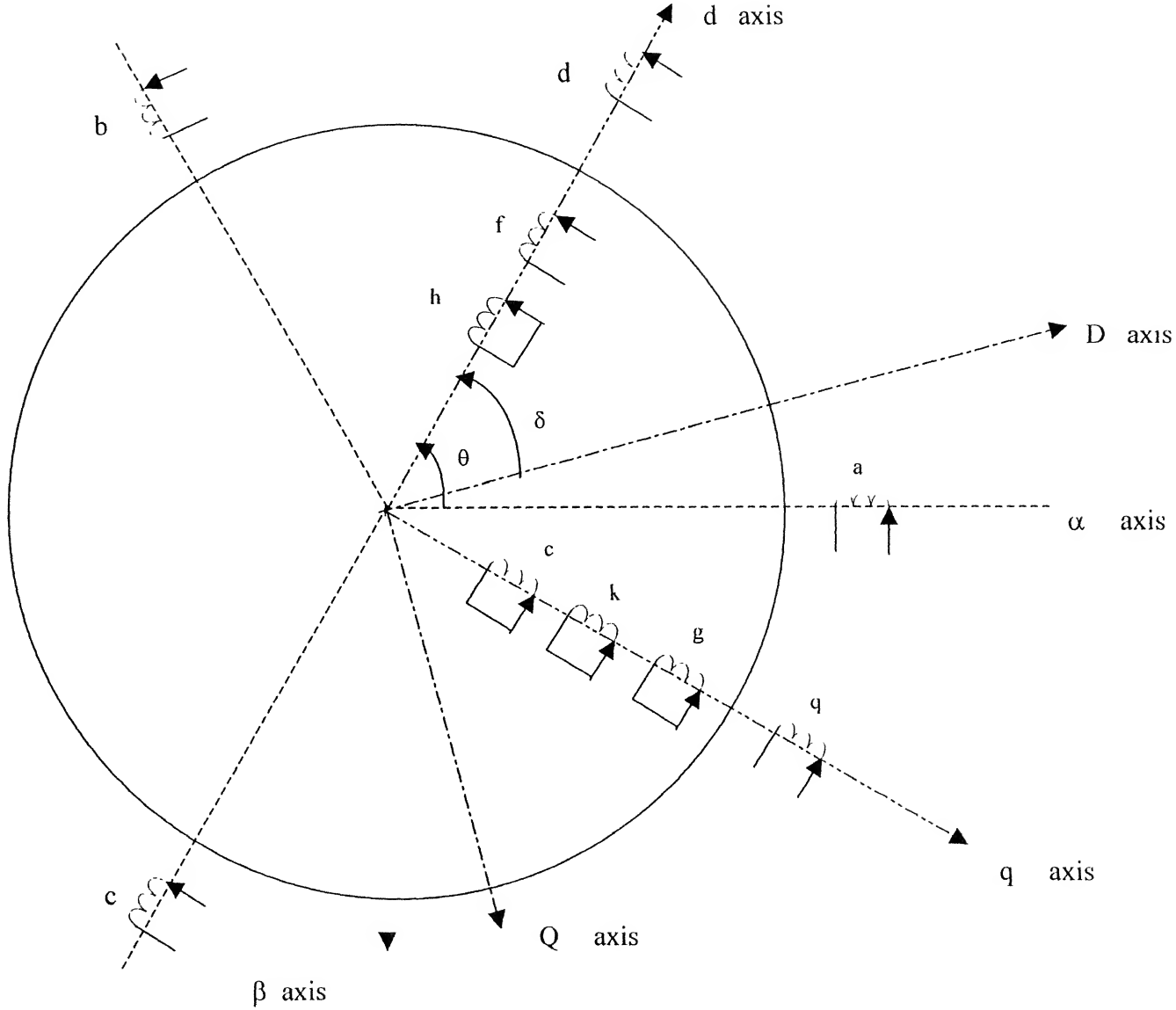

FIG 2.2 SCHEMATIC LAYOUT OF THE WINDINGS OF THE SYNCHRONOUS MACHINE AND THEIR TWO AXIS REPRESENTATION

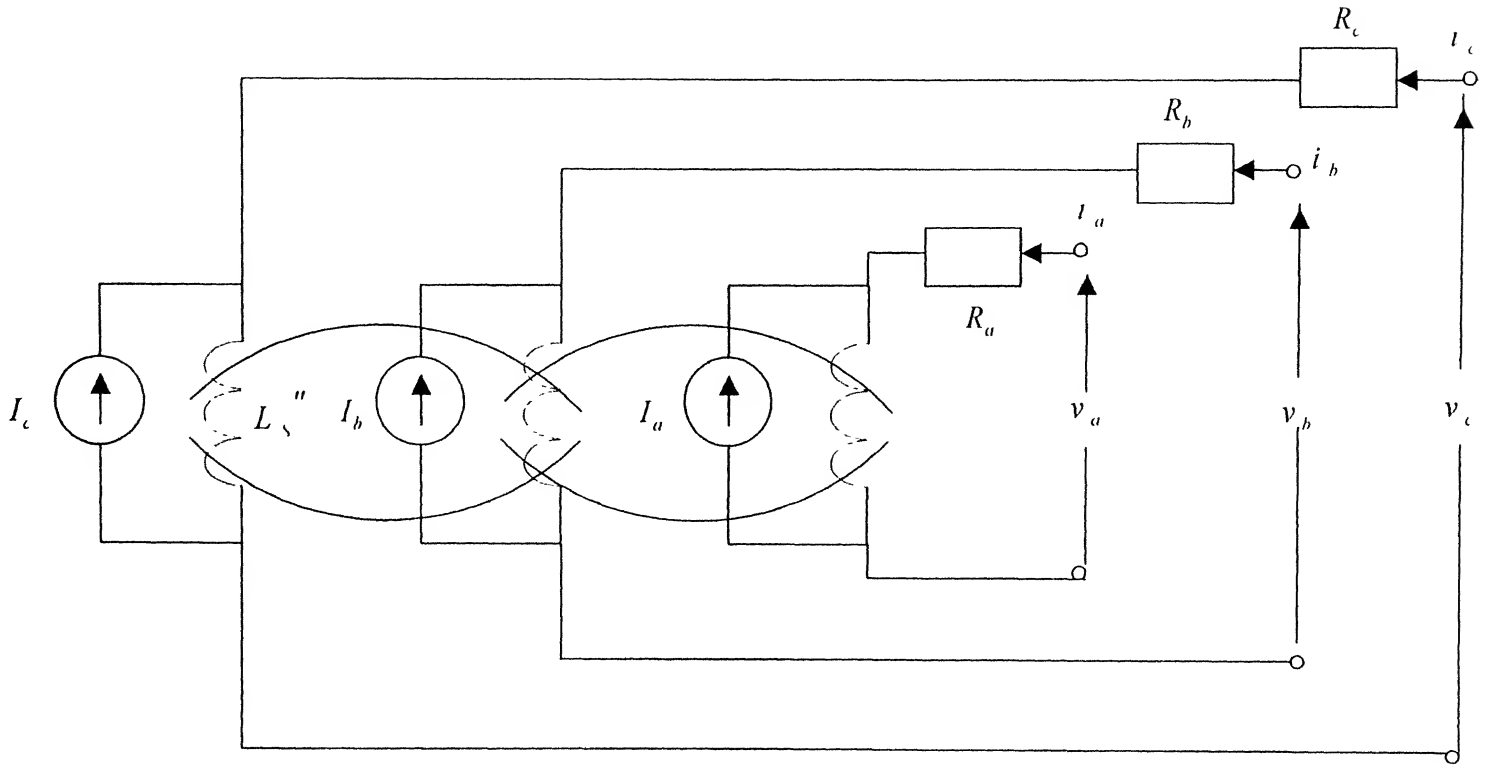

FIG. 2.3 CIRCUIT MODEL FOR THREE PHASE STATOR OF SYNCHRONOUS MACHINE

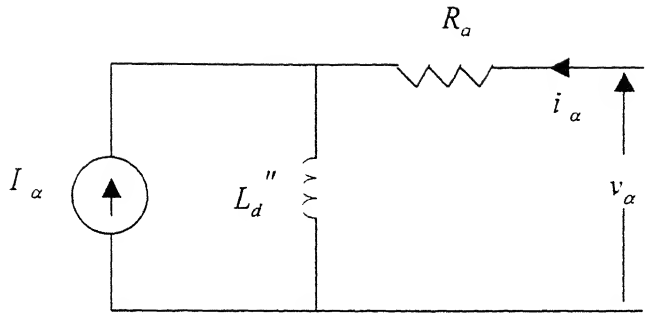

(a) α Axis representation

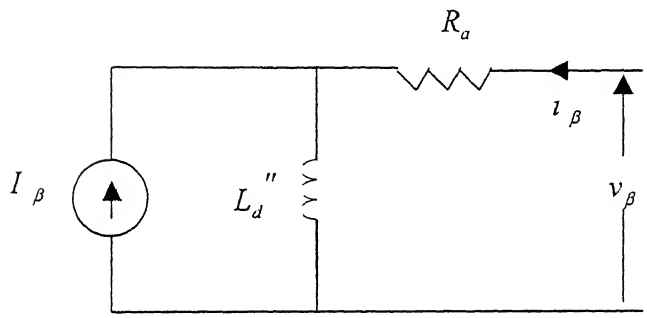

(b) β Axis representation

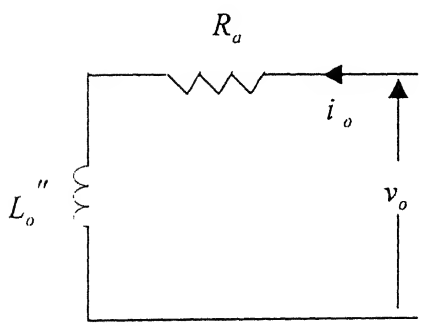

(c) o Axis representation

FIG. 2.4 EQUIVALENT REPRESENTATION OF SYNCHRONOUS MACHINE ON α, β, 0 AXIS

can be transformed to α, β, o components. The advantage of this transformation is that all the three α, β, o component models are uncoupled.

Moreover, α network is identical with β network and is the same as positive sequence network model.

Equivalent source representation of the machine on α, β, o axes is derived in [7] and shown in Fig. 2.4.The equivalent circuit consists of three meshes which are not mutually coupled. R_a denotes the armature resistance. The currents in the meshes correspond to α, β, o components of the armature currents. The relationship between α, β, o components and the phase currents i_a, i_b and i_c is given by

$$\begin{bmatrix} i_a \\ i_b \\ i_c \end{bmatrix} = \begin{bmatrix} \frac{\sqrt{2}}{\sqrt{3}} & 0 & \frac{1}{\sqrt{3}} \\ -\frac{1}{\sqrt{6}} & -\frac{1}{\sqrt{2}} & \frac{1}{\sqrt{3}} \\ -\frac{1}{\sqrt{6}} & \frac{1}{\sqrt{2}} & \frac{1}{\sqrt{3}} \end{bmatrix} \begin{bmatrix} i_\alpha \\ i_\beta \\ i_o \end{bmatrix} \tag{2.3}$$

The dependent current sources in α, β frame of reference are defined as

$$I_\alpha = I_d \cos\theta + I_q \sin\theta \tag{2.4}$$

$$I_\beta = -I_d \sin\theta + I_q \cos\theta \tag{2.5}$$

2.3.2 Rotor Circuits

The rotor flux linkages are defined by

$$\begin{aligned} \Psi_f &= a_1\Psi_f + a_2\Psi_h + b_1 v_f + b_2 i_d \\ \Psi_h &= a_3\Psi_f + a_4\Psi_h + b_3 i_d \\ \dot{\Psi}_g &= a_5\Psi_g + a_6\Psi_k + b_5 i_q \\ \dot{\Psi}_k &= a_7\Psi_g + a_8\Psi_k + b_6 i_q \\ \dot{\Psi}_c &= a_9\Psi_c + b_4 i_q \end{aligned} \tag{2.6}$$

where v_f is the field excitation voltage.

constants $a_1 - a_9$, $b_1 - b_6$ are defined in Appendix A. The d and q components of the machine terminal current are defined by i_d, i_q as

$$i_d = \sqrt{\frac{2}{3}}\left[i_a \cos\theta + i_b \cos(\theta - \frac{2\pi}{3}) + i_c \cos(\theta + \frac{2\pi}{3}) \right]$$

$$i_q = \sqrt{\frac{2}{3}}\left[i_a \sin\theta + i_b \sin(\theta - \frac{2\pi}{3}) + i_c \sin(\theta + \frac{2\pi}{3}) \right]$$

It is noted that currents i_d and i_q are defined with respect to the machine reference frame. However, to have a common axis of representation with the ac network these currents are transformed to D-Q frame of reference which is rotating at synchronous speed ω_0 The following transformation is employed

$$\begin{bmatrix} i_d \\ i_q \end{bmatrix} = \begin{bmatrix} \cos\delta & -\sin\delta \\ \sin\delta & \cos\delta \end{bmatrix} \begin{bmatrix} i_D \\ i_Q \end{bmatrix} \tag{2.7}$$

where i_D , i_Q are the respective components of machine current along D and Q axis . δ is the angle by which d axis leads the D axis .

Substituting eqn (2 7) in eqn. (2.6) and linearizing the resulting equation gives the state equation of the rotor circuits as

$$\dot{x}_R = A_R x_R + B_{R1} u_{R1} + B_{R2} u_{R2} \tag{2 8}$$

where

$$x_R = \begin{bmatrix} \Delta\Psi_f & \Delta\Psi_h & \Delta\Psi_g & \Delta\Psi_k & \Delta\Psi_c \end{bmatrix}^t \quad , \quad u_{R1} = \begin{bmatrix} \Delta\delta & \Delta\omega \end{bmatrix}^t$$

$$u_{R2} = \begin{bmatrix} \Delta i_D & \Delta i_Q \end{bmatrix}^t$$

Matrices A_R , B_{R1} , B_{R2} and B_{R3} are defined in Appendix B,Sec.B.1.

The output equation of the rotor subsystem is developed by utilizing the relationship between I_d , I_q and the rotor flux linkages as given in [6].

$$\begin{aligned} I_d &= c_1 \Psi_f + c_2 \Psi_h \\ I_q &= c_3 \Psi_g + c_4 \Psi_k + c_5 \Psi_c \end{aligned} \tag{2.9}$$

where constants $c_1 - c_5$ are defined in Appendix A.

I_d , I_q are now transformed to D–Q axis components I_D and I_Q, respectively, using the transformation

$$\begin{bmatrix} I_D \\ I_Q \end{bmatrix} = \begin{bmatrix} \cos\delta & \sin\delta \\ -\sin\delta & \cos\delta \end{bmatrix} \begin{bmatrix} I_D \\ I_Q \end{bmatrix} \tag{2.10}$$

The output equations are finally derived as eqns. (B.6), (B.7) and given by

$$y_{R1} = C_{R1} x_R + D_{R1} u_{R1} \tag{2.11}$$

$$y_{R2} = C_{R2} x_R + D_{R2} u_{R1} + D_{R3} u_{R2} \tag{2.12}$$

where $y_{R1} = [\Delta I_D \quad \Delta I_Q]^t, y_{R2} = [\Delta I_D \quad \Delta \dot{I}_Q]^t$

Matrices $C_{R1}, C_{R2}, D_{R1}, D_{R2}, D_{R3}$ and D_{R4} are defined in Appendix B, Sec. B.1 .

2.4 Mechanical System Model

A study of the torsional interaction between turbine - generator and series compensated transmission network necessitates a detailed modeling of the mechanical shaft system. The mechanical system can be described using either the 'multiresonant mechanical model (all - modes model)' [2,12] or the ' modal mechanical model' [2,12]. A comparison of these models is given in [12,14]. The all- modes model is utilized for studies presented in this chapter as it includes the effect of zeroeth mode and accounts for the coupling between different modes .

In the multiresonant model the turbogenerator mechanical system is represented as a linear multi-mass spring dash pot system. Each major rotating element is modeled as a lumped mass represented by its inertia while every shaft element is modeled as a mass-less rotational spring with its stiffness expressed by the spring constant. Viscous damping of each mass and shaft segment is represented by a dash-pot damping A general turbine-generator shaft system model is shown in Fig. 2.5.

The equation of motion of i th mass of the n-mass rotating system is given by

$$\begin{aligned} M_i \ddot{\delta}_i + D_{i-1,i}(\dot{\delta}_i - \dot{\delta}_{i-1}) + D_{i,i}\dot{\delta}_i + D_{i,i+1}(\dot{\delta}_i - \dot{\delta}_{i+1}) + K_{i-1,i}(\delta_i - \delta_{i-1}) \\ + K_{i,i+1}(\delta_i - \delta_{i+1}) = T_{mi} - T_{ei} = T_i \end{aligned} \tag{2.13}$$

where ,

M_i = moment of inertia of ith rotor .

T_{mi} = mechanical torque applied on ith rotor .

T_{ei} = electromagnetic torque on ith rotor due to electromagnetic energy conversion. For turbine rotors this is taken as zero .

δ_i = angle of rotation of ith mass with reference to a fixed reference frame

T_i = net applied torque on ith rotor.

$D_{i,i}$ = self-damping coefficient of ith mass.

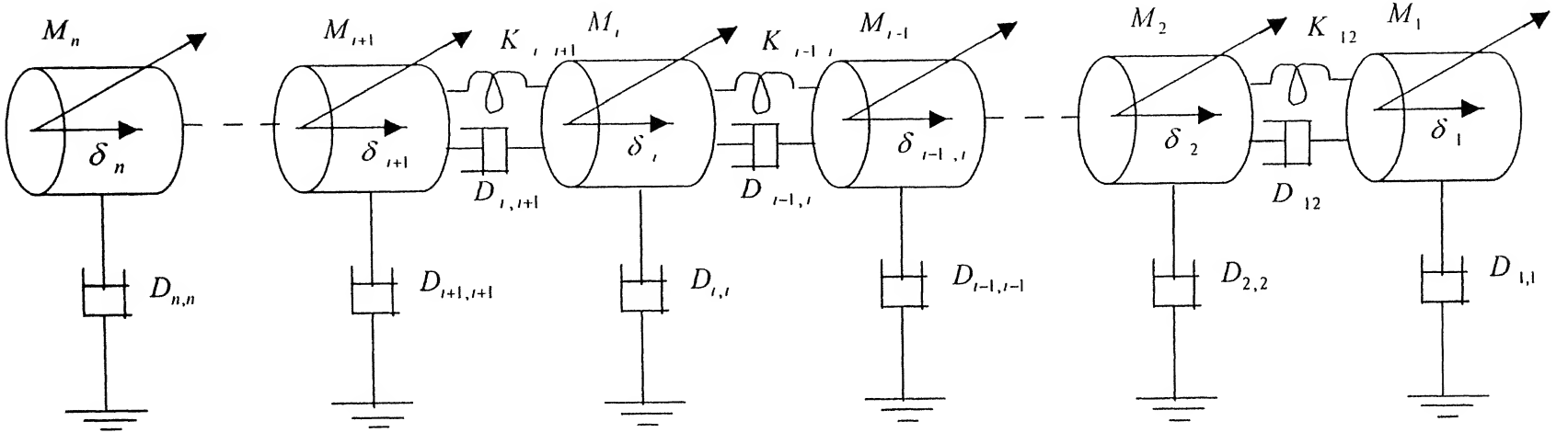

FIG. 2.5 GENERALIZED MODEL OF MECHANICAL SYSTEM

$D_{i,j} = D_{j,i}$ = mutual damping coefficient between ith and jth masses.

$K_{i,j} = K_{j,i}$ = spring constant of the shaft connecting ith and jth masses.

A total of n equations similar to eqn.(2.13) can be written for n masses and combined to result in the following equation of motion

$$M\ddot{\delta} + D\delta + K\delta = T \tag{2.14}$$

where,

M = diagonal matrix of the inertia constants associated with each mass
D = tri-diagonal matrix of damping constants.
K = tri-diagonal matrix of spring constants.
δ = vector representing the angular position of each mass.
T = vector representing the net applied torque on the rotors.

Eqn. (2.14) which describes the torsional motion of masses can be linearized around a quiescent operating point and written in state space form as

$$\dot{x}_M = A_M x_M + B_M u_M \tag{2.15}$$

$$y_M = C_M x_M$$

where $x_M = [\Delta\delta \quad \Delta\dot{\delta}]'$, $y_M = [\Delta\delta_g \quad \Delta\dot{\delta}_g]'$

$\Delta\delta_g$, $\Delta\dot{\delta}_g$ = incremental changes in angular displacement and velocity of the generator mass, respectively.

$$u_M = \Delta T = [\Delta T_1 \quad \Delta T_2 .... \quad \Delta T_i .....\Delta T_{n-1} \quad \Delta T_n]'$$

$$\Delta T_i = \Delta T_{mi} - \Delta T_{ei}$$

It is noted that when turbine – governor dynamics is neglected

$$\Delta T_{mi} = 0$$

while the above state space model has been described for a general n-mass mechanical system, the state and output equations for a specific 6-mass turbine-generator shaft system as utilized for the studies reported in this chapter, are derived in Appendix B,Sec.B.2. This mechanical system, as shown in Fig.B.1, relates to a high pressure turbine, an intermediate pressure turbine, two low pressure turbines, the generator and a rotating exciter. It is described by the following state space equations :

$$\dot{x}_M = A_M x_M + B_{M1} u_{M1} + B_{M2} u_{M2} \tag{2.16}$$

$$y_M = C_M x_M$$

$$x_M = \left[\Delta\delta_1 \quad \Delta\delta_2 \quad \Delta\delta_3 \quad \Delta\delta_4 \quad \Delta\delta_5 \quad \Delta\delta_6 \quad \Delta\dot{\delta}_1 \quad \Delta\dot{\delta}_2 \quad \Delta\delta_3 \quad \Delta\dot{\delta}_4 \quad \Delta\dot{\delta}_5 \quad \Delta\dot{\delta}_6\right]^t$$

$$u_{M1} = \left[\Delta I_D \quad \Delta I_Q\right]^t \quad , \quad u_{M2} = \left[\Delta I_D \quad \Delta i_Q\right]^t \quad , \quad y_M = \left[\Delta\delta_5 \quad \Delta\dot{\delta}_5\right]^t$$

Δi_D , Δi_Q are the incremental D-Q axis components of the current entering generator terminals in the series compensated system .

ΔI_D , ΔI_Q are the incremental D-Q axis components of the dependent current source

A_M , B_{M1} , B_{M2} and C_M are defined in Appendix B , Sec .B.2 .

2.5 Network Model

The network model includes the model of generator stator, transformer, transmission line and the infinite bus. The generator transformer is represented by its leakage reactance. The magnetizing current is neglected. The transmission line is modeled by series R, L and C. The infinite bus is represented as a constant voltage and constant frequency source.

Fig . 2.6 depicts the α- axis representation of the study system shown in Fig. 2.1. I_α is the α component of dependent current source as described in the stator circuit model of synchronous machine . The current entering the generator is represented by i_α. The terminal voltage at infinite bus is indicated by $v_{1\alpha}$. The leakage inductance of the transformer at generator end is denoted by L_{T1} ,whereas L_{T2} represents the inductance of reactor connected to infinite bus .

The equations for the symmetrical network expressed on α- axis are written as

$$L_A \frac{di_\alpha}{dt} = -v_\alpha + v_{1\alpha} - R_A i_\alpha - L_d'' \frac{dI_\alpha}{dt} \tag{2.17}$$

$$C \frac{dv_\alpha}{dt} = i_\alpha \tag{2.18}$$

where $L_A = L + L_{T1} + L_{T2} + L_d''$, $R_A = R + R_a$

The above equations can be rewritten in matrix form as

$$\dot{x}_\alpha = S_1 x_\alpha + S_2 \dot{I}_\alpha + S_3 v_{1\alpha} \tag{2.19}$$

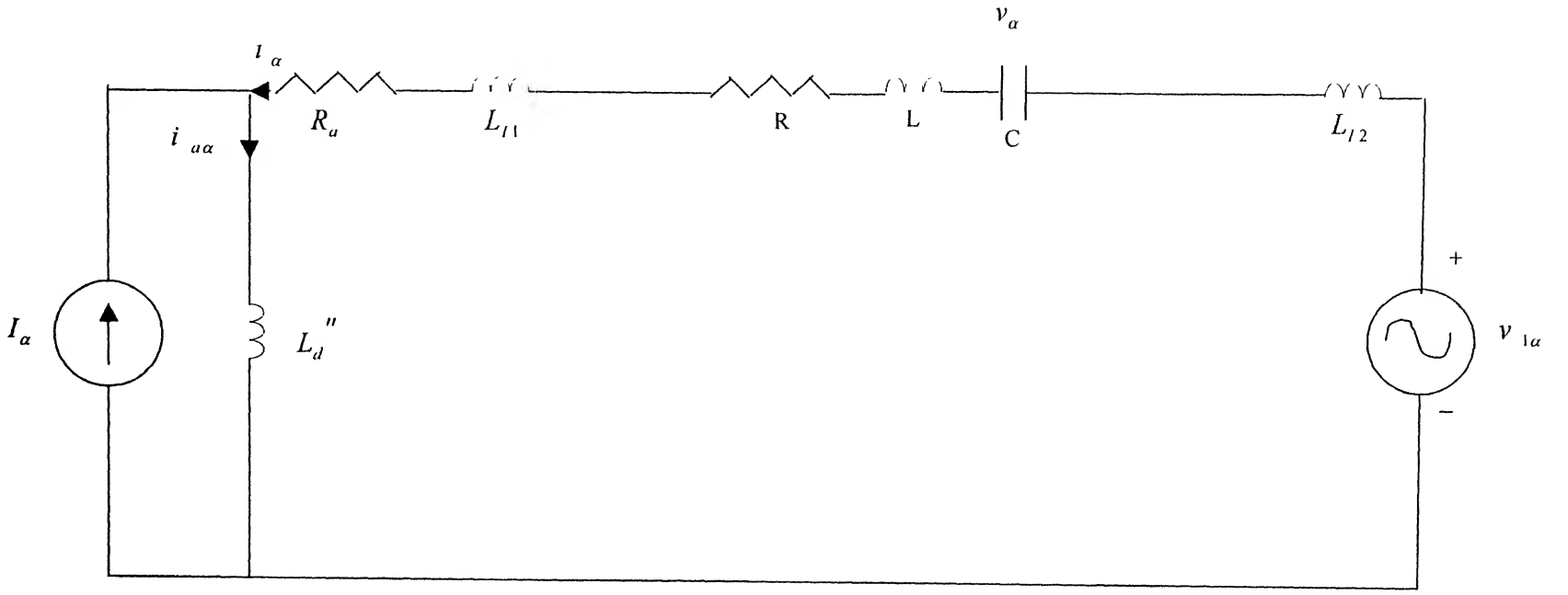

FIG. 2.6 TRANSMISSION NETWORK ON α AXIS FOR IEEE FIRST BENCHMARK MODEL FOR SSR

where $x_\alpha = [i_\alpha \quad v_\alpha]^t$

Matrices S_1 , S_2 and S_3 are defined in Appendix B , Sec. B.3.
Similarly, the equations for the β - network are

$$\dot{x}_\beta = S_1 x_\beta + S_2 I_\beta + S_3 v_{1\beta} \tag{2.20}$$

where $x_\beta = [i_\beta \quad v_\beta]^t$

Since the variables x_α , x_β are sinusoidal quantities in steady state, they result in a time varying system. In order to reduce the overall system to a time invariant one, it is necessary to transform the variables by a D - Q transformation on synchronously rotating reference frame . The D -Q components of the variable x are related to α - β components by the following transformation

$$\begin{bmatrix} x_\alpha \\ x_\beta \end{bmatrix} = \begin{bmatrix} \cos\theta_r I & \sin\theta_r I \\ -\sin\theta_r I & \cos\theta_r I \end{bmatrix} \begin{bmatrix} x_D \\ x_Q \end{bmatrix} \tag{2.21}$$

where $x_D = [i_D \quad v_D]^t$, $x_Q = [i_Q \quad v_Q]^t$

I is an identity matrix of proper dimension. θ_r is the angle by which D-axis leads α - axis .

Equations (2.19) and (2.20) are transformed to D – Q frame of reference using eqn (2.21) and then linearized. It is noted that $\Delta v_{1D} = \Delta v_{1Q} = 0$

The state equation of the series compensated network is finally obtained as

$$\dot{x}_N = A_N x_N + B_{N1} u_{N1} + B_{N2} u_{N2} \tag{2.22}$$

where $x_N = [x_D \quad x_Q]^t$, $u_{N1} = [\Delta I_D \quad I_Q]^t$

$$u_{N2} = [\Delta \dot{I}_D \quad \Delta \dot{I}_Q]^t = \dot{u}_{N1}$$

Matrices A_N , B_{N1} *and* B_{N2} are defined in Appendix B, Sec. B.3.

The current at generator terminals constitutes the output of network model. The corresponding network output equation is given by

$$y_N = C_N x_N \tag{2.23}$$

where $y_V = [\Delta i_D \quad \Delta i_Q]'$

Matrix C_V is defined in Appendix B, Sec B.3.

2.6 Derivation of System Model

The interconnection between the various subsystems can be mathematically described by the following relationship

$$u_I = F_I y_I \tag{2.24}$$

where

u_I = system input vector = $[u_{R1} \quad u_{R2} \quad u_{M1} \quad u_{M2} \quad u_{N1} \quad u_{N2}]'$

y_I = system input vector = $[y_{R1} \quad y_{R2} \quad y_M \quad y_N]'$

Matrix F_I is defined in Appendix B, Sec B.4 .

The state and output equations of all the constituent subsystems are combined to give

$$\dot{x}_I = A_I x_I + B_I u_I \tag{2.25}$$

$$y_I = C_I x_I + D_I u_I \tag{2.26}$$

where $x_I = [x_R \quad x_M \quad x_N]'$

Matrices A_I, B_I, C_I and D_I are defined in Appendix B, Sec . B.4 .
Substituting eqn. (2.26) in eqn. (2.24)

$$u_I = [I - F_I D_I]^{-1} F_I C_I x_I \tag{2.27}$$

Substituting eqn.(2.27) in eqn (2.25) results in

$$\dot{x}_I = A\, x_I \tag{2.28}$$

where

$$A = A_I + B_I [I - F_I D_I]^{-1} F_I C_I$$

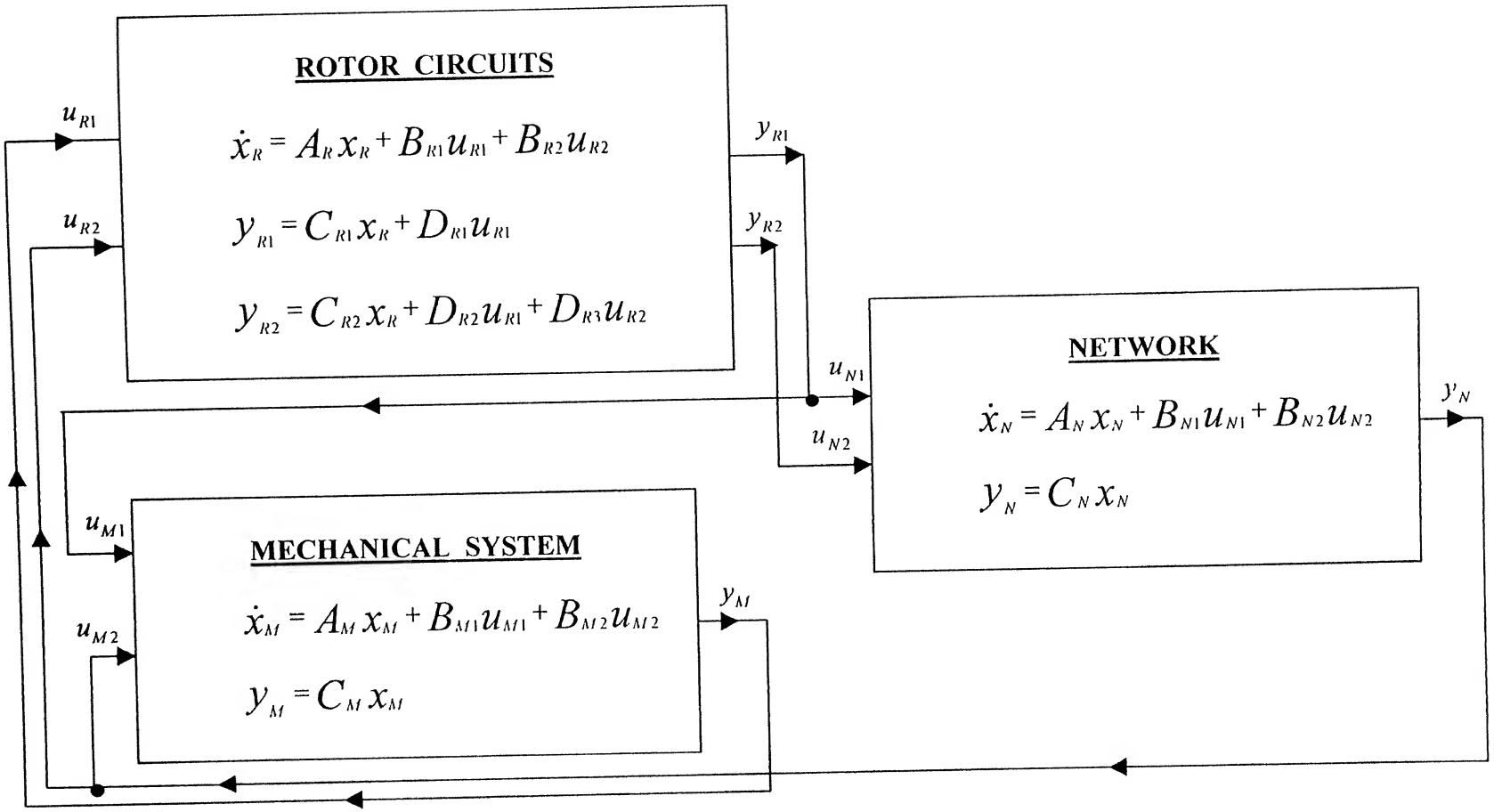

FIG. 2.7 INTERCONNECTION OF VARIOUS SUBSYSTEMS IN OVERALL SYSTEM MODEL

2.7 Eigenvalue Analysis

Eigenvalue analysis has been performed for IEEE First SSR Benchmark System. The operating conditions are chosen to be, generator operating at 803.2 MW. There is no SVC present. When the level of series compensation is such that the electrical frequency of network coincides with the natural frequency of oscillation of any one of the torsional masses, the real part of eigenvalue corresponding to that mode becomes highly positive

Table 2 1 presents the system eigenvalues when network is tuned to different Torsional Modes.

TABLE 2.1 Eigenvalues of IEEE Benchmark System without SVC.

P_g=1.0 p.u. , PF=0.9 Lag

Mode Identification	$X_{C(4)}$=0.178 p.u.	$X_{C(3)}$=0.274 p.u.	$X_{C(2)}$=0.365 p.u.	$X_{C(1)}$=0.454 p.u.
Mode5	0.0 ±j298.1767	0.0 ±j298.1767	0.0 ±j298.1767	0.0 ±j298.1767
Mode4	+1.4279 ±j202.8760	+0.0095 ±j202.7796	-0.0002 ±j202.8626	-0.0023 ±j202.8954
Mode3	+0.0147 ±j160.7544	+1.3816 ±j160.6349	+0.0149 ±j160.3997	+0.0010 ±j160.4985
Mode2	+0.0012 ±j127 0498	+0.0072 ±j127.0920	+0 6715 ±j127.0063	+0.0064 ±j126.9361
Model	+0 0021 ±j99.4066	+0.0190 ±j 99.6600	+0.1248 ±j100.3818	+4 8860 ±j99.2286
Mode0	-0 3321 ±j10.4174	-0.3905 ±j11.2879	-0.4799 ±j12.3397	-0.6222 ±j13.7131
Electrical Mode	-5.3254 ±j202.7614	-4 9425 ±j160.7794	-3.8999 ±j126.9643	-7.3889 ±j99 2066
Supersyn . Mode	-4.7601 ±j551.0233	-4.7973 ±j592.9337	-4.8233 ±j626.2365	-4.8436 ±j654.9739
Generator Rotor Circuits	-40.7906 -25.4118 -3.0801 -0.1287 -0.0676	-40.9539 -25.4264 -3.3957 -0.1333 -0.0871	-41.1552 -25.4457 -3.7929 -0.1429 -0.1016	-41.4114 -25.4733 -4.3401 -0.1599 -0.1100

From the above results, we see that IEEE First SSR Benchmark System is characterizes by 5 torsional modes corresponding to 5 masses of the torsional system. These torsional modes are called as mode 1, mode 2, mode 3, mode 4 and

mode 5 whose frequencies (in radian/sec) are 99, 127, 160, 202 and 298. respectively. There is one mode called as electrical mode, whose frequency matches exactly with that of critically tuned mode. Electrical mode results from the interaction between line inductance and series capacitor.

The eigenvalue results presented in Table 2.1 are in close agreement with the published results [14].

2.8 CONCLUSIONS

In this chapter, system model is developed for IEEE First SSR Benchmark system. The potential instabilities of this system are assessed by an eigenvalue program. This analysis shows that the system is characterized by four unstable torsional modes distributed over a wide frequency range.

The eigenvalue results of Table 2.1 agree with the published results.

Chapter 3

MODELING OF SVC CONTROL SYSTEM

3.1 Introduction

It has been reported earlier [15,23] that a midpoint located SVC can not only improve system stability but also damp subsynchronous oscillations in a single machine infinite bus system. However, this has been demonstrated with auxiliary controllers of SVC utilizing locally available signals and a computed generator frequency signal which has been shown to be quite effective.

In this chapter a new concept is investigated where instead of computing the generator frequency, the actual rotor frequency signal is measured and transmitted over a telecom channel to the remotely located SVC.

This chapter describes the modeling of SVC compensated network, SVC voltage control system and modeling of various SVC auxiliary controllers.

3.2 Study System

The study system is the IEEE First Benchmark System with an SVC placed at the mid point of transmission line, as depicted in Fig 3.1.

3.3 System Model

The system model is derived from the models of constituent subsystems :

(i) Synchronous generator
   (a) Stator circuits
   (b) Rotor circuits
   (c) Mechanical system

(ii) Network

(iii) SVC
   (a) Voltage controller
   (b) Auxiliary feedback controller

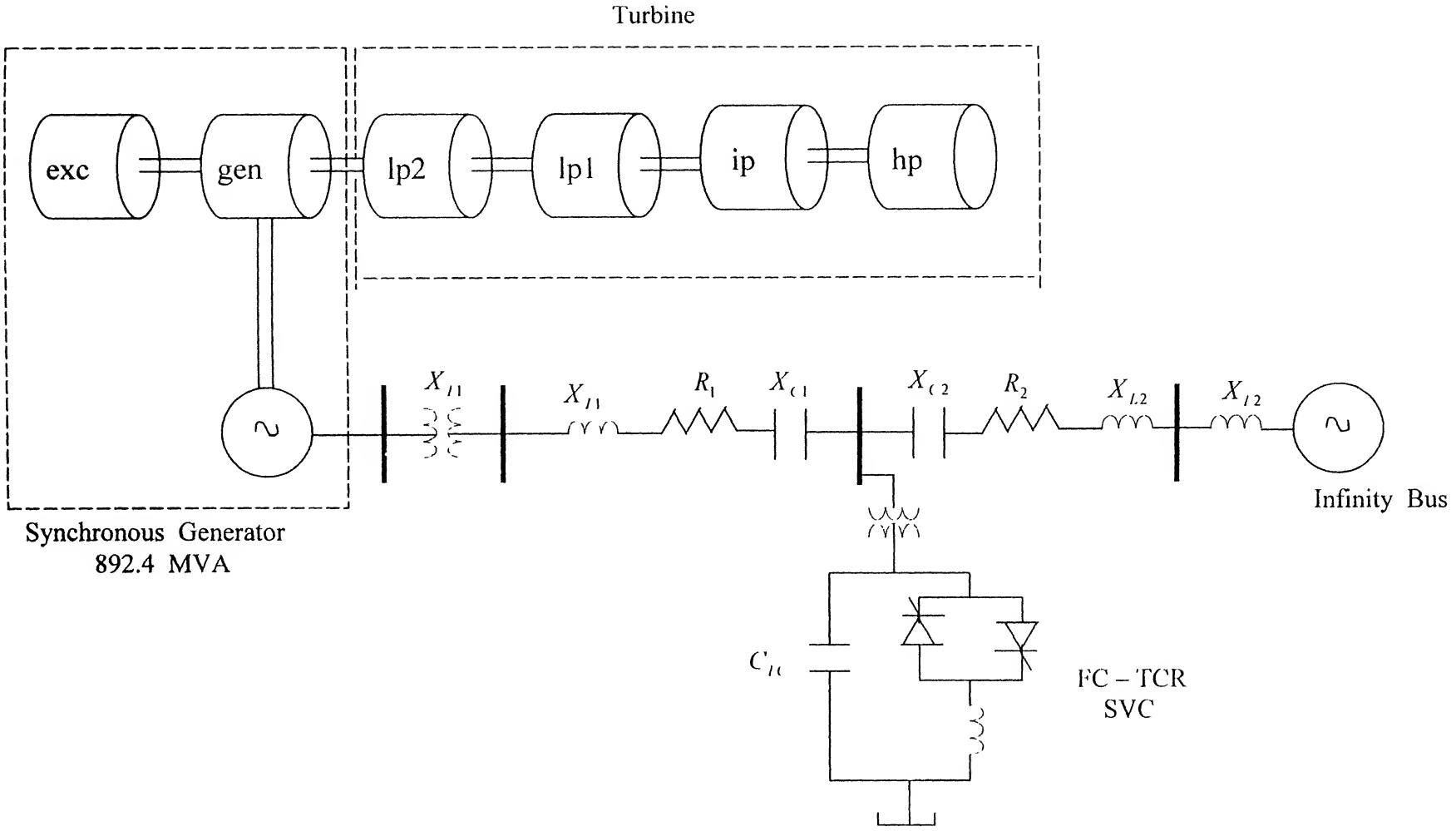

FIG. 3.1 STUDY SYSTEM (IEEE FIRST BENCHMARK SYSTEM WITH AN SVC PLACED AT THE MIDPOINT OF TRANSMISSION LINE)

Component models of the stator and rotor circuits of synchronous generator and mechanical system including representation of various turbine masses and their dynamics have already been derived in Chapter 2. The development of SVC compensated network, SVC voltage control system including TCR transients and all firing control and measurement delays have been described in section 3.3.1 and 3.3.2 respectively.

Modeling of SVC auxiliary controller utilizing various auxiliary signals has been described in section 3.3.4 .

3.3.1 Network Model

The ac network considered for the study system of Fig. 3.1, is similar to that described in Chapter 2 except that the transmission line is segregated into two halves and an SVC is placed at the midpoint of line. The equivalent α - network is shown in Fig 3.2.

R_a denotes the armature resistance of the synchronous generator. I_α is the α component of dependent current source as given in the model of synchronous machine. The current entering the generator is represented by i_α. The voltage and current at infinite bus are represented by $v_{1\alpha}$ and $i_{1\alpha}$ respectively. L_{T1} and L_{T2} represent the leakage inductance of the transformer at generator end and inductance of reactor connected to infinite bus respectively. The SVC bus voltage is indicated by $v_{3\alpha}$ and its current by $i_{3\alpha}$. The two series capacitor voltages are represented by $v_{2\alpha}$ and $v_{4\alpha}$. The transmission line current entering SVC bus from the generator end is denoted by $i_{4\alpha}$. The symbols R_1, L_1, C_{se1} and R_2, L_2, C_{se2} represents the resistance, inductance and capacitance of the two sections of transmission line

The following differential equations are derived for the α - network

$$\frac{di_{1\alpha}}{dt} = -\frac{R_2}{L_B} i_{1\alpha} + \frac{1}{L_B} v_{3\alpha} - \frac{1}{L_B} v_{1\alpha} - \frac{1}{L_B} v_{2\alpha} \tag{3.1}$$

$$\frac{di_\alpha}{dt} = -\frac{R_4}{L_4} i_\alpha + \frac{1}{L_4} v_{3\alpha} - \frac{1}{L_4} v_{4\alpha} - \frac{L''_d}{L_A} \frac{dI_\alpha}{dt} \tag{3.2}$$

$$\frac{dv_{3\alpha}}{dt} = -\frac{1}{C_n} i_\alpha - \frac{1}{C_n} i_{3\alpha} - \frac{1}{C_n} i_{1\alpha} \tag{3.3}$$

$$\frac{dv_{2\alpha}}{dt} = \frac{1}{C_{se2}} i_{1\alpha} \tag{3.4}$$

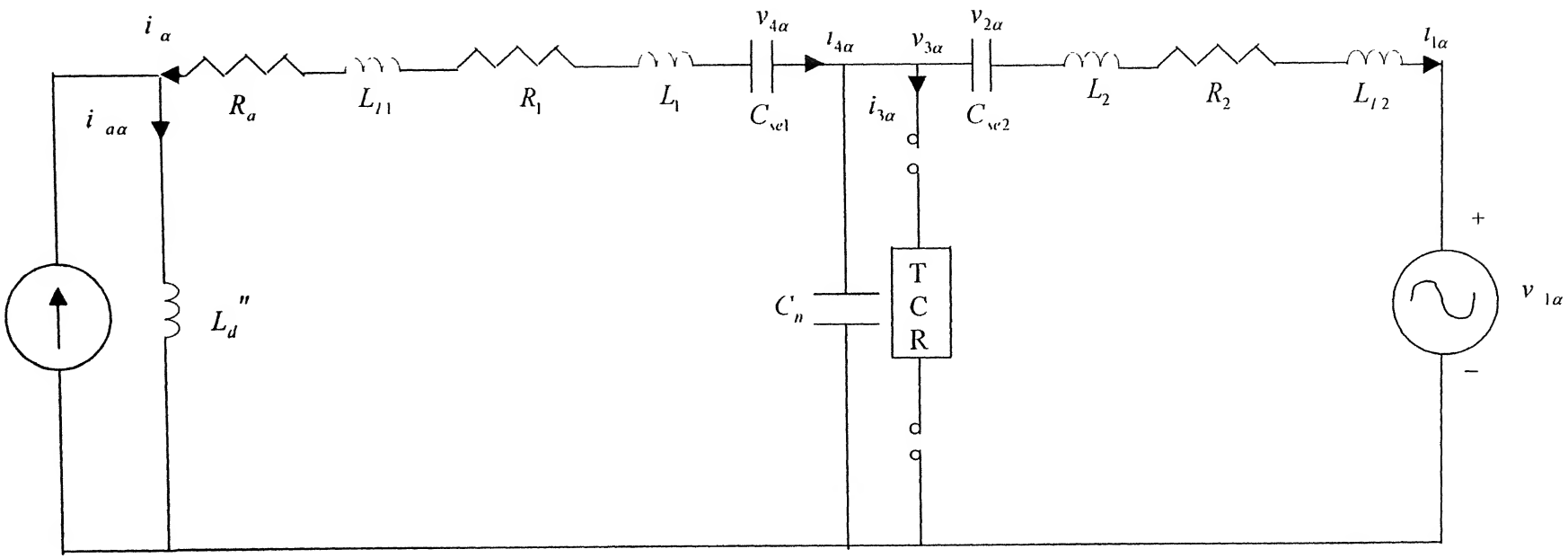

FIG. 3.2 TRANSMISSION NETWORK ON α AXIS FOR IEEE FIRST BENCHMARK MODEL FOR SSR, WHEN SVC IS PLACED AT THE MIDPOINT OF TRANSMISSION LINE

$$\frac{dv_{4\alpha}}{dt} = \frac{1}{C_{sel}} i_{\alpha} \tag{3.5}$$

where $L_4 = L_{T1} + L_1 + L_d''$, $L_B = L_{T2} + L_2$

$R_4 = R_1 + R_a$, $C_n = C_{IC}$

The above equations can be written in matrix form as

$$\dot{x}_{\alpha} = S_1 x_{\alpha} + S_2 i_{3\alpha} + S_3 I_{\alpha} + S_4 v_{1\alpha} \tag{3.6}$$

where $x_{\alpha} = [i_{1\alpha} \quad i_{\alpha} \quad v_{3\alpha} \quad v_{2\alpha} \quad v_{4\alpha}]'$

Matrices S_1 , S_2 , S_3 and S_4 are defined in Appendix C , Sec. C.1. Similarly, the equations for β - network are given by

$$\dot{x}_{\beta} = S_1 x_{\beta} + S_2 i_{3\beta} + S_3 I_{\beta} + S_4 v_{1\beta} \tag{3.7}$$

where $x_{\beta} = [i_{1\beta} \quad i_{\beta} \quad v_{3\beta} \quad v_{2\beta} \quad v_{4\beta}]'$

It is to be noted that vectors x_{α}, x_{β} and matrices S_1, S_2 and S_3 as given above are different from the similar named vectors and matrices as defined in chapter 2 corresponding to the system without SVC.

Eqns.(3.6) and (3.7) are transformed to the synchronously rotating D -Q frame of reference using the transformation described by eqn. (2.21) and are subsequently linearized. Since the infinite bus voltage is constant, Δv_{1D} , $\Delta v_{1Q} = 0$

The state equation of the series compensated network is finally derived as

$$\dot{x}_N = A_N x_N + B_{N1} u_{N1} + B_{N2} u_{N2} + B_{N3} u_{N3} \tag{3.8}$$

where $x_N = [\Delta i_{1D} \quad \Delta i_D \quad \Delta v_{3D} \quad \Delta v_{2D} \quad \Delta v_{4D} \quad \Delta i_{1Q} \quad \Delta i_Q \quad \Delta v_{3Q} \quad \Delta v_{2Q} \quad \Delta v_{4Q}]'$

$u_{N1} = [\Delta i_{3D} \quad \Delta i_{3Q}]'$

$u_{N2} = [\Delta I_D \quad \Delta I_Q]'$

$u_{N3} = [\Delta \dot{I}_D \quad \Delta \dot{I}_Q]' = \dot{u}_{N2}$

Matrices A_N, B_{N1}, B_{N2} and B_{N3} are defined in Appendix C, Sec. C.1 .

The output variables of network model are the current at generator terminals and the SVC bus voltage. The corresponding network output equations are derived as eqns. (C.1,C.2) and given by

$$y_{N1} = C_{N1} x_N \tag{3.9}$$

$$y_{N2} = C_{N2} x_N \tag{3.10}$$

where $y_{N1} = [\Delta i_D \quad \Delta i_Q]'$ and $y_{N2} = [\Delta v_{3D} \quad \Delta v_{3Q}]'$

Matrices C_{N1} and C_{N2} are defined in Appendix C, Sec. C.1.

3.3.2 Static Var Compensator

SVC is a dynamic reactive power device which provides rapid and continuously controllable lagging and leading MVARs. Variation of reactive power can be achieved through both the active and passive control.

3.3.2.1 Operating Characteristic of SVC

Fig. 3.3 shows the steady state control characteristic of an SVC, which represents the relationship between SVC current (or reactive power output) and the bus voltage. The steady state operating point is established at the intersection of the control characteristic with the system load line. For small deviations in the bus voltage around the controller set point V_{ref}, the SVC current is regulated within the control range to provide inductive compensation for voltage rises and capacitive compensation for voltage drops. Thus SVC maintains the terminal voltage at the preset reference V_{ref}. Large changes in the bus voltage force the SVC beyond its control range For severe undervoltages the SVC gets tranformed into an equivalent fixed capacitor having susceptance $B_{LMIN} - B_C$, while for large overvoltages, it reduces to an equivalent shunt reactor of susceptance $B_{LMAX} - B_C$.

The slope of the control characteristic essentially represents a compromise between SVC rating and the voltage stabilizing requirement. It also improves the current sharing between the SVCs operating in parallel. The slope of the control characteristic is typically chosen in the range of 1-10 %.

3.3.2.2 Modeling of SVC Voltage Controller

A small signal model of a general SVC control system is depicted in Fig. 3.5. The terminal voltage perturbation ΔV and the SVC incremental current weighted by the factor K_D representing current droop are fed to the reference junction. T_M represents the measurement time constant which for simplicity is assumed to be equal for both voltage and current measurements. The voltage regulator is assumed to be a proportional-integral (PI) controller. Thyristor control action is represented by an average dead time T_D and a firing delay time T_S. The variation in TCR susceptance is represented by ΔB.

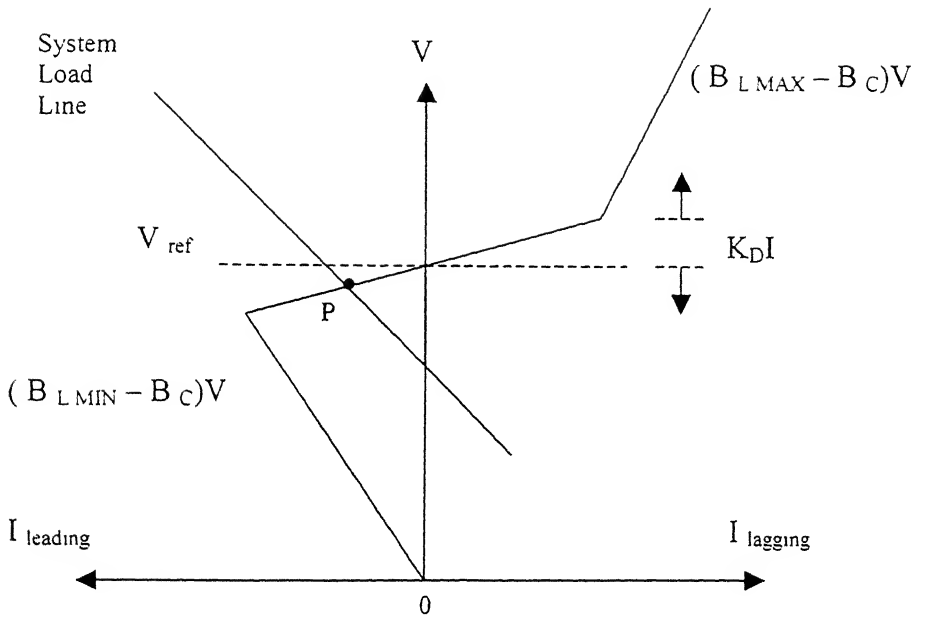

P : operating point

B_C = SVC capacitive susceptance

B_I = SVC inductive susceptance

FIG. 3.3 STEADY STATE CONTROL CHARACTERISTIC OF SVC

In detailed modeling of SVC , TCR transients are being included . The delays associated with SVS controller and measurement unit is also incorporated . The α, β axis currents entering TCR from the network are expressed as

$$L_S \frac{d i_{3\alpha}}{dt} + R_S\, i_{3\alpha} = v_{3\alpha}$$

$$L_S \frac{d i_{3\beta}}{dt} + R_S\, i_{3\beta} = v_{3\beta} \qquad (3.11)$$

where L_S , R_S represent the inductance and resistance of the TCR , respectively .

Transforming equation (3.11) to D-Q frame of reference using equation (2.21) and linearizing , gives

$$\begin{bmatrix} \Delta \dot{i}_{3D} \\ \Delta \dot{i}_{3Q} \end{bmatrix} = \omega_0 \begin{bmatrix} -\frac{1}{Q} & -1 \\ 1 & -\frac{1}{Q} \end{bmatrix} \begin{bmatrix} \Delta i_{3D} \\ \Delta i_{3Q} \end{bmatrix} + \omega_0 B_0 \begin{bmatrix} 1 & 0 \\ 0 & 1 \end{bmatrix} \begin{bmatrix} \Delta v_{3D} \\ \Delta v_{3Q} \end{bmatrix} + \omega_0 \begin{bmatrix} v_{3D0} \\ v_{3Q0} \end{bmatrix} \Delta B \qquad (3.12)$$

where Q = Quality Factor of TCR $= \frac{\omega_0 L_S}{R_S}$, $B = \frac{1}{\omega_0 L_S}$

The following equations can be written for SVS control system

$$\dot{z}_1 = \Delta V_{ref} - z_2 \qquad (3.13)$$

where ΔV_{ref} is the reference voltage perturbation

$$\Delta v_3 - K_D\, \Delta i_3 = z_2 + T_M\, \dot{z}_2 \qquad (3.14)$$

where Δv_3 , Δi_3 are the incremental magnitudes of SVS bus voltage and TCR current.

$$\dot{z}_2 = \frac{1}{T_M}(\Delta v_3 - K_D\, \Delta i_3) - \frac{1}{T_M} z_2 \qquad (3.15)$$

$$-K_P \dot{z}_1 - K_I z_1 = z_3 + T_S \dot{z}_3 \qquad (3.16)$$

Substituting eqn. (3.13) in eqn. (3.16) gives

$$\dot{z}_3 = -\frac{K_I}{T_S} z_1 + \frac{K_P}{T_S} z_2 - \frac{1}{T_S} z_3 - \frac{K_P}{T_S} \Delta V_{ref} \qquad (3.17)$$

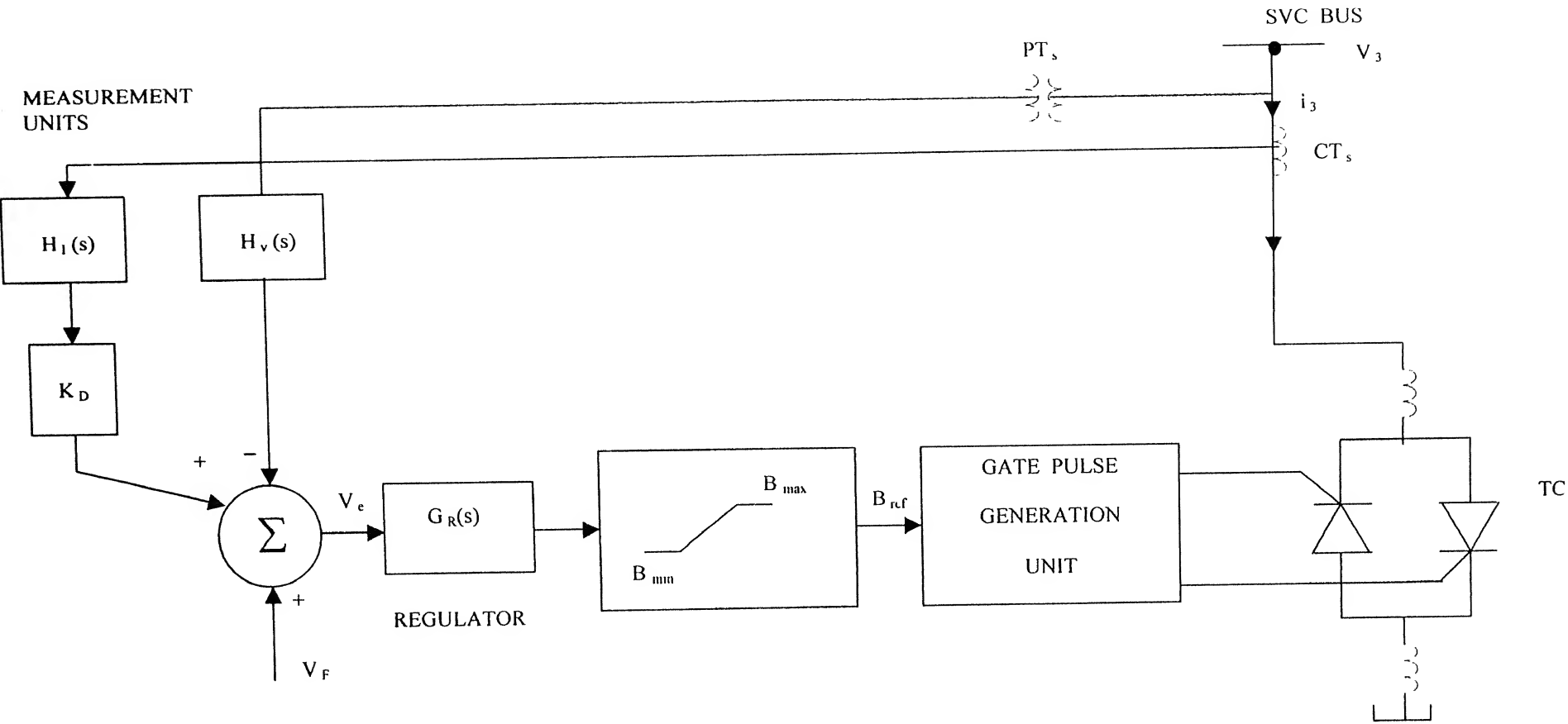

FIG . 3.4 GENERAL CONTROL SYSTEM BLOCK DIAGRAM FOR THYRISTORIZED SVC

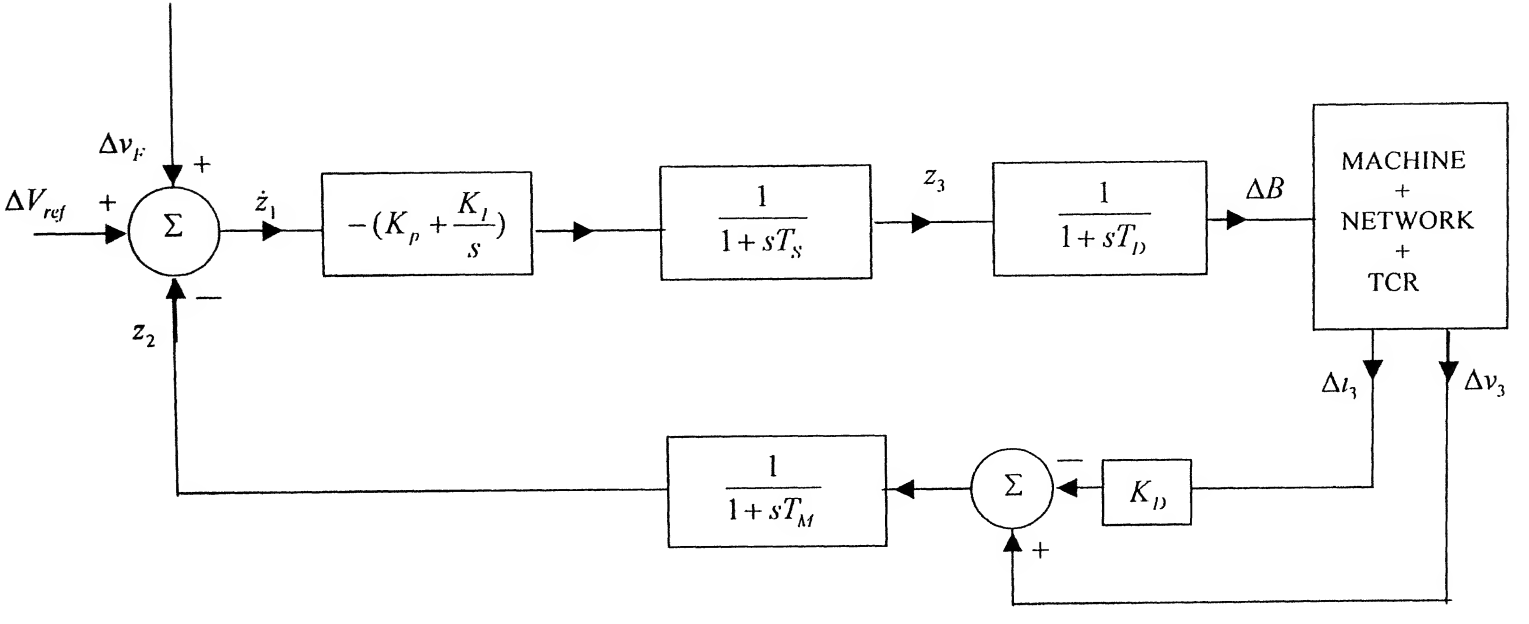

FIG. 3.5 SVC MODEL FOR SMALL SIGNAL ANALYSIS

$$z_3 = \Delta B + T_D \Delta \dot{B} \tag{3.18}$$

or

$$\Delta \dot{B} = \frac{1}{T_D} z_3 - \frac{1}{T_D} \Delta B \tag{3.19}$$

The magnitude of TCR current is given by

$$i_3 = \sqrt{(i_{3D}{}^2 + i_{3Q}{}^2)} \tag{3.20}$$

Linearizing eqn. (3.20)

$$\Delta i_3 = \frac{i_{3D0}}{i_{30}} \Delta i_{3D} + \frac{i_{3Q0}}{i_{30}} \Delta i_{3Q} \tag{3.21}$$

The SVS bus voltage v_3 is also expressed in terms of its D , Q axis components as

$$v_3 = \sqrt{(v_{3D}{}^2 + v_{3Q}{}^2)} \tag{3.22}$$

Linearizing equation (3.22) gives

$$\Delta v_3 = \frac{v_{3D0}}{v_{30}} \Delta v_{3D} + \frac{v_{3Q0}}{v_{30}} \Delta v_{3Q} \tag{3.23}$$

Eqns. (3.21) , (3.23) are substituted in eqn (3.15) to give the state equation corresponding to $\dot{z}_2$.

The state and output equations of the SVC model can then be written as

$$\dot{x}_S = A_S x_S + B_{S1} u_{S1} + B_{S2} u_{S2} + B_{S2} u_{S3} \tag{3.24}$$

$$y_S = C_S x_S + D_S u_{S1} \tag{3.25}$$

where , $x_S = [\Delta i_{3D} \quad \Delta i_{3Q} \quad z_1 \quad z_2 \quad z_3 \quad \Delta B]'$,

$u_{S1} = [\Delta v_{3D} \quad \Delta v_{3D}]'$

$u_{S2} = \Delta V_{ref}$, $u_{S3} = \Delta v_f$, $y_S = [\Delta i_{3D} \quad \Delta i_{3Q}]'$

Matrices A_S , B_{S1} , B_{S2} , C_S and D_S are defined in Appendix C , Sec.C.2

3.3.2.3 Choice of SVC Rating

The dynamic range of SVC is chosen on the basis of reactive power requirement at the SVC bus to control voltage under steady state conditions. This information is obtained from load flow studies which, in addition, provide the voltage magnitudes and phase angles at various buses needed to compute the initial conditions in the system. The SVC bus is assumed to be a PV bus with zero power injection (SVC losses are neglected).

Load flow is then conducted and SVC bus reactive power is computed for varying generator power outputs over whole range of series compensation from 0 % to 90.8 % (a series compensation level corresponding to critical excitation of mode 1). The results are presented in Table 3.1. It is seen that as the generator real power increases from 100 MW to 803.2 MW the SVC reactive power output varies from -4.5 MVA inductive to 250.5 MVA capacitive. Hence, the dynamic range of SVC is chosen as 25 MVA inductive to 275 MVA capacitive. It is important to note that as the SVC configuration is FC-TCR, the reactor is rated larger than the fixed capacitance in order to provide net lagging VARs

.

Table 3.1

Requirement of Reactive Power at SVC Bus (in MVARs)

K=% series compensation

Level of Power Transfer (in MW)	K=0.0	K=35.6	K=54.8	K=73.0	K=90.8
100	3.3	1.7	0.6	-1.1	-4.5
500	94.9	67.0	50.5	31.9	5.3
803.2	250.5	179.3	139.2	96.8	42.2

The slope of the steady state V-I characteristic of SVC which is defined on nominal voltage base and the larger of the two reactive ratings, is taken as 1 % at 275 MVA capacitive reactive power output of SVC.

3.4 Derivation of System Model

The interconnection between the various subsystems can be mathematically described by the following relationship

$$u_T = F_T y_T \tag{3.26}$$

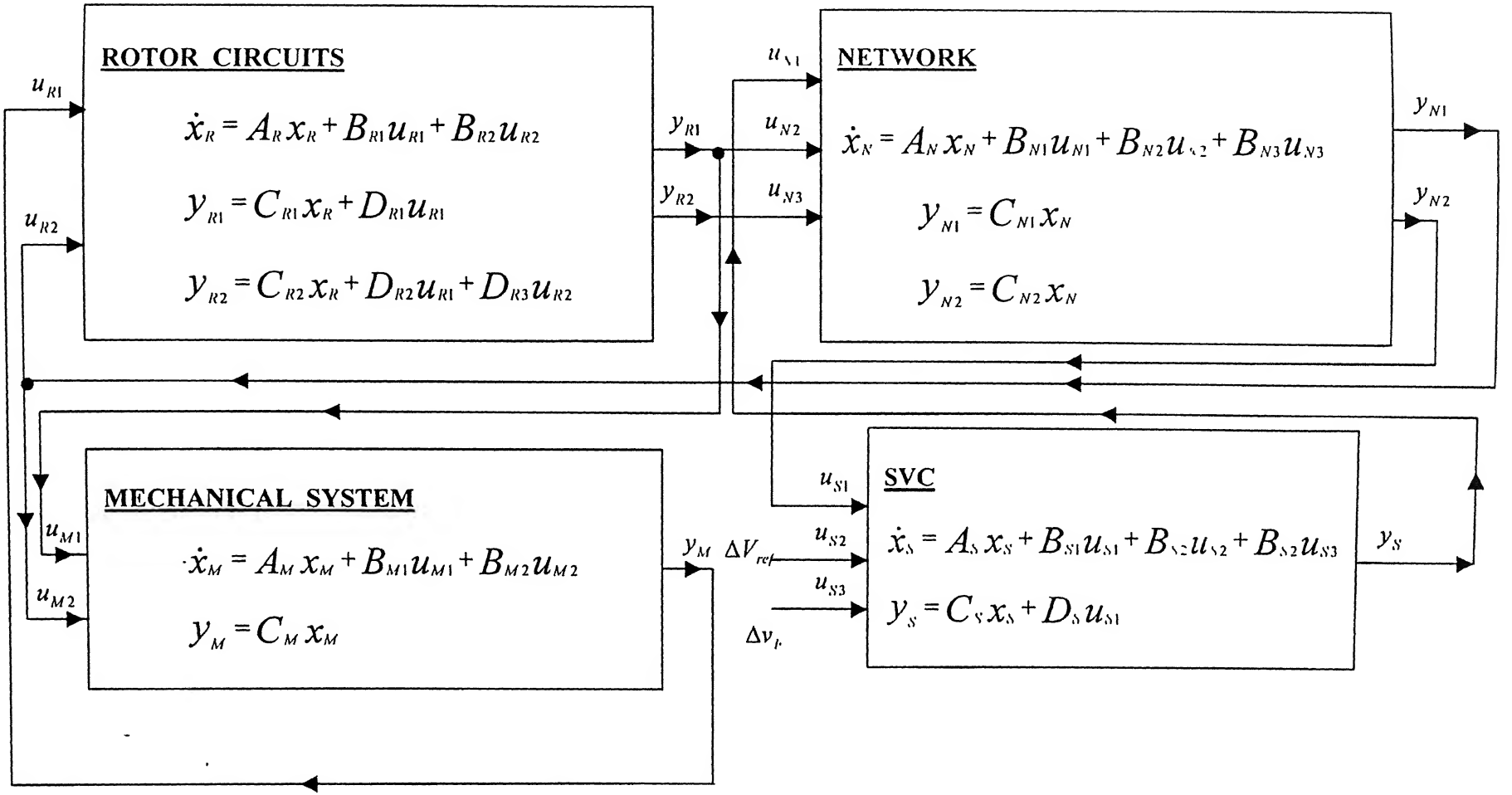

FIG .3.6 INTERCONNECTION OF VARIOUS SUBSYSTEMS IN OVERALL SYSTEM MODEL

where

u_I = system input vector = $[u_{R1} \quad u_{R2} \quad u_{M1} \quad u_{M2} \quad u_{N1} \quad u_{N2} \quad u_{N3} \quad u_{S1}]'$

y_I = system input vector = $[y_{R1} \quad y_{R2} \quad y_M \quad y_{N1} \quad y_{N2} \quad y_S]'$

Matrix F_T is defined in Appendix C ,Sec..C.3 .

The state and output equations of all the constituent subsystems are combined to give

$$\dot{x}_I = A_I x_T + B_I u_T + B u_{S2} + B u_{S3} \tag{3.27}$$

$$y_I = C_I x_I + D_I u_T \tag{3.28}$$

where $x_T = [x_R \quad x_M \quad x_N \quad x_S]'$

Matrices A_T , B_T , B , C_T and D_T are defined in Appendix C,Sec. C.3 .
Substituting eqn. (3.28) in eqn . (3.26)

$$u_I = [I - F_T D_I]^{-1} F_T C_T x_T \tag{3.29}$$

Substituting eqn.(3.29) in eqn. (3.27) results in

$$\dot{x}_I = A\, x_I + B u_{S2} + B u_{S3} \tag{3.30}$$

where

$$A = A_I + B_I [I - F_T D_T]^{-1} F_T C_T$$

$u_{S2} = \Delta v_{ref}$, $u_{S3} = \Delta v_F$

where Δv_F is the output of the auxiliary controller

3.5 SVC Auxiliary Controller Model

This section deals with the development of a state space model for the SVC auxiliary controller. Fig. 3.7 depicts the block diagram of an SVC control system involving feedback of a general auxiliary signal u_C through a controller transfer function G(s). In this analysis the perturbation in SVC reference voltage V_{ref} is assumed to be zero. The state and output equations are derived for this controller with different auxiliary signals. Each signal is mathematically expressed as a function of the state variables of other subsystems. The various signals considered

are line current and CIF, which are locally available and generator frequency available at remote located SVC.

3.5.1 Line Current Auxiliary Controller

The magnitude of transmission line current i_4 entering SVC bus from the generator end, as shown in Fig. 3.1 is given by

$$i_4 = \sqrt{i_{4D}^{\ 2} + i_{4Q}^{\ 2}} \tag{3.31}$$

where i_{4D}, i_{4Q} are the components of line current i_4 along D,Q axis, respectively .

The auxiliary control signal chosen in this case is the perturbation in line current magnitude Δi_4, which is obtained by linearizing eqn .(3.31)

$$\Delta i_4 = \frac{i_{4D0}}{i_{40}} \Delta i_{4D} + \frac{i_{4Q0}}{i_{40}} \Delta i_{4Q} \tag{3.32}$$

this signal can be expressed as

$$u_C = F_{CR} x_R + F_{CM} x_M + F_{CN} x_N + F_{CS} x_S \tag{3.33}$$

where $u_C = \Delta i_4$, $F_{CR} = F_{CM} = F_{CS} = 0$

Matrix F_{CN} is defined in Appendix C, Sec. C.4.1 .

The auxiliary controller is, a priori, assumed to be a simple first order transfer function for this auxiliary signal and all the others described subsequently in this section.

$$G(s) = \frac{\Delta v_F}{\Delta f_S} = K_B \left(\frac{1 + sT_1}{1 + sT_2}\right) \tag{3.34}$$

This controller can be equivalently expressed as

$$G(s) = K_B \frac{T_1}{T_2} + K_B \left(\frac{1 - T_1/T_2}{1 + sT_2}\right) \tag{3.35}$$

A block diagram of this auxiliary controller is displayed in Fig. 3.8. The corresponding state and output equations are given by

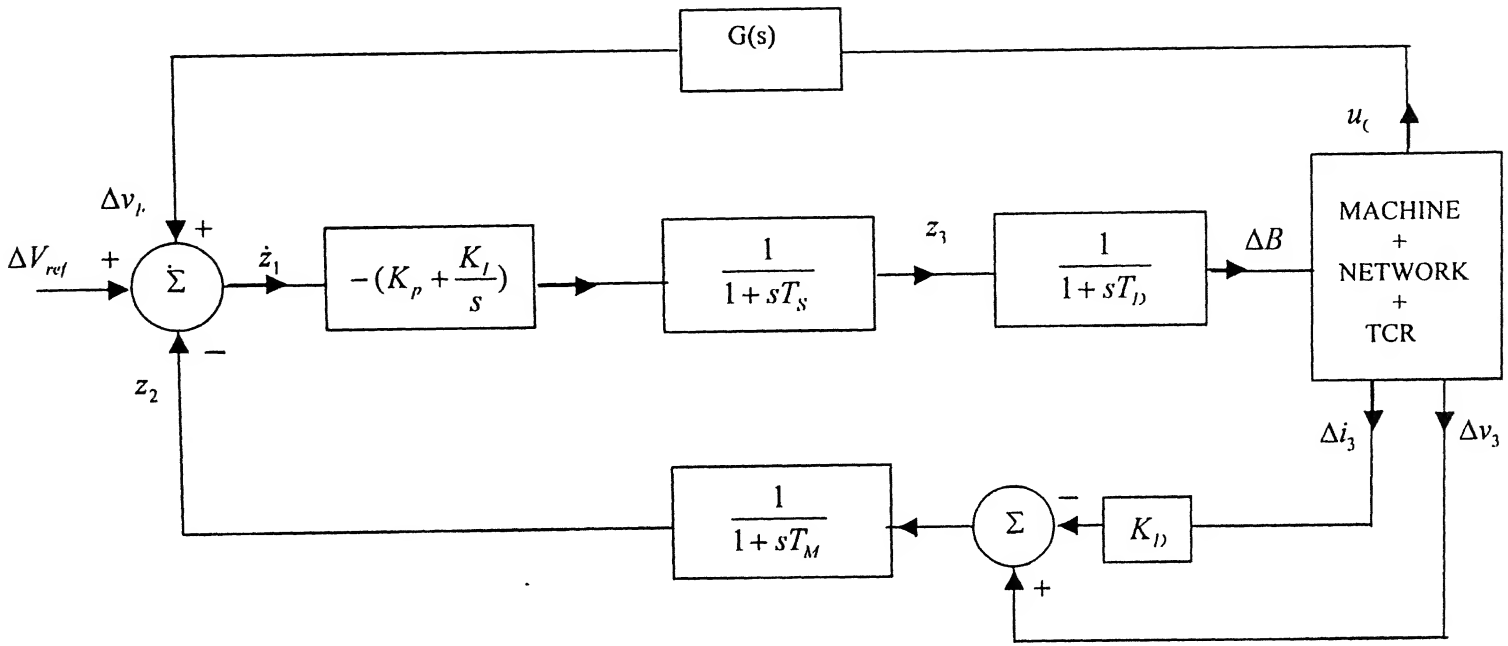

FIG.3.7 SVC CONTROL SYSTEM WITH AUXILIARY FEEDBACK

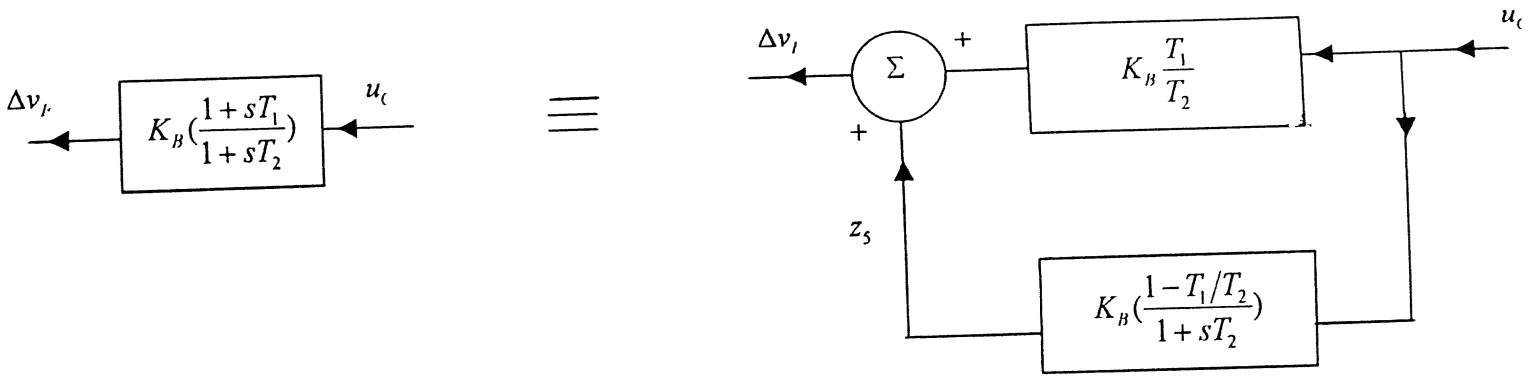

FIG . 3.8 BLOCK DIAGRAM OF A GENERAL FIRST ORDER AUXILIARY SVC CONTROLLER

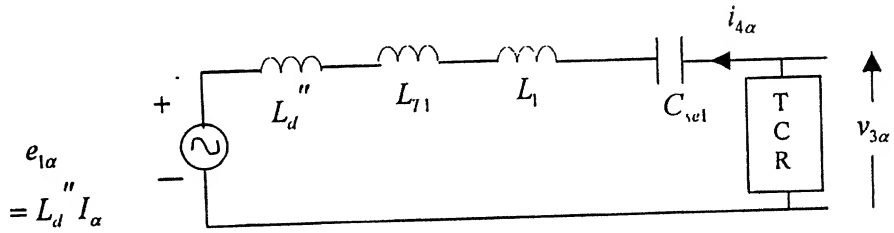

FIG. 3.9 SIMPLIFIED α - AXIS REPRESENTATION OF THE STUDY SYSTEM FOR OBTAINING CIF SIGNAL

$$\dot{x}_C = A_C x_C + B_C u_C \tag{3.36}$$

$$y_C = C_C x_C + D_C u_C \tag{3.37}$$

where $x_C = [z_5]$, $y_C = \Delta v_F$

Matrices A_C, B_C, C_C and D_C are defined in Appendix C, Sec.C.4.1

3.5.2 Computed Internal Frequency (CIF) Auxiliary Controller

Computed internal frequency is a control signal derived from the generating source frequency. Since the generating station and SVC are located far apart from each other, the CIF signal is computed from parameters which are available at the SVC bus. The quantities utilized for the computation of CIF signal are bus voltage, transmission line current at the SVC bus and the reactance between generator internal voltage and SVC terminals. The derivation procedure is given below.

The α axis network of the study system including synchronous generator, transformers and transmission network shown in Fig. 3.2 is simplified to a form depicted in Fig. 3.9. For computing CIF signal, only the section between generator and SVC is considered. The resistances of the generator stator and transmission line is neglected. The fixed capacitor is considered as placed on the right of TCR and hence, is ignored in this analysis. The dependent current source representing the generator is transformed to an equivalent voltage source behind subtransient inductance. L_E represents the total inductance between SVC and the equivalent voltage source and is given by

$$L_E = L_d'' + L_{T1} + L \tag{3.38}$$

where

L_d'' = subtransient inductance of the generator.

L_{T1} = inductance of transformer at generator end.

L = inductance of transmission line segment between the generator transformer and SVC.

The α, β axis components of the internal voltage e_1 of synchronous generator is given by

$$e_{1\alpha} = v_{3\alpha} + L_E \frac{di_{4\alpha}}{dt} \tag{3.39}$$

$$e_{1\beta} = v_{3\beta} + L_E \frac{di_{4\beta}}{dt} \tag{3.40}$$

where $v_{3\alpha}$, $v_{3\beta}$ are the components of SVC bus voltage v_3 along α , β axis respectively. $i_{4\alpha}$, $i_{4\beta}$ are the components of line current i_4 along α , β axis respectively

Transforming eqns. (3.39) and (3.40) to D-Q frame of reference using eqn. (2.21) results in

$$e_{1D} = v_{3D} + L_E \dot{i}_{4D} + \omega_0 L_E i_{4Q} \tag{3.41}$$

$$e_{1Q} = v_{3Q} + L_E \dot{i}_{4Q} - \omega_0 L_E i_{4D} \tag{3.42}$$

where e_{1D} , e_{1Q} are the D and Q axis components of the internal voltage e_1 respectively.

The angle δ_1 of the internal voltage e_1 is computed as

$$\delta_1 = \tan^{-1}\left(\frac{e_{1Q}}{e_{1D}}\right) \tag{3.43}$$

Linearizing eqn. (3.43)

$$\Delta\delta_1 = \frac{e_{1D0}}{e_{10}^2}\Delta e_{1Q} - \frac{e_{1Q0}}{e_{10}^2}\Delta e_{1D} \tag{3.44}$$

The computed internal frequency (CIF) signal $\Delta\omega_1$ is then obtained by differentiating eqn. (3.44)

$$\Delta\omega_1 = \frac{d}{dt}\Delta\delta_1 = \frac{e_{1D0}}{e_{10}^2}\Delta\dot{e}_{1Q} - \frac{e_{1Q0}}{e_{10}^2}\Delta\dot{e}_{1D} \tag{3.45}$$

The expression for $\Delta\omega_1$ in general matrix notation is derived in Appendix C as eqn. (C.11) and given by

$$u_C = F_{CR}x_R + F_{CM}x_M + F_{CN}x_N + F_{CS}x_S \tag{3.46}$$

where $u_C = \Delta\omega_1$

Matrices F_{CR}, F_{CM} and F_{CN} are defined in Appendix C, Sec. C..4.4 .

The state and output eqn. Of the corresponding auxiliary controller are given by eqns.(3.36) and (3.37) respectively .

3.5.3 Remote Frequency (RF) Auxiliary Controller

The remote frequency signal is the actual measured value of generator rotor frequency which is transmitted over a telecom channel to the midpoint located SVC. This signal is associated with a time delay T_{TD} which includes both the measurement and telecom delay. Fig 3.10. represents the block diagram for remote frequency auxiliary controller .

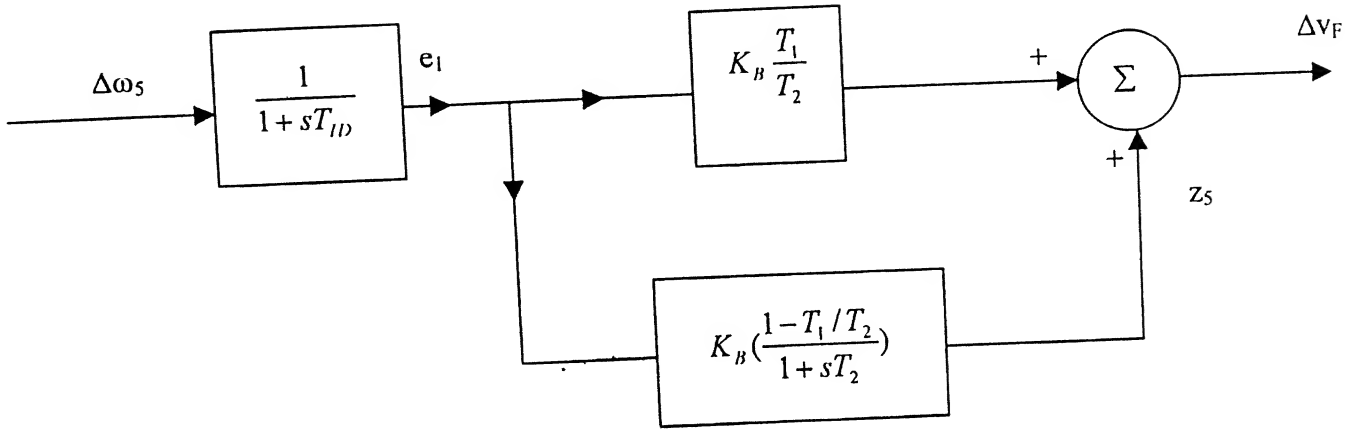

FIG 3.10 BLOCK DIAGRAM OF REMOTE FREQUENCY AUXILIARY CONTROLLER

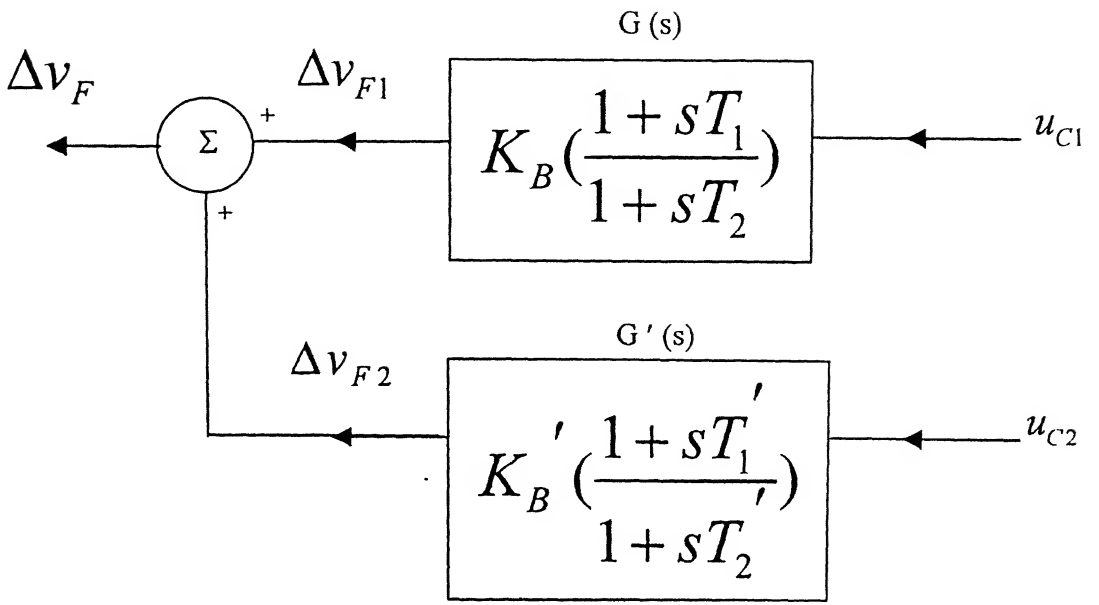

FIG .3.11 BLOCK DIAGRAM OF AUXILIARY CONTROLLER WITH COMPOSITE SIGNAL FEEDBACK

The following eqns. can be written for remote frequency auxiliary controller.

$$\dot{e}_1 = (-\frac{1}{T_{ID}})e_1 + (\frac{1}{T_{ID}})\Delta\omega_5 \tag{3.47}$$

$$\dot{z}_5 = [A_C]z_5 + [B_C]e_1 \tag{3.48}$$

$$\Delta v_F = [C_C]z_5 + [D_C]e_1 \tag{3.49}$$

The state and output equations are derived for this auxiliary controller as :

$$\dot{x}_C = A'_C x_C + B'_C u_C \tag{3.50}$$

$$y_C = C'_C x_C \tag{3.51}$$

where $x_C = [z_5 \quad e_1]'$, $y_C = \Delta v_F$, $u_C = \Delta\omega_5$

$$A'_C = \begin{bmatrix} A_C & B_C \\ 0 & (-\frac{1}{T_{ID}}) \end{bmatrix} \quad , \quad B'_C = \begin{bmatrix} 0 \\ (\frac{1}{T_{ID}}) \end{bmatrix}$$

$$C'_C = [C_C \quad D_C]$$

Matrices A_C , B_C , C_C and D_C have been defined in Appendix C , Sec . C 4.1

3.5.4 Composite Line Current and RF Auxiliary Controller

The auxiliary signal in this case comprises a combination of line current and remote frequency (RF) signals with the objective of utilizing the beneficial contribution of both towards the damping of different torsional modes.

The control scheme for composite controller is illustrated in block diagram form in Fig 3.11, where u_{C1} and u_{C2} correspond, respectively to the line current and RF control signals. Although, the auxiliary controller configurations are same for both the signals, they are referred as G(s) and G'(s) for line current and RF signals, respectively. The state and output equations of the two individual controllers, as derived in section 3.5.1, can be rewritten as

Line Current

$$\dot{x}_{C1} = A_C x_{C1} + B_C u_{C1} \tag{3.52}$$

$$y_{C1} = C_C x_{C1} + D_C u_{C1} \tag{3.53}$$

where $x_{C1} = [z_{51}]$, $u_{C1} = \Delta i_4$, $y_{C1} = \Delta v_{F1}$

Matrices A_C, B_C, C_C and D_C are defined in Sec. 3.3.1.

Remote Frequency (RF)

$$\dot{x}_{C2} = A_C x_{C2} + B_C u_{C2} \tag{3.54}$$

$$y_{C2} = C_C x_{C2} + D_C u_{C2} \tag{3.55}$$

where $x_{C2} = [z_{52}]$, $u_{C2} = \Delta\omega_5$, $y_{C2} = \Delta v_{F2}$

The state equation of the composite auxiliary controller is obtained by combining eqns.(3.52) and (3.54)

$$\dot{x}_C = A_C' x_C + B_C' u_C \tag{3.56}$$

where $x_C = [x_{C1} \quad x_{C2}]'$, $u_C = [u_{C1} \quad u_{C2}]'$

$$A_C' = \begin{bmatrix} A_C & 0 \\ 0 & A_C \end{bmatrix} , \quad B_C' = \begin{bmatrix} B_C & 0 \\ 0 & B_C \end{bmatrix}$$

The auxiliary controller output is given by

$$\Delta v_F = \Delta v_{F1} + \Delta v_{F2} \tag{3.57}$$

The output equation of composite auxiliary controller is then obtained by adding eqns . (3.53) and (3.55)

$$y_C = C_C' x_C + D_C' u_C \tag{3.58}$$

where $y_C = \Delta v_F$

$$C_C' = [C_C \quad C_C] , \quad D_C' = [D_C \quad D_C]$$

The modeling of composite line current and CIF signals is also derived in a similar manner.

3.6 Derivation of System Model (With SVC Auxiliary Controller)

The procedure given in Sec. 3.4 is utilized to combine the state and output equations of the series compensated network, SVC voltage controller and SVC auxiliary controller as developed in this chapter with those of the generator rotor circuit and mechanical system derived in Chapter 2, to result in the state equation of the overall system as

$$\dot{x} = Ax \tag{3.59}$$

where $x = [x_R \quad x_M \quad x_N \quad x_S \quad x_C]'$

The general auxiliary controller eqn.(3.36) is simply appended to the system matrix A defined by eqn.(3.30), to result in the modified system matrix.

3.7 Conclusions

In this chapter, the model for IEEE First Benchmark system together with an SVC placed at the midpoint of transmission line is developed. Further the models of SVC voltage controller and different auxiliary controllers viz. line current, computed internal frequency (CIF) and remote frequency (RF) signal are obtained. Models are also derived for composite auxiliary signals in the combination of line current and CIF, and line current and remote frequency.

Chapter 4

SYSTEM STUDIES

4.1 Introduction

This chapter presents eigenvalue results for IEEE First SSR Benchmark System with an SVC placed at the midpoint of transmission line. SVC is employed in the Benchmark system with the objective to damp torsional oscillations It is important to note that if an SVC is placed at the midpoint of transmission line, then it also serves the purpose of improving dynamic stability. Eigenvalue results are presented for all the four critical series compensation levels for Benchmark system, i.e. 35.6 %, 54.8 %, 73 % and 90.8 %, at which network is tuned to mode 4, mode 3, mode 2 and mode 1, respectively. System studies are done with SVC voltage controller alone and with different auxiliary stabilizing signals viz., line current, CIF, remote frequency signal and combination of line current with CIF and remote frequency signal, individually.

4.2 Case Study

The study system is the IEEE First SSR Benchmark System with an SVC placed at the midpoint of transmission line. The midpoint connected FC-TCR static var compensator is rated at 275 MVA leading to 25 MVA lagging. The operating value of generator power is taken to be 803 MW. The load flow data is given in Appendix D.

The modeling of synchronous generator and turbine generator mechanical system has already been described in Chapter 2, whereas the modeling of network, SVC voltage controller and auxiliary controllers is described in chapter 3. The data corresponding to generator, rotor spring mass parameters and SVC voltage controller including all control system delays is given in Appendix D. To represent the worst damping condition all self and mutual damping coefficients are assumed to be zero.

The objective of this case study is to examine the effectiveness of different auxiliary signals i.e. line current, CIF, remote frequency signal and combination of line current with CIF and remote frequency signal in damping torsional oscillation

modes. Eigenvalue analysis is employed to obtain the loci of critical system modes with varying controller parameters each taken one at a time, for each auxiliary controller. Based on these root loci, ranges are determined for the controller parameters (K_B , T_1 and T_2) which result in damping of all or most of the critical system modes. A suitable set of parameters lying in this range is then selected. The controller parameters which result in maximum damping of all or most of the critical system modes are chosen as optimal for the particular auxiliary controller .

System studies are done at all the four critical series compensation levels : 35.6 %, 54.8 %, 73 % and 90.8 % where torsional modes 4, 3, 2 and 1, respectively, are critically destabilized .

4.2.1 Selection of voltage controller parameters

For selecting voltage controller parameters K_I (integral gain) and K_p (proportional gain) the following technique is adopted. For selecting K_I , first the torsional system is removed from the rest of the system. The proportional gain K_p is set to zero and K_I is varied over a wide range. From eigenvalue results root loci is plotted for sensitive eigenvalues. The value of K_I for which the rotor mode is most stable and all other system modes are also reasonably stable is chosen as optimal value of K_I For selecting K_p , torsional system is incorporated and K_I is fixed at this optimal value. Then K_p is varied and corresponding root loci is plotted. The value of K_p at which the undamping of torsional modes is reduced is chosen as the optimal value of K_p. These values of K_p and K_I are utilized for all the system studies .

For IEEE First SSR Benchmark System with an SVC placed at the midpoint of transmission line, the optimal values of K_p and K_I are found to be +2.6 and +90.0 respectively.

4.2.2 Case 1 : Line Compensation = 35.6 % (Network tuned to mode 4)

To begin with, the effect of SVC with pure voltage control in damping the torsional modes, is examined. Table 4.1 lists the system eigenvalues without SVC and with an SVC having voltage controller alone. It is seen that voltage controller alone has very little effect on the stability of torsional oscillations.

Different auxiliary signals are now investigated in respect of their ability to stabilize the various torsional modes, these are :

(i) line current
(ii) CIF
(iii) Remote frequency (RF)
(iv) line current + CIF
(v) line current + RF

4.2.2.1 Line Current Auxiliary Controller

Eigenvalue analysis is performed to examine system stability as affected by the line current auxiliary controller parameters. Loci of eigenvalues sensitive to variation in K_B, T_1 and T_2, each taken at a time, are plotted in Figs 4.1, 4.2 and 4.3, respectively.

From Fig. 4.1, it is observed that for $-0.41 \leq K_B \leq -0.39$, all the torsional modes except mode 4 are successfully damped. As K_B is reduced from -0.41, the mode 4 tends towards stability, but the electrical mode tends towards instability. At $K_B = -0.42$ rotor mode becomes unstable whereas at $K_B = -0.46$ mode 4 becomes stable, but this results in a high degree of destabilization of electrical mode. To study the effect of parameters T_1 and T_2, a value of $K_B = -0.41$ is selected at which all other modes except mode 4 are stable.

The loci of critical eigenvalues as T_1 is varied is illustrated in Fig. 4 2. It is observed that for values of $0.096 \leq T_1 \leq 0.099$, all other modes except mode 4 are stable. As T_1 is increased from 0.099, mode 4 tends towards stability but electrical mode and rotor mode tends towards instability. At T_1=0.12, mode 4 becomes stable but rotor mode and electrical mode becomes unstable.

Fig. 4.3 shows the behavior of critical roots with variation in T_2. For $0.0207 \leq T_2 \leq 0.022$, all other modes except mode 4 are stable. As T_2 is increased from 0.015 to 0.022, rotor mode and electrical mode tend towards stability, whereas mode 4 towards instability. The eigenvalue results corresponding to line current controller parameters which result in reduced undampings of mode 4 are shown in Table 4.1.

From the above root loci, it is evident that line current controller is unable to damp all the system modes simultaneously at 35.6 % compensation.

4.2.2.2 CIF Auxiliary Controller

The variation of critical eigenvalues with variation in K_B for CIF auxiliary controller is exhibited in Fig. 4.4. It is observed that as K_B is increased from 0.0025 to 0.0085, rotor mode and SVC mode tend towards instability whereas mode 2, mode 3, mode 4 and electrical mode tends towards stability.

Fig. 4.5 shows the behavior of critical roots with variation in T_1. It is seen that as T_1 is increased from 0.0001 to 0.0015, the rotor mode, and SVC mode tend towards instability whereas mode 1, mode 2, mode 3, mode 4 and electrical mode tend towards stability.

Fig. 4.6 shows the behavior of critical roots with variation in T_2. It is seen that CIF could not stabilize modes 3, 4, SVC mode and rotor mode.System eigenvalues for a set of parameters chosen from the ranges described above are listed in Table 4.1.

4.2.2.3 Remote Frequency (RF) Auxiliary Controller

The variation of critical eigenvalues with K_B for RF auxiliary controller is

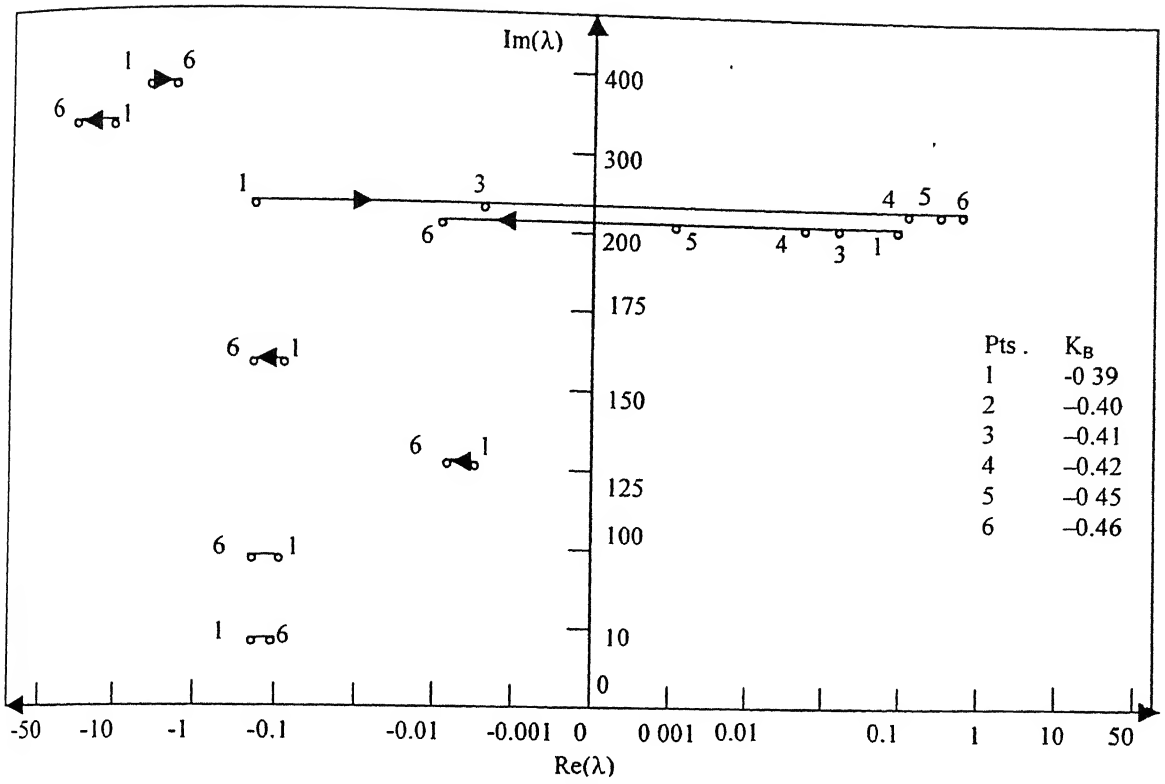

FIG 4.1 ROOT LOCI WITH VARIATION IN K_B FOR LINE CURRENT AUXILIARY CONTROLLER . LINE COMPENSATION = 35.6 % . T_1 = 0.099 Sec . , T_2 = 0.0207 Sec .

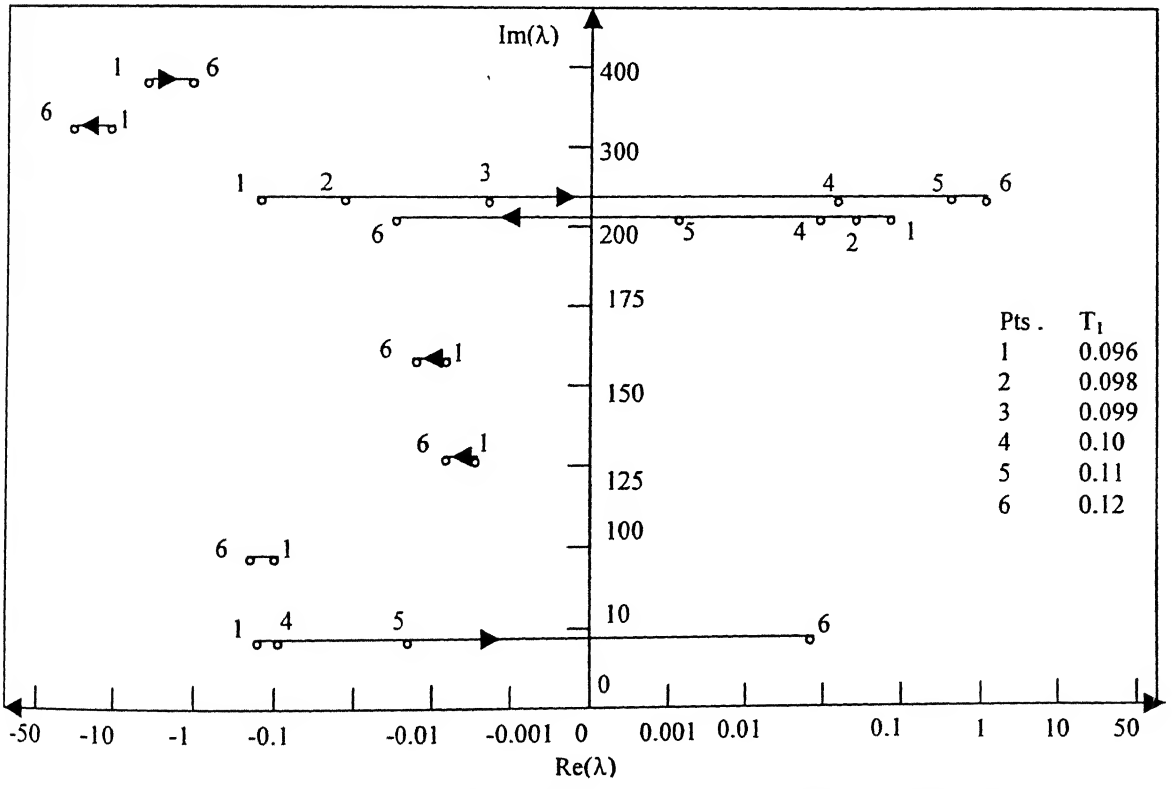

FIG 4.2 ROOT LOCI WITH VARIATION IN T_1 FOR LINE CURRENT AUXILIARY CONTROLLER . LINE COMPENSATION = 35.6 % . K_B = -0.41 , T_2 = 0.0207 Sec .

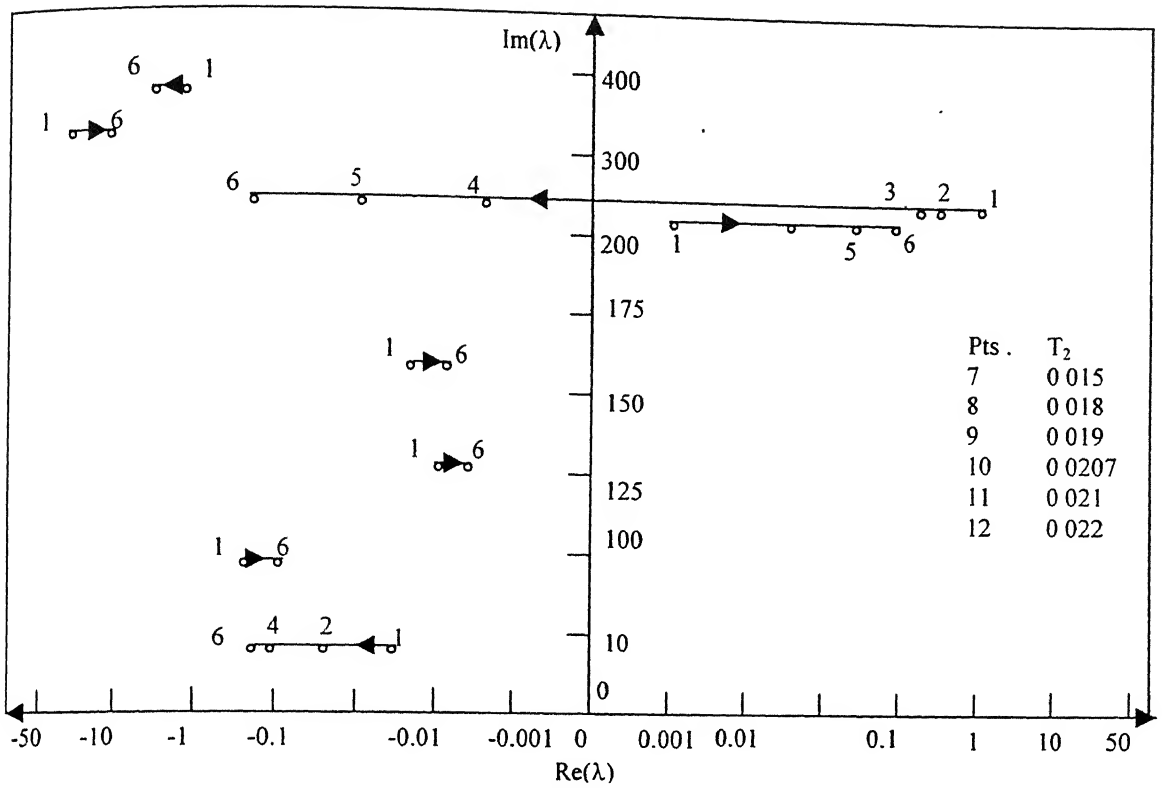

FIG . 4.3 ROOT LOCI WITH VARIATION IN T_2 FOR LINE CURRENT AUXILIARY CONTROLLER . LINE COMPENSATION = 35.6 % . K_B = -0.41 , T_1 = 0.099 Sec .

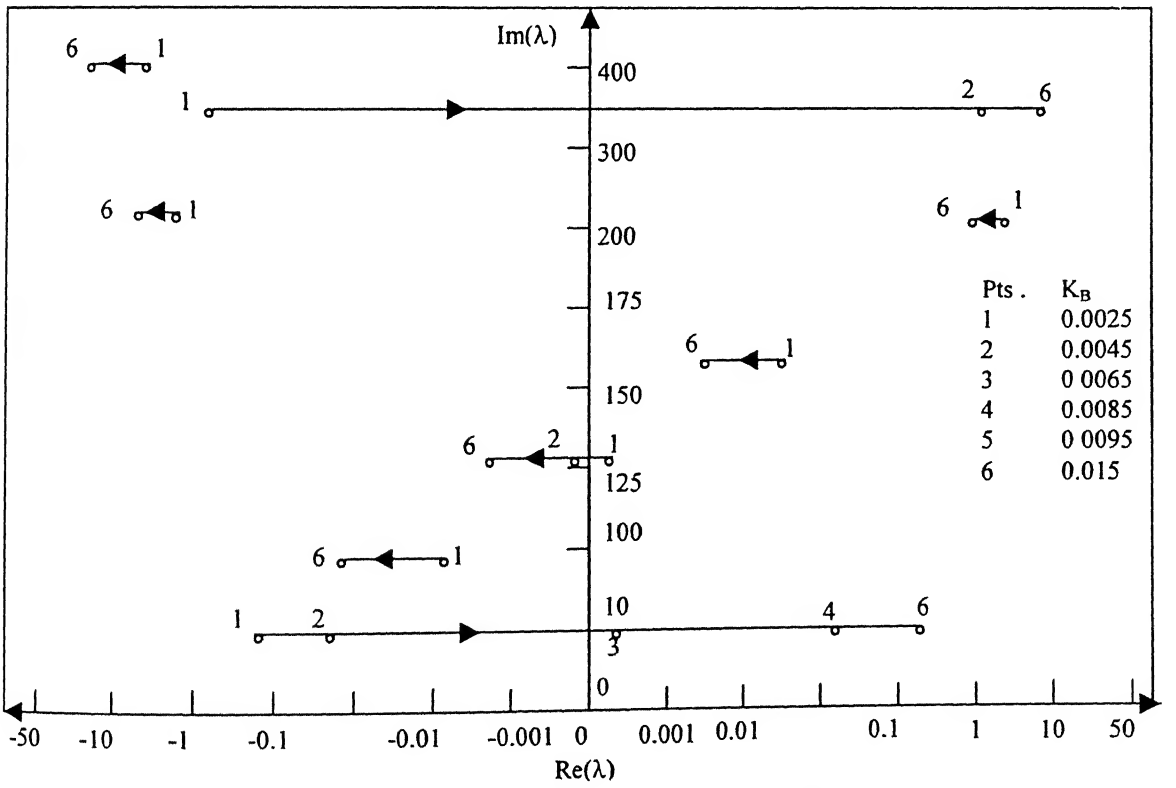

FIG . 4.4 ROOT LOCI WITH VARIATION IN K_B FOR CIF AUXILIARY CONTROLLER . LINE COMPENSATION = 35.6 % . T_1 = 0.0007 Sec . , T_2 = 0.018 Sec .

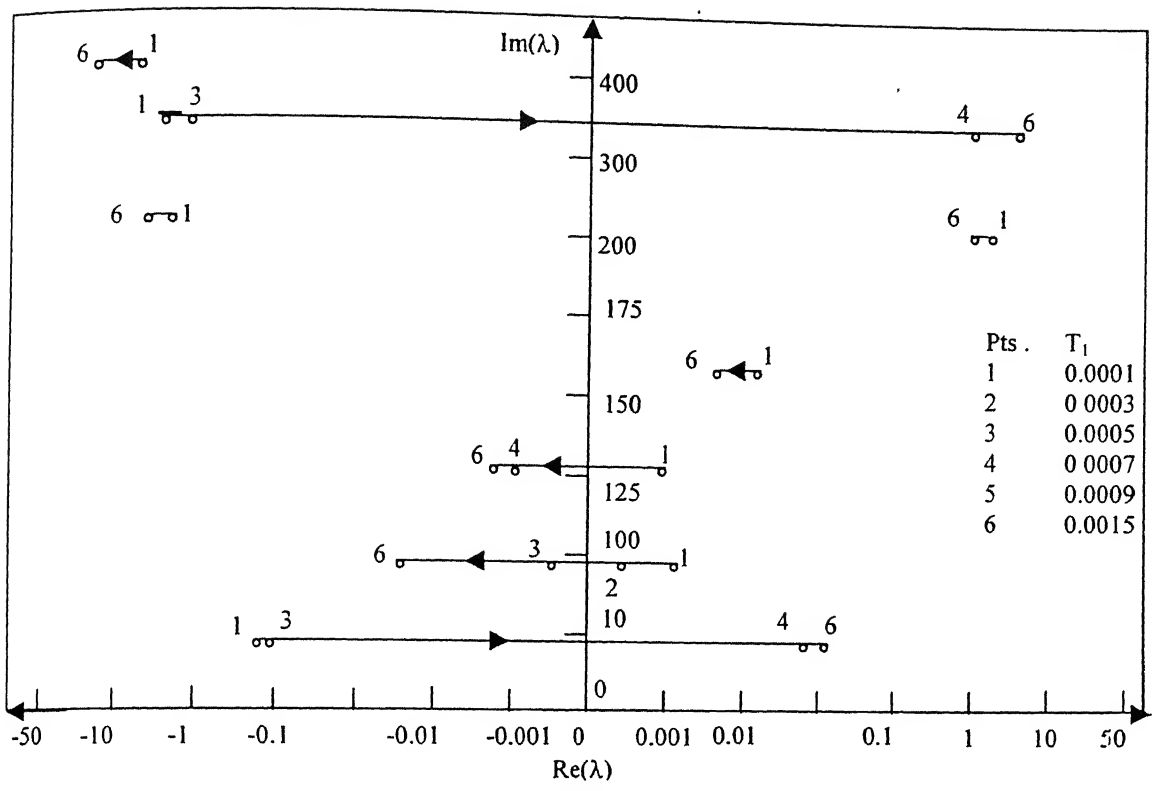

FIG . 4.5 ROOT LOCI WITH VARIATION IN T_1 FOR CIF AUXILIARY CONTROLLER . LINE COMPENSATION = 35.6 % . K_B = 0.0085 , T_2 = 0.018 Sec .

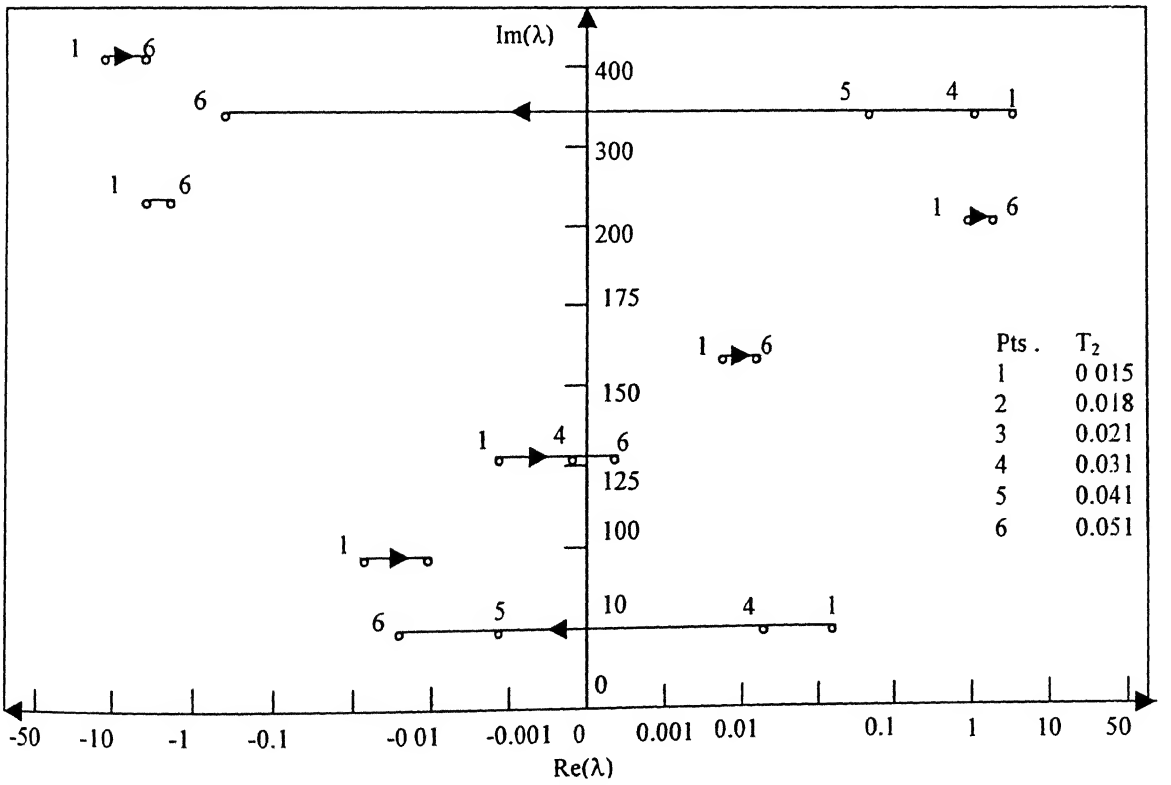

FIG . 4.6 ROOT LOCI WITH VARIATION IN T_2 FOR CIF AUXILIARY CONTROLLER . LINE COMPENSATION = 35.6 % . K_B = 0.0085 , T_1 = 0.0007 Sec .

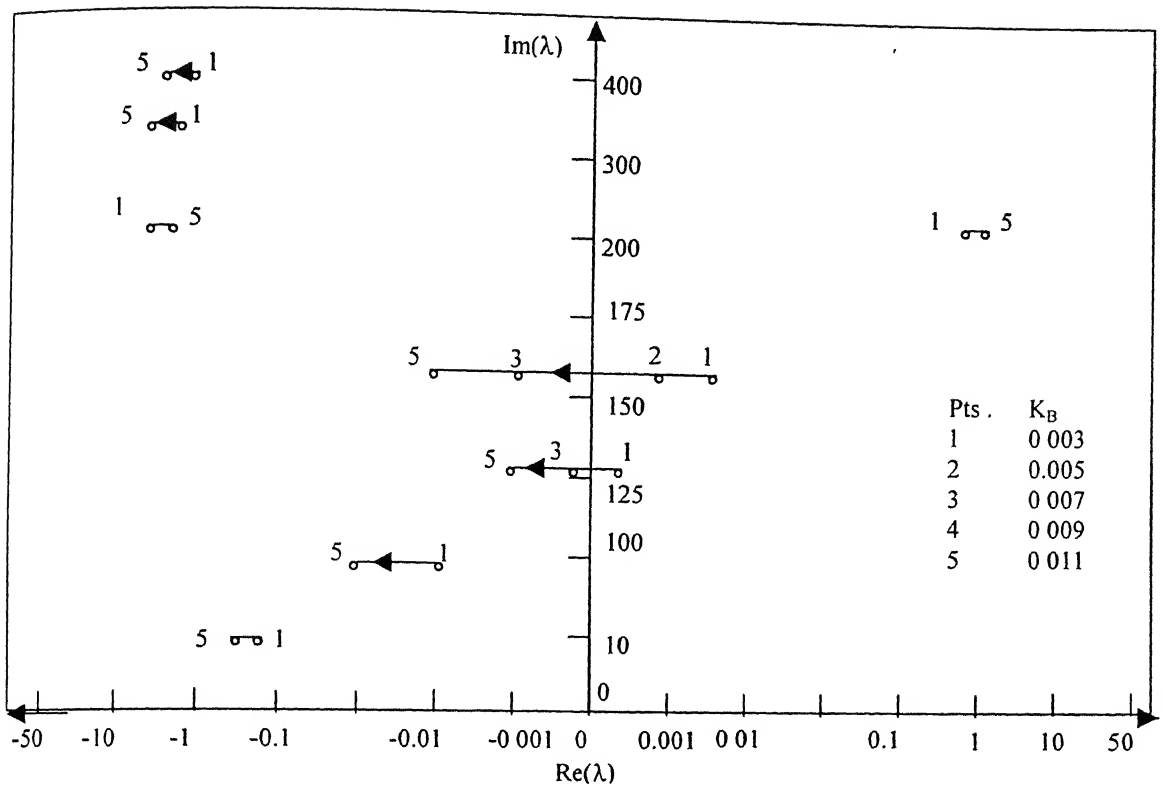

FIG . 4.7 ROOT LOCI WITH VARIATION IN K_B FOR RF AUXILIARY CONTROLLER . LINE COMPENSATION = 35.6 % . T_1 = 0.043 Sec . , T_2 =9.0 E - 6 Sec .

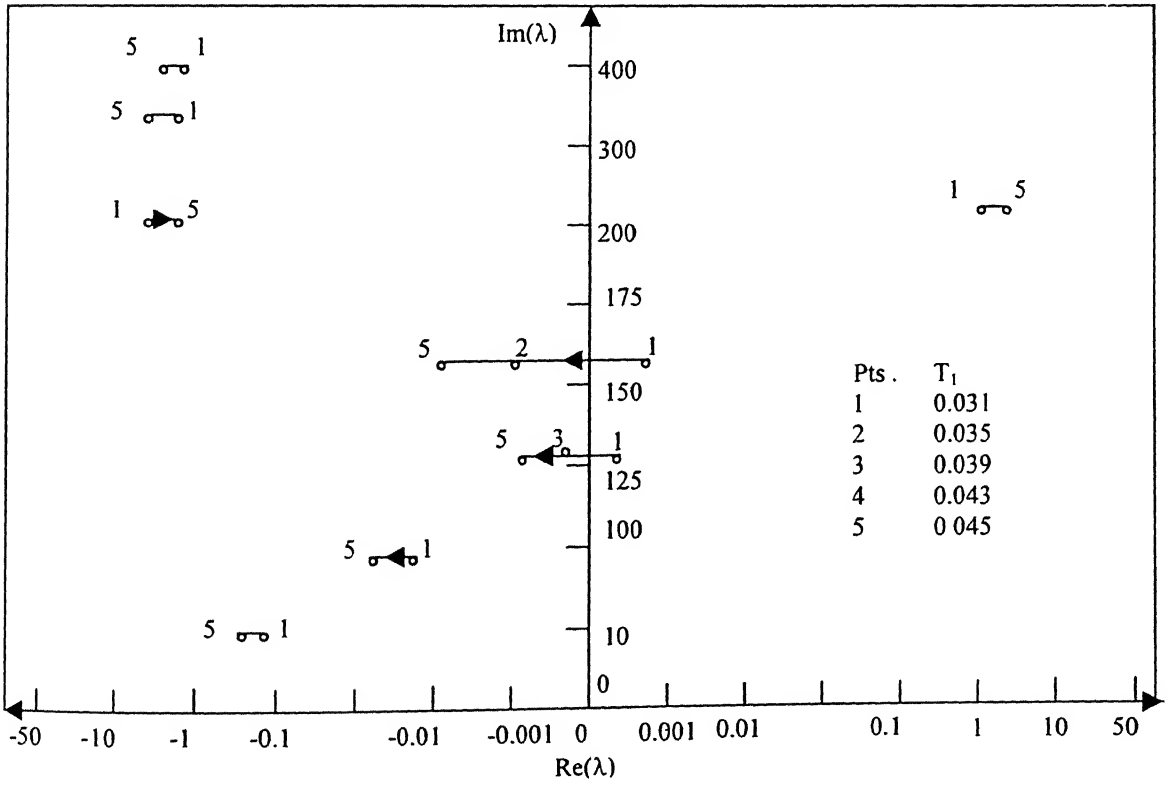

FIG . 4.8 ROOT LOCI WITH VARIATION IN T_1 FOR RF AUXILIARY CONTROLLER . LINE COMPENSATION = 35.6 % . K_B = 0.009 , T_2 = 9.0 E - 6 Sec .

shown in Fig. 4.7. It is observed that for $0.007 \leq K_B \leq 0.011$, all the torsional modes except mode 4 are successfully damped. As K_B is reduced from $K_B = 0.007$, modes 2 and 3 become unstable.

Fig. 4.8 shows the behavior of critical roots with variation in T_1. It is seen that all the modes except mode 4 are stable for $0.039 \leq T_1 \leq 0.045$.

Fig. 4.9 shows the behavior of critical roots with variation in T_2. It is seen that all the modes except mode 4 are stable for $9.0\,E\text{-}7 \leq T_2 \leq 9.0\,E\text{-}5$.
System eigenvalues for a set of parameters chosen from the ranges described above are listed in table 4.1.

For this signal, the telecom delay has been chosen to be 5.0 ms, and the same value has been utilized for all studies reported in this chapter.

4.2.2.4 Line Current + CIF Auxiliary Controller

A study of the eigenvalues given in Table 4.1 reveals that none of the auxiliary controller line current, CIF and RF alone can stabilize mode 4, if stability of all other modes are also to be ensured simultaneously. Therefore , the effect of composite line current and CIF signals is studied .

The variation of critical eigenvalues with K'_B for (LC +CIF) auxiliary controller is shown in Fig. 4.10. It is observed that for $0.0080 \leq K'_B \leq 0.0085$, all the torsional modes including mode 4 are successfully damped. As K'_B is reduced from $K'_B = 0.0080$, mode 4 becomes unstable. As K'_B is increased from $K'_B = 0.0085$, the rotor mode becomes unstable .

Fig. 4.11 shows the behavior of critical roots with variation in T'_1. It is seen that all the system modes are damped for $0.0006 \leq T'_1 \leq 0.0007$. As T'_1 is reduced from $T'_1 = 0.0006$, electrical mode becomes unstable, whereas if T'_1 is increased from 0.0007 electrical mode becomes unstable.

Similarly, from the root loci displayed in Fig. 4.12, it is seen that whole system is stable for $0.018 \leq T'_2 \leq 0.020$. As T'_2 is reduced from $T'_2 = 0.018$, rotor mode becomes unstable, whereas if T'_2 is increased from 0.020 electrical mode becomes unstable.

System eigenvalues for a set of parameters chosen from the ranges described above which ensure complete system stability are listed in Table 4.1.

4.2.2.5 Line Current + Remote Frequency (RF) Auxiliary Controller

The variation of critical eigenvalues with K'_B for (LC +RF) auxiliary controller is shown in Fig. 4.13. It is observed that for $0.014 \leq K'_B \leq 0.018$, all the torsional modes including mode 4 are successfully damped. As K'_B is reduced from $K'_B = 0.014$, mode 4 becomes unstable, however as K'_B is increased from $K'_B = 0.018$, electrical mode becomes unstable.

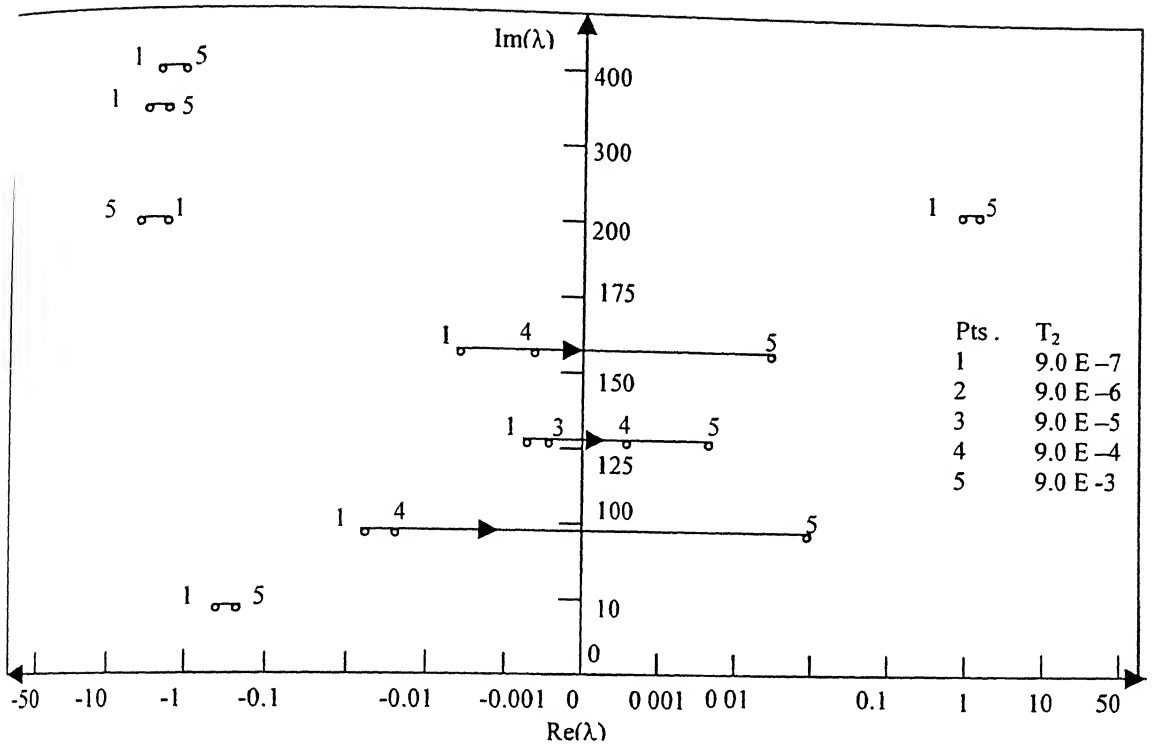

; 4.9 ROOT LOCI WITH VARIATION IN T_2 FOR RF AUXILIARY CONTROLLER. LINE COMPENSATION = 35.6 %. K_B = 0.009 , T_1 = 0.043 Sec

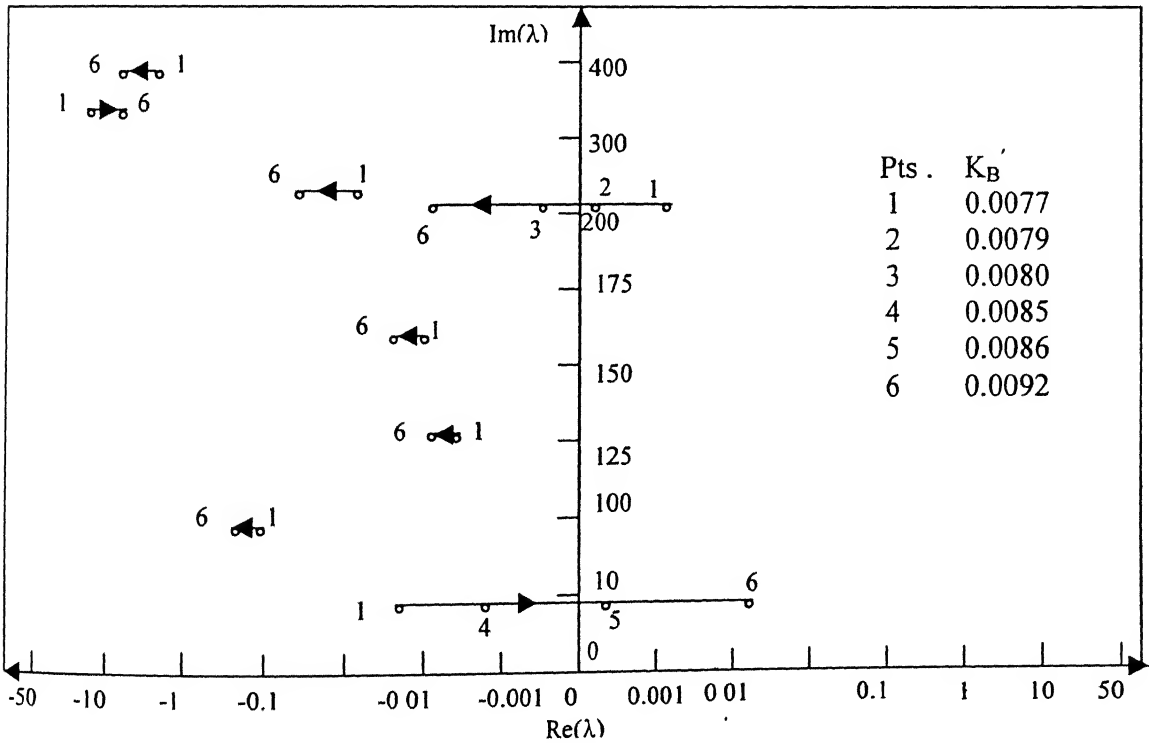

IG. 4.10 ROOT LOCI WITH VARIATION IN K_B' FOR COMPOSITE (LINE CURRENT + CIF) AUXILIARY CONTROLLER. LINE COMPENSATION = 35.6 %. T_1' = 0.0007 Sec. , T_2' = 0.018 Sec. K_B = -0.475 , T_1 =0.084 Sec. , T_2 =0.0245 Sec.

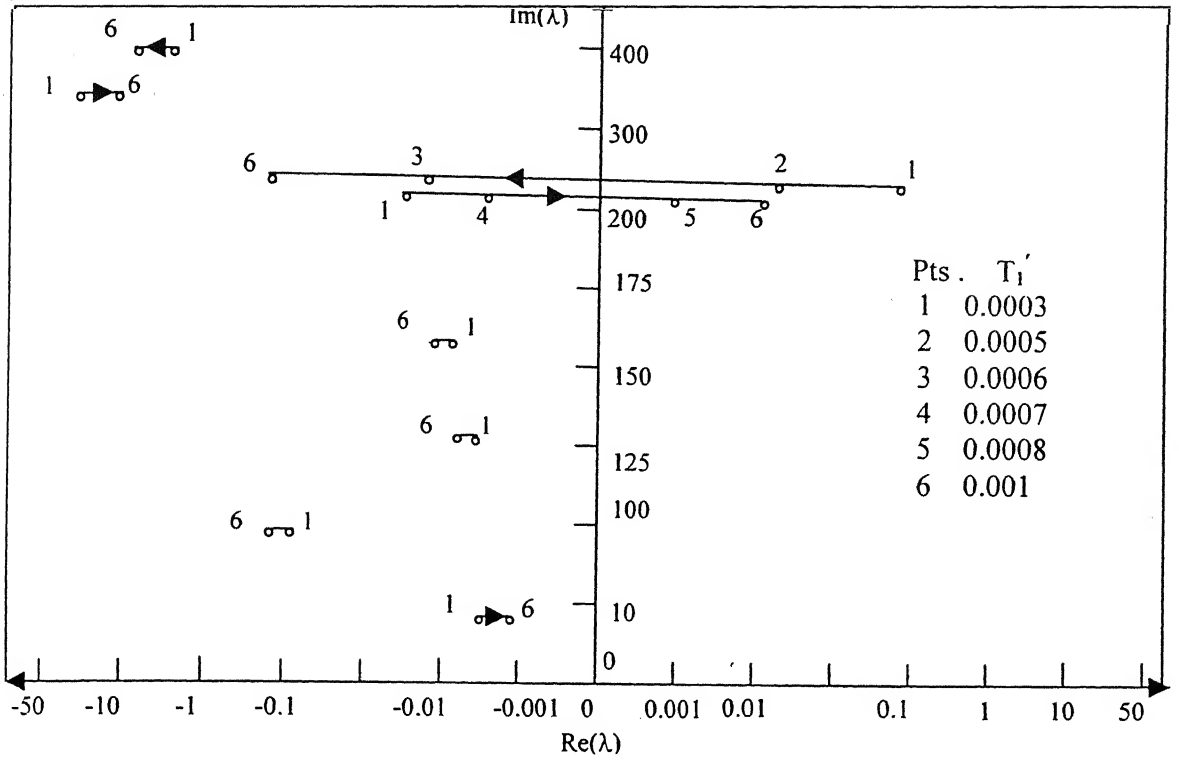

FIG . 4.11 ROOT LOCI WITH VARIATION IN T_1' FOR COMPOSITE (LINE CURRENT + CIF) AUXILIARY CONTROLLER .
LINE COMPENSATION = 35.6 % . K_B' = 0.0085 , T_1' = 0.018 Sec .
K_B = -0.475 , T_1 =0.084 Sec . , T_2 =0.0245 Sec .

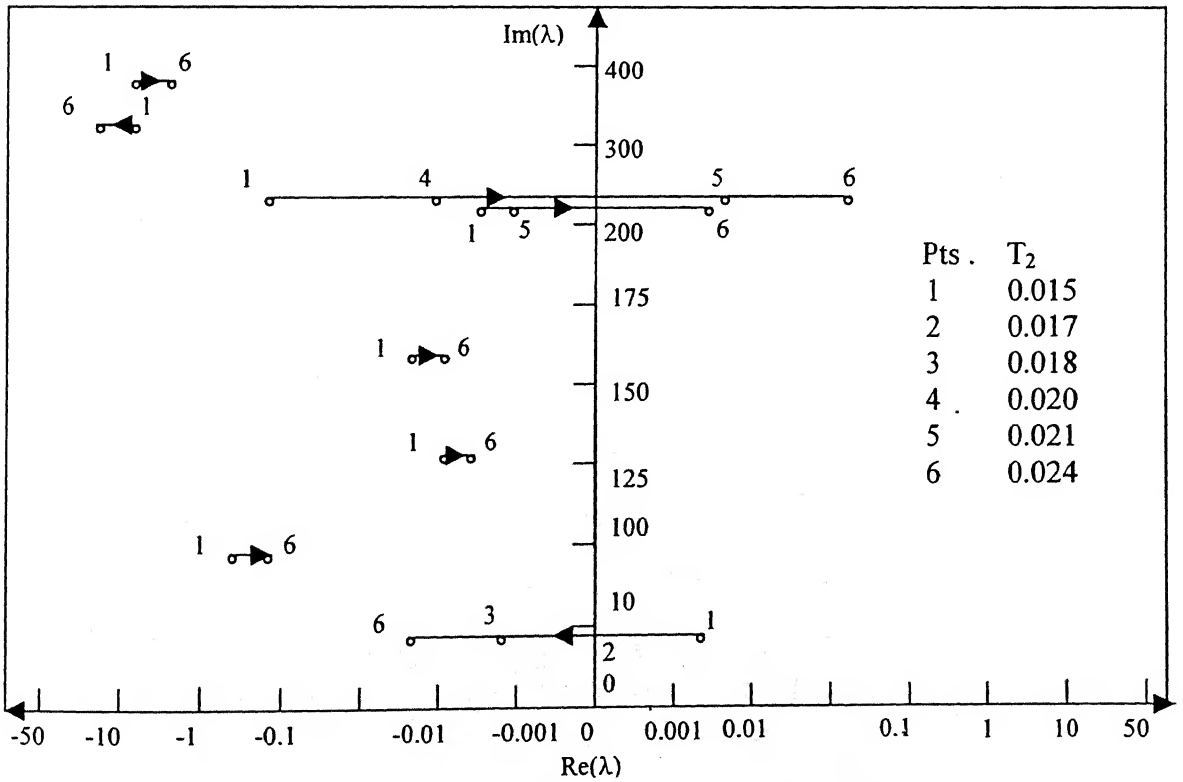

FIG . 4.12 ROOT LOCI WITH VARIATION IN T_2 FOR COMPOSITE (LINE CURRENT + CIF) AUXILIARY CONTROLLER .
LINE COMPENSATION = 35.6 % . K_B' = 0.0085 , T_1' = 0.0007 Sec .
K_B = -0.475 , T_1 =0.084 Sec . , T_2 =0.0245 Sec .

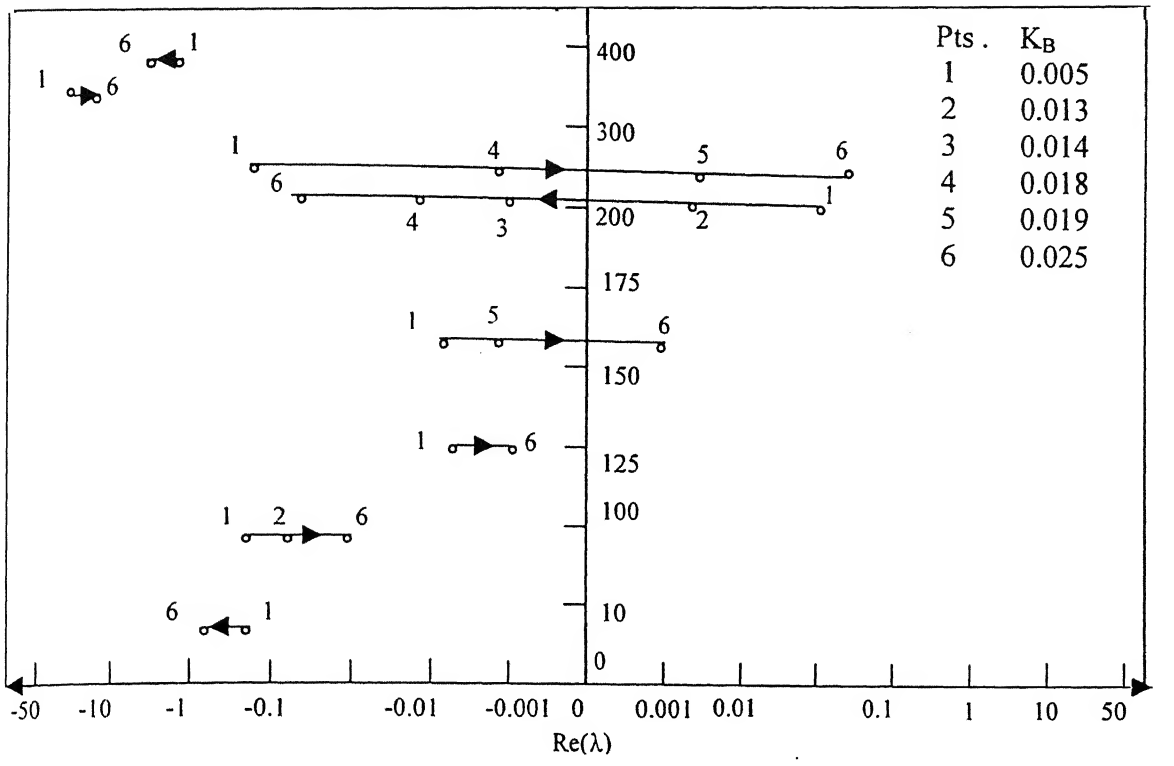

G . 4.13 ROOT LOCI WITH VARIATION IN K_B' FOR COMPOSITE (LINE CURRENT + RF) AUXILIARY CONTROLLER .
LINE COMPENSATION = 35.6 % . T_1' = 0.009 Sec . , T_2' = 0.007 Sec . , T_D =0.005 Sec .
K_B = -0.44 , T_1 =0.08 Sec . , T_2 =0.017 Sec .

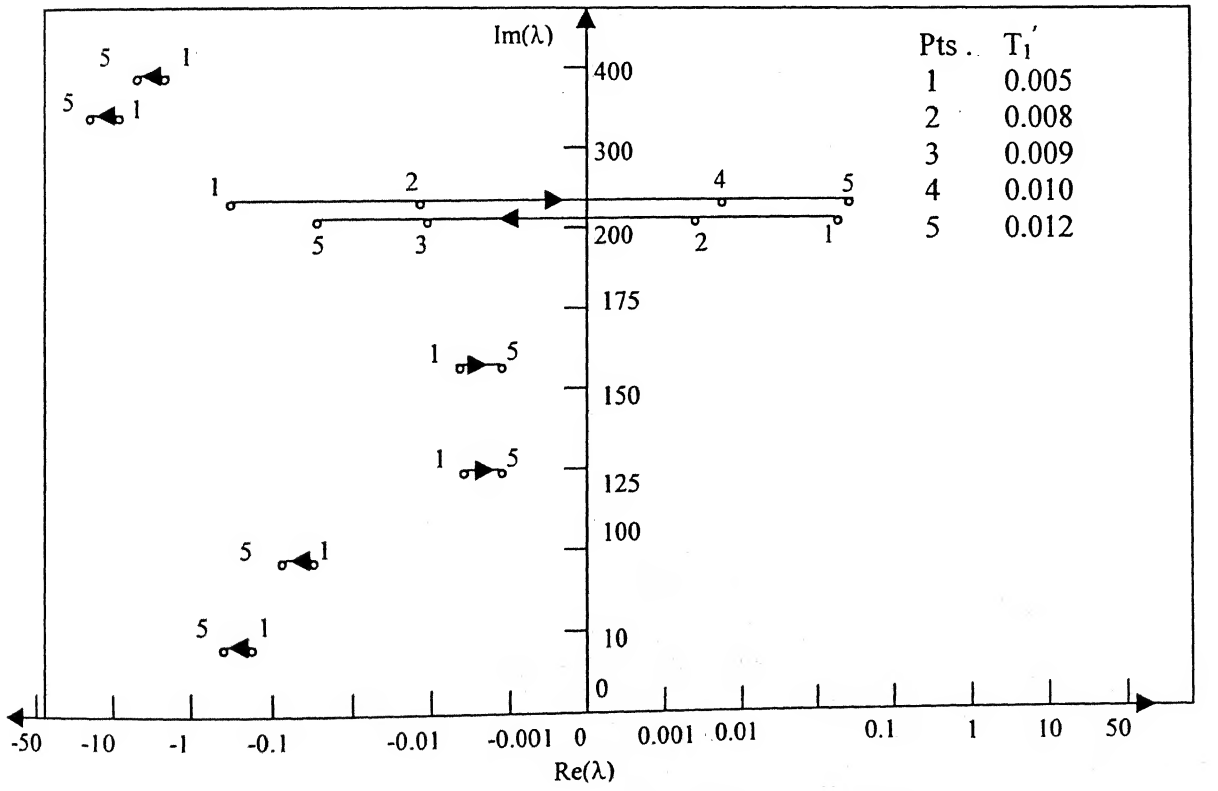

FIG . 4.14 ROOT LOCI WITH VARIATION IN T_1' FOR COMPOSITE (LINE CURRENT + RF) AUXILIARY CONTROLLER .
LINE COMPENSATION = 35.6 % . K_B' = 0.016 , T_2' = 0.007 Sec . , T_D = 0.005 Sec .
K_B = -0.44 , T_1 =0.08 Sec . , T_2 =0.017 Sec .

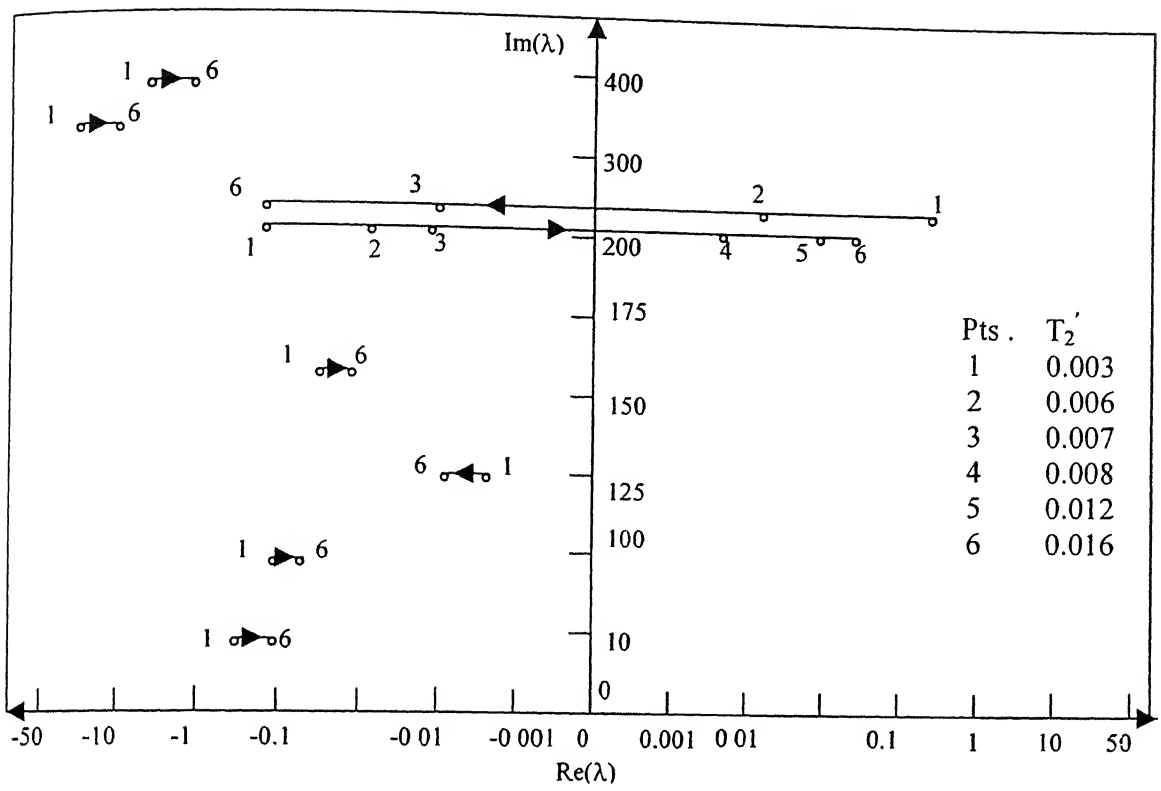

FIG . 4.15 ROOT LOCI WITH VARIATION IN T_2' FOR COMPOSITE (LINE CURRENT + RF) AUXILIARY CONTROLLER .
LINE COMPENSATION = 35.6 % . K_B' = 0.016 , T_1' = 0.009 Sec . , T_D =0.005 Sec . K_B = -0.44 , T_1 =0.08 Sec . , T_2 =0.017 Sec .

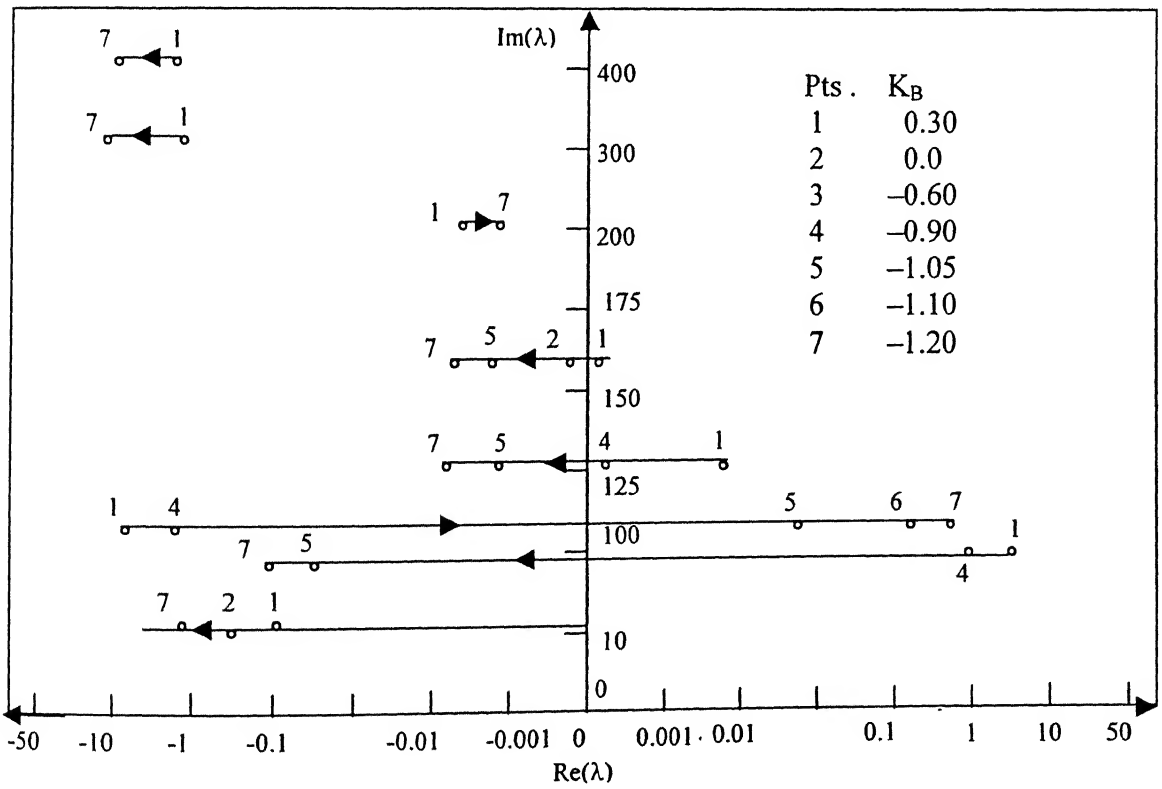

FIG . 4.16 ROOT LOCI WITH VARIATION IN K_B FOR LINE CURRENT AUXILIARY CONTROLLER . LINE COMPENSATION = 90.8 % . T_1 = 0.019 Sec . , T_2 = 0.017 Sec

TABLE 4.1

SYSTEM EIGENVALUES FOR SVC VOLTAGE CONTROLLER AND DIFFERENT AUXILIARY CONTROLLERS. LINE SERIES COMPENSATION = 35.6 %

Mode Identification	Without SVC	Voltage Controller	Line Current	CIF	RF	Line Current +CIF	Line Current +RF
Network		-5.6048 ± j 1942.0 -6.1032 ± j 1187.8 -4.076 ± j 395.42	-5.1215 ± j.1942.2 -4.7929 ± j 1188.1 -4.7433 ± j 386.25	-5.7632 ± j 1942 2 -6.5214 ± j 1187.9 -11.0477 ± j 405.2	-5.6033 ± j 1942.0 -6.1016 ± j 1187.8 -4.3780 ± j 395 3	-5.3508± j 1942.2 -5.1663 ± j 1187.9 -7.2587 ± j 393 40	-5 0955 ± j 1942.2 -4.7230 ± j 1188.1 -4.5467 ± j386.002
Mode 5	0.0± j 298.17	0.0± j298.17	0.0± j 298.1767	0.0 ± j 298.1767	0.0 ± j 298.1767	0.0± j 298.17	0 0± j 298.1767
Mode 4	+1.4279±j202.8	+1.4059 ± j 202.8	+0.0650 ± j 203.93	+1.2024 ± j 203 05	-4 9536 ± j 201 99	-0.0044 ± j 203 97	-0 0143 ± j 204 10
Mode 3	+0.0147± j160.7	+0.0145 ± j 160.7	-0.0112 ± j 160.74	+0.0085 ± j 160.74	-0.0066 ± j 160 78	-0.0134 ± j 160.75	-0.0037 ± j 160.75
Mode 2	+0.0012± j127.0	+0 0010 ± j 127.0	-0.0077 ± j 127.05	-0.0012 ± j 127.04	-0.0007 ± j 127 06	-0.0084 ± j 127.05	-0.0037 ± j 127.05
Mode 1	+0.0021± j99.40	+0.0018 ± j 99.36	-0.1383 ± j 99.39	-0.0349 ± j 99.37	-0.0397 ± j 99 51	-0.1604 ± j99 420	-0.0887 ± j 99.433
Mode 0	-0.3321± j10.41	-0.1947 ± j 10.35	-0.1077 ± j 8 82	+0.0615 ± j 10.15	-0.3788 ± j 10.39	-0.0023 ± j 8.4233	-0.4509 ± j 8 9686
Elect. Mode	-5.3254± j202.7	-5.3894 ± j 202.87	-0.0031 ± j 211.43	-5.9217 ± j 203.24	+1.4577 ± j 203.92	-0.0610 ± j 210.89	-0.0236 ± j 211.84
S . S . Mode	-4 7601± j551.0	-4.7702 ± j 551.04	-3.7880 ± j 552 45	-4.6147 ± j 550.90	-4.7398 ± j 551.03	-3.8315 ± j 552.15	-3.7642 ± j 552.53
Generator Rotor Circuits	-40.79 , -25.41 -3.08 , -0.1287 -0.0676	-40.72 , -25.31 -4.008 , -0.1527 -0.1089	-41.78 , -25.25 -3.57 , -0.1353 -0.0944	-40.73 , -25.05 -4.32 , -0 1530 -0 1090	-40.71 , -25.31 -4.0323 , -0.1524 -0.1088	-42.13 , -25.14 -3.7791 , -0.0898 -0.1333	-41.52 , -25.27 -3.5232 , -0.1340 -0.0918
SVC		-612.35 , -407.11 -176 28 , -17.548 -4.2278 ± j 359 67	-602.94 , -406.72 -124.69 , -92.32 -15.56 -19.7072 ± j 345.4	-612.98 , -407.14 -176.71 , -57 33 -16.58 + 4.6770 ± j 348.3	-612.55 , -407 13 -205.38 , -170.00 -17.43 , -1.1 E +5 -4.5893 ± j 359.79	-603 71 , -406.76 -136 82 , -75 91 -53.00 , -14.93 -15.8545 ± j 339.9	-602.23 ,-406.684 -198.48 ,-146.139 -15.7679 -112.6798 ± j 23.5 -20.2715 ± j 344.0
Optimum Auxiliary ControllerParameter		K_p = 0.26 K_I = 90.0	K_B = -0.41 T_1 = 0.099 T_2 = 0.0207	K_B = 0.0085 T_1 = 0.0007 T_2 = 0.018	K_B = 0.009 T_1 = 0.043 T_2 = 9 0 E - 6	LC CIF K_B=-0 475,K_B'=0 0085 T_1=0 084 , T_1'= 0 0007 T_2= 0 0245,T_2 = 0 018	LC RF K_B= -0.44 , K_B'= 0 016 T_1=0 08 , T_1'= 0 009 T_2= 0 017,T_2'= 0 007

Elect . Mode : Electrical Mode , S . S. Mode . Super-synchronous Mode
Time Constants T_1 and T_2 are expressed in seconds

TABLE 4.2

SYSTEM EIGENVALUES FOR SVC VOLTAGE CONTROLLER AND DIFFERENT AUXILIARY CONTROLLERS . LINE SERIES COMPENSATION = 54.8 %

Mode Identification	Without SVC	Voltage Controller	Line Current	Line Current + CIF	Line Current + RF
Network		-5.5908 ± j 1954.3570 -6.0733 ± j 1200.1624 -4.2433 ± j 408.1346	-5.1685 ± j1954.5289 -4.9472 ± j 1200.4020 -7.4363 ± j 399.5897	-5.1710 ± j 1954.4812 -5.0260 ± j 1200.4206 -6.8619 ± j 400.3675	-5.0758 ± j 1954.5707 -4.7011 ± j 1200 4721 -7.3813 ± j 397 8930
Mode 5 Mode 4 Mode 3 Mode 2 Mode 1 Mode 0	0.0± j298.1767 +0 0095 ± j 202.7796 +1.3816 ± j 160.6349 +0.0072 ± j 127 0920 +0.0190 ± j 99.6600 -0.3905 ± j 11.2879	0.0± j 298.1767 +0.0041 ± j 202.7733 +1.3335 ± j 160.6610 +0.0077 ± j 127.0897 +0.0206 ± j 99 6371 -0.2963 ± j 11.2686	0.0 ± j 298.1767 -0.0258 ± j 202.7375 +0 0205 ± j 161.2159 -0.0040 ± j 127.0775 -0.0969 ± j 99.6023 -0.2135 ± j 9.5596	0.0 ± j 298.1767 -0.0229 ± j 202.7407 +0.0226 ± j 161 2714 -0 0037 ± j 127.0784 -0.0908 ± j 99.6062 -0.3573 ± j 9 6169	0.0± j 298.1767 -0 0066 ± j 202 6712 -0.0016 ± j 161.1134 -0.0051 ± j 127.0764 -0 1055 ± j 99 5977 -0.4113 ± j 9 6193
Elect . Mode S . S . Mode	-4.9425 ± j 160.7794 -4 7973 ± j 592.9337	-5 0919 ± j 160.9631 -4.8100 ± j 592.9815	-0.0010 ± j 171.8962 -3.9065 ± j 594.0390	-0.0084 ± j 170 9428 -3.9689 ± j 593.9145	-0.0287 ± j 175.1326 -3.7580 ± j 594.2907
Generator Rotor Circuits	-40.9539 , -25.4264 -3.3957 , -0.1333 -0.0871	-40.9040 , -25 3689 -4.4001 , -0.1584 -0.1101	-25.2292 , -3.9482 -0.1399 , -0.0997 -46 1934 + j 2.9405	-44.5144 , -25 2532 -3.7998 , -0.1384 -0.0979	-42.2612 , -25 2823 -3 7473 , -0.1371 -0.0960
SVC		-612.3169 , -407.2558 -178.5174 , -14.0945 -4.4470 ± j 347.8371	-46.1934 - j 2.9405 -604.3054 , -406.9299 -153.3967 , -12.3537 -16.3542 ± j 336.7300	-606 0311 , -407 0991 -152.5634 , -60 5598 -50.4082 , -13.0364 -16.3322 ± j 338.1678	-602 2465 , -406.8379 -199.0747 , -168 4871 -138.8458 , -76.3018 -13.2787 -19 3098 ± j 332.9645
Optimum Auxiliary Controller Parameters		K_p = +0.26 K_I = +90.0	K_B = -0.41 T_1 = 0.127 T_2 = 0.0298	LC RF K_B = -0.445 , K_B' = -0 0001 T_1 = 0.094 , T_1' = 0 0099 T_2 = 0.027 , T_2' = 0 0165	LC RF K_B = -0.475 , K_B' = 0.005 T_1 = 0.09 , T_1' = 0.009 T_2 = 0.02 , T_2' = 0.006

Elect . Mode : Electrical Mode , S . S. Mode : Super-synchronous Mode

Time Constants T_1 and T_2 are expressed in seconds

TABLE 4.3

SYSTEM EIGENVALUES FOR SVC VOLTAGE CONTROLLER AND DIFFERENT AUXILIARY CONTROLLERS . LINE SERIES COMPENSATION = 73.0 %

Mode Identification	Without SVC	Voltage Controller	Line Current	Line Current + CIF	Line Current + RF
Network		-5.5765 ± j 1966.5351 -6.0440 ± j 1212.3519 -4.3584 ± j 420.4799	-5.1269 ± j1966.7110 -4.8622 ± j 1212.6149 -8.6695 ± j 411.8048	-4.3659 ± j 1965.7231 -4.6678 ± j 1214.2987 -1.1838 ± j 400.9834	-5.1398 ± j 1966.7057 -4.8961 ± j 1212.6062 -8.6031 ± j 412.0649
Mode 5	0.0 ± j 298.1767	0.0± j 298.1767	0.0± j 298.1767	0.0 ± j 298.1767	0.0± j 298.1767
Mode 4	-0.0002 ± j 202.8626	–0.0044 ± j 202.8622	-0.0108 ± j 202.8794	-0.0194 ± j 202.8325	-0.0003 ± j 202.8583
Mode 3	+0.0149 ± j 160.3997	+0.0131 ± j 160.3981	-0.0359 ± j 160.2421	-0.0210 ± j 160.2776	-0.0105 ± j 160.2278
Mode 2	+0.6715 ± j 127.0063	+0.6147 ± j 127.0421	+0.0047 ± j 127.1609	+0.0024 ± j 127.2987	-0.0007 ± j 127.1717
Mode 1	+0.1248 ± j 100.3818	+0.1421 ± j 100.3561	-0.0430 ± j 99.8922	-0.0419 ± j 100.1114	-0.0584 ± j 99.9195
Mode 0	-0.4799 ± j 12.3397	-0.4207 ± j 12.3589	-0.4033 ± j 10.5283	-0.8406 ± j 11.2124	-0.7264 ± j 10.4729
Elect . Mode	-3.8999 ± j 126.9643	-4.2361 ± j 127.2406	-0.0109 ± j 144.3823	-0.0025 ± j 137.1270	-0.0267 ± j 143.7184
S . S . Mode	-4.8233 ± j 626.2365	-4.8383 ± j 626.3200	-3.8878 ± j 627.3364	-4.2392 ± j 627.1768	-3.9117 ± j 627.3052
Generator Rotor Circuits	-41.1552 , -25.4457 -3.7929 ,-0.1429 -0.1016	-41.1177 , -25.4113 -4.9355 ,-0.1635 -0.1108	-25.2159 , -4.2789 -0.1432 , -0.1019 -42.5148 + j 5.8624	-43.2679 , -25.3797 -3.8116 , -0.1442 -0.1027	-25.2555 , -3.7907 -0.1372 , -0.0950 -43.0728 + j 5.3642
SVC		-612.2737 , -407.3800 -180.4202 , -10.8831 -4.6933 ± j 336.2759	-42.5148 - j 5.8624 -603.7014 , -407.0382 -158.7284 , -110.0356 -17.2343 ± j 323.7314	-608.4864 , -407.2286 -181.4170 , -94.2175 -53.5790 , -11.5823 -19.7914 ± j 347.4773	-43.0728 - j 5.3642 -603.9595 , -407.0485 -159.3692 , -10.8906 -200.1020 ± j 3.5441 -16.7851 ± j 324.2228
Optimum Auxiliary Controller Parameters		K_p = +0.26 K_I = +90.0	K_B = -0.45 T_1 = 0.127 T_2 = 0.03	LC CIF K_B= -0.423 ,K_B' = -0.0084 T_1 = 0.07 , T_1' = 0.0015 T_2 = 0.0213 , T_2' = 0.009	LC RF K_B= -0.582 , K_B' = 0.0033 T_1 = 0.089 , T_1' = 0.007 T_2 = 0.028 , T_2' = 0.005

Elect . Mode : Electrical Mode , S . S. Mode : Super-synchronous Mode

Time Constants T_1 and T_2 are expressed in seconds .

Fig. 4.14 shows the behavior of critical roots with variation in T'_1. It is seen that all the system modes are damped only for $T'_1 = 0.009$. As T'_1 is reduced from $T'_1 = 0.009$, mode 4 becomes unstable, whereas if T'_1 is increased from 0.009 electrical mode becomes unstable.

Similarly, from the root loci displayed in Fig. 4.15, it is seen that whole system is stable only for $T'_2 = 0.007$. As T'_2 is reduced from $T'_2 = 0.007$, electrical mode becomes unstable, whereas if T'_2 is increased from 0.007 mode 4 becomes unstable. System eigenvalues for a set of parameters chosen from the ranges described above are listed in Table 4.1.

4.2.3 Case 2 : Line Compensation = 54.8 % (Network tuned to mode 3)

Root loci studies were conducted for all signals as described in the previous section, and the best controllers were obtained.

Eigenvalue results with these different auxiliary controllers are presented in Table 4.2.

4.2.4 Case 3 : Line Compensation = 73.0 % (Network tuned to mode 2)

Eigenvalue results with different optimized auxiliary controllers are presented in Table 4.3.

4.2.5 Case 4 : Line Compensation = 90.8 % (Network tuned to mode 1)

The variation of critical eigenvalues with K_B for line current auxiliary controller is shown in Fig. 4.16. It is observed that for $-1.20 \leq K_B \leq -1.05$, all the system modes except electrical mode are successfully damped. As K_B is increased from $K_B = -1.05$, electrical mode becomes stable but mode 1 and mode 2 becomes unstable.

Fig. 4.17 shows the behavior of critical roots with variation in T_1. It is seen that all the modes except mode 1 are stable for $0.019 \leq T_1 \leq 0.021$ whereas for $0.016 \leq T_1 \leq 0.018$ all other modes except electrical mode are damped. .

Fig. 4.18 shows the behavior of critical roots with variation in T_2. It is seen that for $0.0172 \leq T_2 \leq .0.0174$ all the system modes are stable.

Thus , we see that at critical compensation level of 90.8 % , line current auxiliary controller alone is able to damp all the system modes .

Eigenvalue results with line current auxiliary controller are presented in Table 4.4 .

To sum up, the system eigenvalues for the stabilizing composite (LC + RF) auxiliary controller for different critical levels of series compensation are presented in Table 4.5.

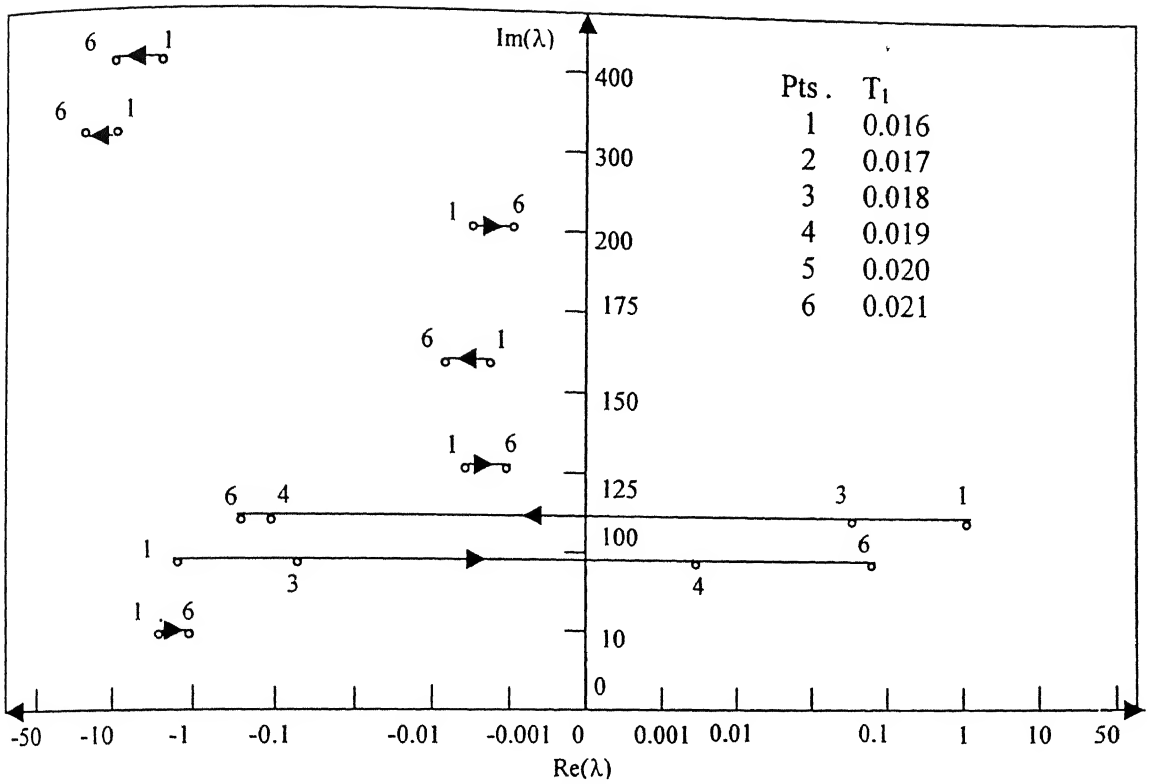

FIG . 4.17 ROOT LOCI WITH VARIATION IN T_1 FOR LINE CURRENT AUXILIARY CONTROLLER . LINE COMPENSATION = 90.8 % . K_B = -1.05 , T_2 = 0.017 Sec .

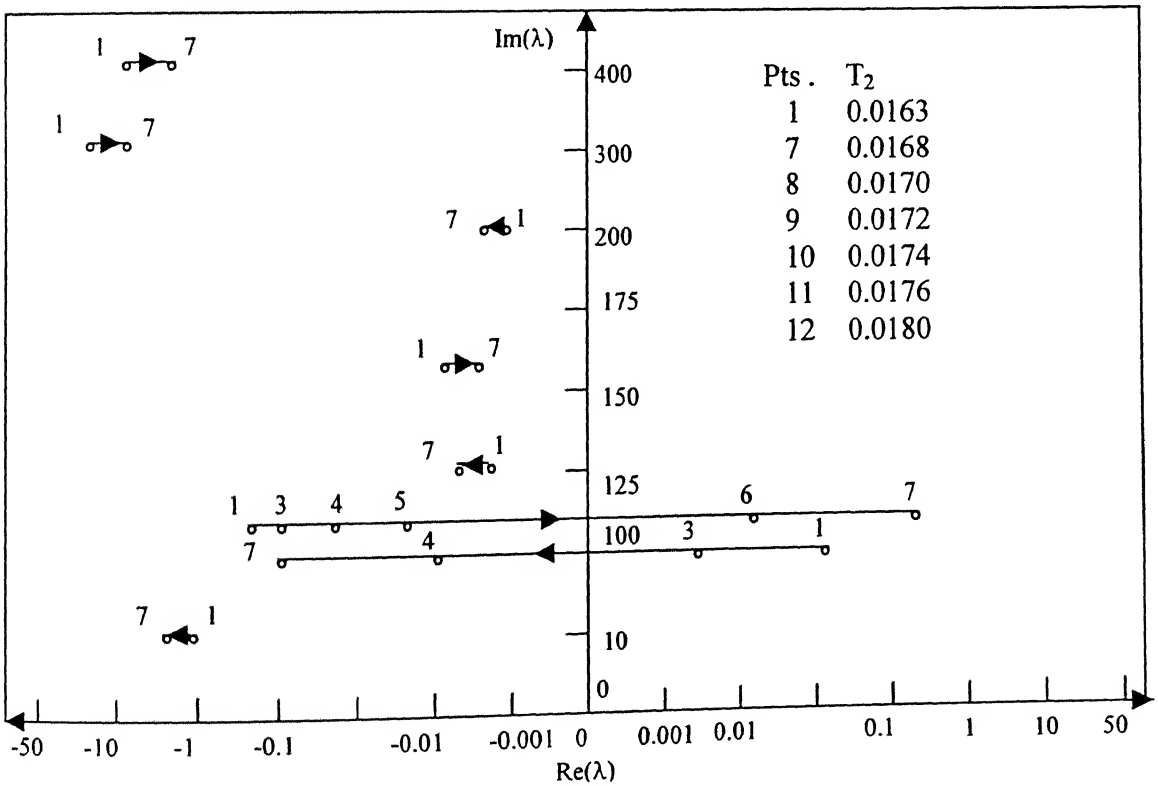

FIG . 4.18 ROOT LOCI WITH VARIATION IN T_2 FOR LINE CURRENT AUXILIARY CONTROLLER . LINE COMPENSATION = 90.8 % . K_B = -1.05 , T_1 = 0.019 Sec .

TABLE 4.4

SYSTEM EIGENVALUES FOR SVC VOLTAGE CONTROLLER AND LINE CURRENT AUXILIARY CONTROLLER .LINE SERIES COMPENSATION = 90.8 %

Mode Identification	Without SVC	Voltage Controller	Line Current
Network		-5.5585 ± j 1980.3259 -6.0100 ± j 1226.1544 -4.4370 ± j 434.1739	-5.2945 ± j 1980.4234 -5.3232 ± j 1226.2960 -7.7367 ± j 429.5042
Mode 5 Mode 4 Mode 3 Mode 2 Mode 1 Mode 0	0.0 ± j 298.1767 -0.0002 ± j 202.8626 +0.0010 ± j 160.4985 +0.0064 ± j 126.9361 +4.8860 ± j 99.2286 -0.6222 ± j 13.7131	0.0± j 298.1767 –0.0058 ± j 202.9012 –0.0008 ± j 160.5022 +0.0073 ± j 126.9368 +4.6077 ± j 99.3452 -0.5776 ± j 13.7705	0.0± j 298.1767 -0.0022 ± j 202.9172 -0.0059 ± j 160.5003 -0 0035 ± j 126.8890 -0.0341 ± j 102.5796 -1.7716 ± j 11.7127
Elect . Mode S . S . Mode	-7.3889 ± j 99.2066 -4.8436 ± j 654.9739	-7.7771 ± j 99.4540 -4.8616 ± j 655.1249	-0.0234 ± j 108.5859 -4.2767 ± j 655.6576
Generator Rotor Circuits	-41.4114 , -25.4733 -4.3401 , -0.1599 -0.1100	-41.3855 , -25.4550 -6.1279 , -0.1678 -0.1112	-40.9137 , -25.5840 -2.3993 , -0.1277 -0.0578
SVC		-612.2080 , -407.5084 -182.0978 , -7.2661 -4.9725 ± j 323.3045	-607.3270 ,-407.3222 -172.8613 ,-57.4574 -11.9191 -12.0288 ± j 316.2570
Optimum Auxiliary Controller Parameters		K_p = +0.26 K_I = +90.0	K_B = -1.05 T_1 = 0.019 T_2 = 0.0174

Elect . Mode : Electrical Mode , S . S. Mode : Super-synchronous Mode

Time Constants T_1 and T_2 are expressed in seconds .

TABLE 4.5

SYSTEM EIGENVALUES FOR THE STABILIZING COMPOSITE (LC+RF) AUXILIARY CONTROLLERS FOR DIFFERENT CRITICAL LEVELS OF SERIES COMPENSATION

Mode Identification	% compensation =35.6	% compensation =54.8	% compensation =73.0	% compensation =90.8
Network	-5.0955 ± j 1942.2912 -4.7230 ± j 1188.1626 -4.5467 ± j386.0024	-5.0758 ± j 1954.5707 -4.7011 ± j 1200.4721 -7.3813 ± j 397.8930	-5.1398 ± j 1966.7057 -4.8961 ± j 1212.6062 -8.6031 ± j 412.0649	-5.2945 ± j 1980.4234 -5.3232 ± j 1226.2960 -7.7367 ± j 429.5042
Mode 5 Mode 4 Mode 3 Mode 2 Mode 1 Mode 0	0.0± j 298.1767 -0.0143 ± j 204.1061 -0.0037 ± j 160.7555 -0.0037 ± j 127.0526 -0.0887 ± j 99.4330 -0.4509 ± j 8.9686	0.0± j 298.1767 -0.0066 ± j 202.6712 -0.0016 ± j 161.1134 -0.0051 ± j 127.0764 -0.1055 ± j 99.5977 -0.4113 ± j 9.6193	0.0± j 298.1767 -0.0003 ± j 202.8583 -0.0105 ± j 160.2278 -0.0007 ± j 127.1717 -0.0584 ± j 99.9195 -0.7264 ± j 10.4729	0.0± j 298 1767 -0.0022 ± j 202.9172 -0.0059 ± j 160.5003 -0.0035 ± j 126.8890 -0.0341 ± j 102.5796 -1.7716 ± j 11.7127
Elect . Mode S . S . Mode	-0.0236 ± j 211.8459 -3.7642 ± j 552.5340	-0.0287 ± j 175.1326 -3.7580 ± j 594.2907	-0.0267 ± j 143.7184 -3.9117 ± j 627.3052	-0.0234 ± j 108.5859 -4.2767 ± j 655.6576
Generator Rotor Circuits	-41.5220 , -25.2711 -3.5232 , -0.1340 -0.0918	-42.2612 , -25.2823 -3.7473 , -0.1371 -0.0960	-25.2555 , -3.7907 -0.1372 , -0.0950 -43.0728 + j 5.3642	-40.9137 , -25.5840 -2.3993 , -0.1277 -0.0578
SVC	-602.2328 ,-406.6841 -198.4830 ,-146.1392 -15.7679 -112.6798 ± j 23.5379 -20.2715 ± j 344.0237	-602.2465 , -406.8379 -199.0747 , -168.4871 -138.8458 , -76.3018 -13.2787 -19.3098 ± j 332.9645	-43.0728 -j 5.3642 -603.9595 , -407.0485 -159.3692 , -10.8906 -200.1020 ± j 3.5441 -16.7851 ± j 324.2228	-607.3270 ,-407.3222 -172.8613 ,-57.4574 -11.9191 -12.0288 ± j 316.2570
Optimum Auxiliary Controller Parameters	LC RF K_B = -0.44 , K_B' = 0.016 T_1 = 0.08 , T_1' = 0.009 T_2 = 0.017 , T_2' = 0.007	LC RF K_B = -0.475 , K_B' = 0.005 T_1 = 0.09 , T_1' = 0.009 T_2 = 0.02 , T_2' = 0.006	LC RF K_B = -0.582 , K_B' = 0.0033 T_1 = 0.089 , T_1' = 0.007 T_2 = 0.028 , T_2' = 0.005	LC K_B = -1.05 T_1 = 0.019 T_2 = 0.0174

Elect . Mode : Electrical Mode , S . S. Mode : Super-synchronous Mode

Time Constants T_1 and T_2 are expressed in seconds .

4.3 Discussions

Mode 4 stabilization

- From eigenvalue results presented in Table 4.1, for series compensation level of 35.6 % when mode 4 is critically destabilized, we see that SVC voltage controller alone has very little effect on the stability of torsional modes. This necessitates the need of auxiliary controller in addition to voltage controller. Therefore different auxiliary signals such as line current (LC), CIF, remote frequency (RF) and combination of line current with CIF and remote frequency are considered. It is observed that line current alone is unable to damp mode 4 , and CIF alone is unable to damp modes 3, 4, rotor mode and SVC mode while maintaining stability of all other modes. Remote frequency signal alone can not stabilize the electrical mode but enhances the stability of mode 4. Since none of the auxiliary signals alone are able to stabilize all the system modes, a need is felt to study the composite effect of two auxiliary signals. Hence the influence of (LC + CIF) and (LC +RF) composite auxiliary controllers is examined. It is found that both (LC + CIF) and (LC + RF) auxiliary controllers are able to stabilize the system. However, with (LC + CIF) auxiliary controller the stability of mode 4 and rotor mode are lower in comparison to those ensured by (LC + RF) auxiliary controller.

  Hence (LC + RF) auxiliary controller is better than (LC + CIF) auxiliary controller .

Stabilization of mode 3 and mode 2

- From eigenvalue results presented in Tables 4.2 and 4.3, for critical series compensation levels of 54.8 % and 73 % respectively, it is observed that line current alone is unable to stabilize the critically tuned mode while stabilizing the rest of the system modes.. It is seen that (LC + CIF) combination is unable to stabilize the critically tuned mode at 54.8 % and 73 %, even though it could stabilize the system at 35.6 % . However, the (LC + RF) composite signal is able to stabilize all the system modes at 54.8 % and 73 % series compensation.

Stabilization of mode 4

- From eigenvalue results presented in Table 4.4, for critical series compensation level of 90.8 % when mode 1 is critically destabilized, it is seen that line current auxiliary controller alone is able to stabilize the system.

  As torsional oscillations are invariably caused by the interaction between the transmission line current and the turbine – generator mechanical

system, it can be expected that the line current signal will contain information regarding the torsional oscillations and hence constitutes a useful control signal.

- From the eigen value results presented in Table 4.5, we see that over whole range of series compensation level, line current signal needs lead compensation ($T_1 > T_2$) with negative gain constant (K_B). With increase in series compensation level, magnitude of gain increases and the phase lead (ratio of T_1 / T_2) decreases.

- CIF signal needs lag compensation ($T_1 > T_2$) for all cases, however gain constant is positive for mode 4 but negative with modes 3 and 2.

  Remote frequency (RF) signal needs lead compensation with positive gain constant. With increase in series compensation level, magnitude of gain decreases, whereas ratio of (T_1 / T_2) increases.

4.4 CONCLUSIONS

Eigenvalue analysis is conducted for the IEEE First SSR Benchmark System with an SVC placed at the midpoint of transmission line. The efficacy of various individual and composite signals is investigated at all the four critical levels of series compensation. The following conclusions are made:

- Line current signal can damp all modes only at very high series compensation level of 90.8 %.

- The performance of remote frequency signal is better than CIF when considered in combination with line current.

- A combination of line current and remote frequency auxiliary controller is able to stabilize all the system modes for all the critical series compensation levels. Similar results were not obtained with combination of line current and CIF.

- Both the remote frequency and line current signals require phase lead controllers.

Chapter 5

STUDY OF TELECOM DELAYS AND LOCATION OF SVC ON SSR MITIGATION

5.1 Introduction

In the previous chapter, it has been studied that a combination of line current and remote frequency signal is able to damp all the torsional modes at all critical series compensation levels. In this chapter the influence of telecom delays associated with remote frequency signal on the stability of torsional modes is investigated.

In this chapter an attempt is also made to study the effectiveness of different auxiliary signals when SVC is placed at the generator end.

In this chapter, system studies are specifically done for series compensation level of 35.6 %, at which mode 4 is critically destabilized. This compensation level is chosen because eigenvalue results presented in Table 1.1 for IEEE First SSR Benchmark System reveals that the undamping of mode 4 at 35.6 % is much higher than undamping of modes 3 and 2 at 54.8 % and 73 % respectively. Although, undamping of mode 1 at 90.8 % is higher, this level of series compensation is too high to come in realistic range.

5.2 Influence of Telecom Delays on System Stability

In the previous chapter it has been studied that with a telecom delay of 5 ms. the system is stable with (line current + RF) auxiliary controller for all the critical levels of series compensation. In this section, the effect of varying telecom delays on system stability has been studied for critical series compensation level of 35.6 %, when mode 4 is critically destabilized. Eigenvalue analysis is done for telecom delays of 1.0 ms, 2.5 ms, 5.0 ms and 7.5 ms. Eigenvalues with varying telecom delays for (line current + RF) auxiliary controller are presented in Table 5.1 .

TABLE 5.1

EFFECT OF VARIATION IN TELECOM DELAY (T_{TD}) OF REMOTE FREQUENCY SIGNAL ON SYSTEM STABILITY. LINE SERIES COMPENSATION = 35.6 %

Mode Identification	T_{TD} = 1.0 ms	T_{TD} = 2.5 ms	T_{TD} = 5.0 ms	T_{TD} = 7.5 ms
Network	-5.1419 ± j 1941.2706 -4.8488 ± j 1188.1332 -4.7378 ± j 386.5497	-5.1187 ± j 1942.2810 -4.7858 ± j 1188.1482 -4.6441 ± j 386.2745	-5.0955 ± j 1942.2912 -4.7230 ± j 1188.1626 -4.5467 ± j 386.0024	-5.0998 ± j 1942.2886 -4.7345 ± j 1188.1571 -4.5934 ± j 386.0388
Mode 5 Mode 4 Mode 3 Mode 2 Mode 1 Mode 0	0.0± j298.1767 -0.1888 ± j 204.2461 -0.0063 ± j 160.7619 -0.0038 ± j127.0547 -0.0914 ± j 99.4546 -0.4524 ± j 9.0922	0.0± j 298.1767 -0.1139 ± j 204.2053 -0.0046 ± j 160.7598 -0.0036 ± j 127.0540 -0.0899 ± j 99.4476 -0.4521 ± j 9.0292	0.0± j 298.1767 -0.0143 ± j 204.1061 -0.0037 ± j 160.7555 -0.0037 ± j 127.0526 -0.0887 ± j 99.4330 -0.4509 ± j 8.9686	0.0± j 298.1767 +0.0252 ± j 204.0945 -0.0034 ± j 160.7534 -0.0037 ± j 127.0519 -0.0862 ± j 99.4262 -0.5009 ± j 8.8875
Elect . Mode S . S . Mode	-0.2362 ± j 210.6115 -3.8381 ± j 552.3999	-0.1136 ± j 211.1727 -3.8018 ± j 552.4667	-0.0236 ± j 211.8459 -3.7642 ± j 552.5340	-0.0011 ± j 211.7268 -3.7655 ± j 552.5186
Generator Rotor Circuits	-41.4909 , -25.2729 -3.5764 , -0.1354 -0.0946	-41.5068 , -25.2719 -3.5499 , -0.1347 -0.0932	-41.5220 , -25.2711 -3.5232 , -0.1340 -0.0918	-41.5437 , -25.2717 -3.4601 , -0.1329 -0.0890
SVC	-603.2875 , -406.7320 -999.9715 , -144.2867 -15.8743 -113.1832 ± j 14.2070 -18.5004 ± j 346.0413	-602.6367 , -406.5410 -400.2523 , -144.4761 -15.8260 -112.9613 ± j 19.6340 -19.3563 ± j 345.0709	-602.2328 ,-406.6841 -198.4830 ,-146.1392 -15.7679 -112.6798 ± j 23.5379 -20.2715 ± j 344.0237	-602.3759 , -406.6922 -15.8922 -110.2839 ± j18.4143 -140.4068 ± j 13.5031 -20.2335 ± j 344.3246
Optimum Auxiliary Controller Parameters	LC RF K_B = -0.40 , K_B' = 0.016 T_1 = 0.08 , T_1' = 0.009 T_2 = 0.017 , T_2' = 0.007	LC RF K_B = -0.42 , K_B' = 0.016 T_1 = 0.08 , T_1' = 0.009 T_2 = 0.017 , T_2' = 0.007	LC RF K_B = -0.44 , K_B' = 0.016 T_1 = 0.08 , T_1' = 0.009 T_2 = 0.017 , T_2' = 0.007	LC RF K_B = -0.475 , K_B' = 0.016 T_1 = 0.0756 , T_1' = 0.0099 T_2 = 0.0175 , T_2' = 0.007

Elect . Mode : Electrical Mode , S . S. Mode : Super-synchronous Mode

Time Constants T_1 and T_2 are expressed in seconds .

TABLE 5.2
SYSTEM EIGENVALUES WHEN SVC IS PLACED AT THE GENERATOR END.
LINE SERIES COMPENSATION = 35.6 %

Mode Identification	Without SVC	Line Current	Generator Frequency
Network		-2.4451 ±j 1971.8016 -3.1640 ±j 1217.6910 -0.6997 ±j 377.5360	-2.5864 ±j 1971.7453 -3.5368 ±j 1217.6101 -1.7498 ±j 377.7372
Mode 5 Mode 4 Mode 3 Mode 2 Mode 1 Mode 0	0.0± j 298.17 +1.4279±j202.8 +0.0147± j160.7 +0.0012± j127.0 +0.0021± j99.40 -0.3321± j10.41	0.0 ±j 298.1767 +1.3732 ±j 204.7526 –0.0012 ±j 160.7309 -0.0026 ±j 127.0449 -0.0463 ±j 99.3467 -0.0108 ±j 9.5806	0.0 ±j 298.1767 -1.8543 ±j 201.3241 -0.0534 ±j 160.7143 -0.0113 ±j 127.0517 -0.1255 ±j 99.4316 -0.1991 ±j 10.5510
Elect. Mode S. S. Mode	-5.3254± j202.7 -4.7601± j551.0	-1.7631 ±j 205.7681 -2.0598 ±j 551.8722	-0.0121 ±j 206.0467 -2.5370 ±j 551.3222
Generator Rotor Circuits	-40.79 , -25.41 -3.08 , -0.1287 -0.0676	-38.9504 , -25.2478 -5.4865 , -0.1905 -0.1154	-40.5704 , -25.0702 -5.7799 , -0.1158 -0.1960
SVC		-608.8108 , -407.1918 -166.0534 , -32.7858 -14.9127 -13.0416 ±j 367.7227	-611.4976 , -407.2988 -174.2928 , -17.7726 -1.1 E + 5 , -1.0 E + 11 -6.6598 ±j 374.3282
Optimum Auxiliary Controller Parameters		K_B = -0.17 T_1 = 0.10 T_2 = 0.045	K_B = + 0.0053 T_1 = 0.043 T_2 = 9.0 E - 6

Elect. Mode : Electrical Mode , S. S. Mode : Super-synchronous Mode
Time Constants T_1 and T_2 are expressed in seconds.

5.3 Influence of SVC location on the effectiveness of different auxiliary signals

In this section, the effect of line current and generator frequency auxiliary signals is examined when SVC is placed at the generator end, for critical series compensation level of 35 6 %, i.e. when mode 4 is critically destabilized. Table 5.2 presents the eigenvalue results with line current and generator frequency auxiliary signals when SVC is placed at the generator end. Both these signals are considered individually.

5.4 Discussions

- From eigenvalue results presented in Table 5.1, it is concluded that at critical series compensation level of 35.6 %, the system is stable for telecom delay (T_{TD}) ranging from 1.0 ms to 5.0 ms. However for T_{TD}=7.5 ms, the system was unstable. As telecom delay is reduced from 5.0 ms to 2.5 ms, damping of mode 4 is increased approximately 8 times whereas that of electrical mode by 5 times. If telecom delay is further reduced i.e. from 5.0 ms to 1.0 ms, then damping of mode 4 is increased 13 times and of electrical mode by 10 times.

  Thus we see that telecom delay associated with remote frequency signal has significant effect on the stability of critical mode (in present case mode 4) and the electrical mode, whereas rest of the system modes are not much affected. The performance of (line current + remote frequency) auxiliary controller when tuned to modes 3 and 2, i.e. at critical compensation levels 54.8 % and 73 % has been investigated in chapter 4 with a time delay of 5.0 ms which is observed to give pessimistic results. If telecom delay can be reduced, then the system stability can be further improved.

SVC located at Generator End

- From eigenvalue results presented in Table 5.2, it is concluded that when SVC is placed at the generator end, line current auxiliary controller alone could not stabilize mode 4, but generator frequency auxiliary controller alone was able to stabilize whole system at critical compensation level of 35.6 %. If we compare the eigenvalue results of generator frequency auxiliary controller presented in Table 5.2 with that of (line current + remote frequency) auxiliary controller presented in Table 4.1, both for critical series compensation level of 35.6 %, then it can be concluded that an SVC placed at the generator end is much more effective than midpoint located SVC in damping the torsional oscillations. This behavior is very much expected because when SVC

is placed at the generator end then there is no time delay associated with generator frequency signal, hence generator frequency signal alone is much more effective than composite line current + remote frequency auxiliary controller.

It is important to note that if an SVC is placed at the generator end then it is solely dedicated to the damping of subsynchronous oscillations [14] and can not be simultaneously employed for any other purpose such as improvement of dynamic stability limit. Since SVC is an expensive device, therefore midpoint location of SVC is more justified both from technical and economical points of view.

5.5 CONCLUSIONS

- The telecom delay associated with remote frequency signal plays a significant role in system stabilization. The lower the telecom delay, better is the damping of torsional modes. A fast communication technique such as fibre optics is therefore recommended.

- It has been revalidated that an SVC placed at generator terminals and employing rotor frequency auxiliary feedback is able to damp subsynchronous oscillations.

Chapter 6

CONCLUSIONS

6.1 General

Static var compensators (SVC) are traditionally placed at the generator terminals to mitigate subsynchronous oscillations (SSO) in series compensated electric power transmission systems. An auxiliary control [14] of the SVC employing generator rotor frequency feedback is shown to be adequate for damping SSO. These SVCs suffer from the disadvantage that they are exclusively employed for SSO suppression and can not be utilized for achieving any other objective simultaneously. It may be understood that SVCs are very expensive equipment which need to be utilized most optimally.

It has been reported [15] that an SVC located at the midpoint of a series compensated line can be utilized for dual purposes of damping SSO and stability enhancement. Controllers of these SVCs have been designed based on a combination of line current signal and computed value of generator internal frequency (CIF). Both these signals utilize local measurements, as the current trend in power systems practice is to use local signals for the sake of reliability.

In this thesis an altogether new concept of SVC control employing a remote generator frequency signal transmitted over a telecom line, is presented. The motivation for this new investigation is provided because of two reasons :

(i) Signals such as "current margin" are successfully transmitted over telecom lines in HVDC transmission systems in a reliable manner, over the world.

(ii) Since generator rotor frequency is the most effective signal when SVC is connected at the generator terminals, it is thought that the same signal, if made available at the remotely located SVC, may also prove to be substantially effective. While the previous work [15,23] attempted to synthesize this signal based on the local measurements, in this thesis the same rotor frequency signal is actually measured and transmitted over telecom channels.

In this thesis the study system is chosen to be the IEEE First SSR Benchmark System. This is suitably modified to connect an SVC at the midpoint of the transmission line. Different auxiliary signals such as line current, CIF, remote frequency signal and combination of line current with CIF and remote frequency signal are examined in respect of their effectiveness in stabilizing the torsional oscillation modes. The auxiliary controller is, a priori, assumed to be a simple lead - lag transfer function. System studies are done for all the four critical series compensation levels, i.e. 35.6 %, 54.8 %, 73 % and 90.8 % at which mode 4, mode 3, mode 2 and mode 1, respectively, are critically destabilized.

It is observed that a pure voltage control of SVC has minimal effect on the stability of torsional oscillation modes, which is expected since voltage control does not contribute electric damping. When the network is critically compensated, which may not be realistic, a combination of line current and remote frequency signal is successful in damping torsional oscillations at critical compensation levels of 35.6 %, 54.8 % and 73 %. At critical compensation level of 90.8 %, line current auxiliary controller alone is able to stabilize the system. Eigenvalue results of this thesis clearly show that (line current + RF) combination is much superior to (line current + CIF) even with a time delay of 5 ms.

It has been shown that with a time delay of 5 ms, the study system is stable with (line current + remote frequency) auxiliary controller over whole range of critical series compensation. It is further shown that the lower is the value of telecom delay, better is the stability of torsional modes.

It is concluded in this thesis that this remote rotor frequency signal together with line current signal can be successfully applied for damping all the torsional modes at all the critical levels of series compensation. The performance of remote rotor frequency signal is much better than the computed internal frequency signal.

This concept of remotely transmitted signal is being investigated for the first time in the control of static var compensators to damp subsynchronous oscillations.

6.2 Scope for Future Work

- To study the capability of SVC auxiliary controllers in damping torsional oscillations for **IEEE Second Benchmark System for SSR** and even on big sized realistic systems.

- To study the performance with exact CIF auxiliary controller for midpoint located SVC , where transients associated with inductor and capacitor are taken into account.

- To validate the eigenvalue results obtained in chapter 4 and 5 through EMTDC/PSCAD simulation , in which it is possible to model all the system nonlinearities .

APPENDIX A

SYNCHRONOUS MACHINE MODEL PARAMETERS

In this Appendix, expressions are given for the various constants which are used in the synchronous machine model [6].

The constants $a_1 - a_9$ are defined as

$$\begin{bmatrix} a_1 & a_2 \\ a_3 & a_4 \end{bmatrix} = -\frac{w_o}{x_f x_h - x^2_{fh}} \begin{bmatrix} R_f x_h & -R_f x_{fh} \\ -R_h x_{fh} & R_h x_f \end{bmatrix}$$

$$\begin{bmatrix} a_5 & a_6 \\ a_7 & a_8 \end{bmatrix} = -\frac{w_o}{x_g x_k - x^2_{gk}} \begin{bmatrix} R_g x_k & -R_g x_{gk} \\ -R_k x_{gk} & R_k x_g \end{bmatrix}$$

$a_9 = -1 / T_{coil}$; T_{coil} is the time constant of dummy coil (small value chosen arbitrarily = 0.1 msec)

The constants $b_1 - b_6$ are defined as

$$b_1 = \frac{w_o R_f}{x_{df}} \quad , \quad \begin{bmatrix} b_2 \\ b_3 \end{bmatrix} = \frac{w_o}{x_f x_h - x^2_{fh}} \begin{bmatrix} R_f (x_{df} x_h - x_{dh} x_{fh}) \\ R_h (x_f x_{dh} - x_{fh} x_{df}) \end{bmatrix}$$

$$\begin{bmatrix} b_5 \\ b_6 \end{bmatrix} = \frac{w_o}{x_g x_k - x^2_{gk}} \begin{bmatrix} R_g (x_{qg} x_k - x_{qk} x_{gk}) \\ R_k (x_g x_{qk} - x_{gk} x_{qg}) \end{bmatrix}$$

$$b_4 = \sqrt{x_c (x_q'' - x_d'')}$$

$w_o = 2\pi f$; f is the system frequency

The constants $c_1 - c_5$ are given as

$$c_1 = \frac{x_{df}x_h - x_{dh}x_{fh}}{x_d^{"}(x_f x_h - x_{fh}^2)}$$

$$c_2 = \frac{x_{dh}x_f - x_{fh}x_{df}}{x_d^{"}(x_f x_h - x_{fh}^2)}$$

$$c_3 = \frac{x_{qg}x_k - x_{qk}x_{gk}}{x_d^{"}(x_g x_k - x_{gk}^2)}$$

$$c_4 = \frac{x_{qk}x_g - x_{gk}x_{qg}}{x_d^{"}(x_g x_k - x_{gk}^2)}$$

$$c_5 = \frac{1}{x_d^{"}}\sqrt{\frac{x_q^{"} - x_d^{"}}{x_c}}$$

where

x_f , x_h , x_g , x_k are reactances of the rotor coils specified by the subscripts.

x_c is the reactance of the dummy coil (chosen = x_q)

R_f , R_h , R_g , R_k are resistances of the rotor coils specified by the subscripts.

x_{df} , x_{dh} , x_{fh} , x_{gk} , x_{qg} , x_{qk} are mutual reactances between rotor coils specified by the subscripts.

The resistances and reactances of the various rotor coils are defined as follows :

$$x_{df} = x_{dh} = x_{fh} = x_d - x_l \quad , \qquad x_{qg} = x_{qk} = x_{qc} = x_{gk} = x_q - x_l$$

$$x_{hl} = \frac{(x_d^{"} - x_l)(x_d^{'} - x_l)}{(x_d^{'} - x_d^{"})} \quad , \qquad x_{fl} = \frac{(x_d^{'} - x_l)x_{df}}{(x_d - x_d^{'})}$$

$$x_{gl} = \frac{(x_q^{"} - x_l)(x_q^{'} - x_l)}{(x_q^{'} - x_q^{"})} \quad , \qquad x_{kl} = \frac{(x_q^{'} - x_l)x_{qk}}{(x_q - x_q^{'})}$$

$$x_f = x_{df} + x_{fl} \quad , \quad x_h = x_{df} + x_{hl}$$

$$x_g = x_{qk} + x_{gl} \quad , \quad x_k = x_{qk} + x_{kl}$$

$$R_f = \frac{x_{df}^{\,2}}{w_o T_{do}^{'}(x_d - x_d^{'})} \quad , \quad R_h = \frac{(x_d^{'} - x_l)^2}{w_o T_{do}^{''}(x_d^{'} - x_d^{''})}$$

$$R_g = \frac{(x_q^{'} - x_l)^2}{w_o T_{qo}^{''}(x_q^{'} - x_q^{''})} \quad , \quad R_k = \frac{x_{qk}^{\,2}}{w_o T_{qo}^{'}(x_q - x_q^{'})}$$

where

x_l is the stator leakage reactance.

x_d , $x_d^{'}$, $x_d^{''}$ are the direct axis synchronous, transient and subtransient reactances respectively.

x_q , $x_q^{'}$, $x_q^{''}$ are the quadrature axis synchronous, transient and subransient reactances respectively.

$T_{do}^{'}$, $T_{do}^{''}$ are the direct axis transient and subtransient open circuit time constants respectively.

$T_{qo}^{'}$, $T_{qo}^{''}$ are the quadrature axis transient and subtransient open circuit time constants respectively.

APPENDIX B

DETAILS OF SYSTEM MODEL DESCRIBED IN CHAPTER 2

B.1 Rotor Circuits

Substituting eqn.(2.7) in eqn.(2.6)

$$\begin{aligned}
\dot{\Psi}_f &= a_1\Psi_f + a_2\Psi_h + b_1 v_f + b_2\cos\delta\, i_D - b_2\sin\delta\, i_Q \\
\Psi_h &= a_3\Psi_f + a_4\Psi_h + b_3\cos\delta\, i_D - b_3\sin\delta i_Q \\
\dot{\Psi}_g &= a_5\Psi_g + a_6\Psi_k + b_5\sin\delta i_D + b_5\cos\delta i_Q \\
\Psi_k &= a_7\Psi_g + a_8\Psi_k + b_6\sin\delta i_D + b_6\cos\delta i_Q \\
\dot{\Psi}_c &= a_9\Psi_c + b_4\sin\delta i_D + b_4\cos\delta i_Q
\end{aligned} \tag{B.1}$$

The state equation for the rotor circuits is obtained by linearizing eqn. (B.1)

$$\dot{x}_R = A_R x_R + B_{R1}u_{R1} + B_{R2}u_{R2} \tag{B.2}$$

where

$$x_R = [\Delta\Psi_f\ \Delta\Psi_h\ \Delta\Psi_g\ \Delta\Psi_k\ \Delta\Psi_c\ ]' \quad , \quad u_{R1} = [\Delta\delta\quad \Delta\omega]'$$

$$u_{R2} = [\Delta i_D\quad \Delta i_Q]'$$

$$A_R = \begin{bmatrix} a_1 & a_2 & 0 & 0 & 0 \\ a_3 & a_4 & 0 & 0 & 0 \\ 0 & 0 & a_5 & a_6 & 0 \\ 0 & 0 & a_7 & a_8 & 0 \\ 0 & 0 & 0 & 0 & a_9 \end{bmatrix} \quad , \quad B_{R1} = \begin{bmatrix} -b_2 i_{q0} & 0 \\ -b_3 i_{q0} & 0 \\ b_5 i_{d0} & 0 \\ b_6 i_{d0} & 0 \\ b_4 i_{d0} & 0 \end{bmatrix}$$

$$B_{R2} = \begin{bmatrix} b_2 \cos\delta_0 & -b_2 \sin\delta_0 \\ b_3 \cos\delta_0 & -b_3 \sin\delta_0 \\ b_5 \sin\delta_0 & b_5 \cos\delta_0 \\ b_6 \sin\delta_0 & b_6 \cos\delta_0 \\ b_4 \sin\delta_0 & b_4 \cos\delta_0 \end{bmatrix}$$

$i_{d0} = \cos\delta_0 i_{D0} - \sin\delta_0 i_{Q0}$

$i_{q0} = \sin\delta_0 i_{D0} + \cos\delta_0 i_{Q0}$

Substituting eqn. (2.9) in eqn. (2.10) gives

$$I_D = c_1 \cos\delta \Psi_f + c_2 \cos\delta \Psi_h + c_3 \sin\delta \Psi_g + c_4 \sin\delta \Psi_k + c_5 \sin\delta \Psi_c$$

$$I_Q = -c_1 \sin\delta \Psi_f - c_2 \sin\delta \Psi_h + c_3 \cos\delta \Psi_g + c_4 \cos\delta \Psi_k + c_5 \cos\delta \Psi_c \qquad \text{(B.3)}$$

Differentiating eqn. (2.9)

$$\dot{I}_d = c_1 \dot{\Psi}_f + c_2 \dot{\Psi}_h$$

$$\dot{I}_q = c_3 \dot{\Psi}_g + c_4 \dot{\Psi}_k + c_5 \dot{\Psi}_c \qquad \text{...(B.4)}$$

Eqn. (2.10) is also differentiated to give

$$\begin{bmatrix} \dot{I}_D \\ \dot{I}_Q \end{bmatrix} = \begin{bmatrix} \cos\delta & \sin\delta \\ -\sin\delta & \cos\delta \end{bmatrix} \begin{bmatrix} \dot{I}_d \\ \dot{I}_q \end{bmatrix} + \frac{d\delta}{dt} \begin{bmatrix} -\sin\delta & \cos\delta \\ -\cos\delta & -\sin\delta \end{bmatrix} \begin{bmatrix} I_d \\ I_q \end{bmatrix} \qquad \text{(B.5)}$$

The flux derivative terms in eqn. (B.4) are replaced by their respective expressions obtained from the rotor state equations (B.2). $\dot{I}_d$, $\dot{I}_q$ so obtained are substituted in eqn. (B.5). The resulting equation together with eqn. (B.3) are now linearized to give the output equations of rotor circuit as

$$y_{R1} = C_{R1} x_R + D_{R1} u_{R1} \qquad \text{(B.6)}$$

$$y_{R2} = C_{R2} x_R + D_{R2} u_{R1} + D_{R3} u_{R2} \qquad \text{(B.7)}$$

where $y_{R1} = [\Delta I_D \quad \Delta I_Q]'$, $y_{R2} = [\Delta \dot{I}_D \quad \Delta \dot{I}_Q]'$

The **nonzero** elements of the different matrices are defined as

$C_{R1}(1,1) = c_1 \cos\delta_0$

$C_{R1}(1,2) = c_2 \cos\delta_0$

$C_{R1}(1,3) = c_3 \sin\delta_0$

$C_{R1}(1,4) = c_4 \sin\delta_0$

$$C_{R1}(1,5) = c_5 \sin\delta_0$$
$$C_{R1}(2,1) = -c_1 \sin\delta_0$$
$$C_{R1}(2,2) = -c_2 \sin\delta_0$$
$$C_{R1}(2,3) = c_3 \cos\delta_0$$
$$C_{R1}(2,4) = c_4 \cos\delta_0$$
$$C_{R1}(2,5) = c_5 \cos\delta_0$$
$$C_{R2}(1,1) = (c_1 a_1 + c_2 a_3)\cos\delta_0$$
$$C_{R2}(1,2) = (c_1 a_2 + c_2 a_4)\cos\delta_0$$
$$C_{R2}(1,3) = (c_3 a_5 + c_4 a_7)\sin\delta_0$$
$$C_{R2}(1,4) = (c_3 a_6 + c_4 a_8)\sin\delta_0$$
$$C_{R2}(1,5) = c_5 a_9 \sin\delta_0$$
$$C_{R2}(2,1) = -(c_1 a_1 + c_2 a_3)\sin\delta_0$$
$$C_{R2}(2,2) = -(c_1 a_2 + c_2 a_4)\sin\delta_0$$
$$C_{R2}(2,3) = (c_3 a_5 + c_4 a_7)\cos\delta_0$$
$$C_{R2}(2,4) = (c_3 a_6 + c_4 a_8)\cos\delta_0$$
$$C_{R2}(2,5) = c_5 a_9 \cos\delta_0$$
$$D_{R1}(1,1) = I_{Q0}$$
$$D_{R1}(2,1) = -I_{D0}$$
$$D_{R2}(1,1) = -(c_1 b_2 + c_2 b_3)\, i_{q0} \cos\delta_0 + (c_3 b_5 + c_4 b_6 + c_5 b_4)\, i_{d0} \sin\delta_0$$
$$D_{R2}(1,2) = I_{Q0}$$
$$D_{R2}(2,1) = (c_1 b_2 + c_2 b_3)\, i_{q0} \sin\delta_0 + (c_3 b_5 + c_4 b_6 + c_5 b_4)\, i_{d0} \cos\delta_0$$
$$D_{R2}(2,2) = -I_{D0}$$
$$D_{R3}(1,1) = c_1 b_1 \cos\delta_0$$
$$D_{R3}(2,1) = -c_1 b_1 \sin\delta_0$$
$$D_{R4}(1,1) = (c_1 b_2 + c_2 b_3)\cos^2\delta_0 + (c_3 b_5 + c_4 b_6 + c_5 b_4)\sin^2\delta_0$$
$$D_{R4}(1,2) = -(c_1 b_2 + c_2 b_3)\sin\delta_0 \cos\delta_0 + (c_3 b_5 + c_4 b_6 + c_5 b_4)\sin\delta_0 \cos\delta_0$$
$$D_{R4}(2,1) = -(c_1 b_2 + c_2 b_3)\sin\delta_0 \cos\delta_0 + (c_3 b_5 + c_4 b_6 + c_5 b_4)\sin\delta_0 \cos\delta_0$$
$$D_{R4}(2,2) = (c_1 b_2 + c_2 b_3)\sin^2\delta_0 + (c_3 b_5 + c_4 b_6 + c_5 b_4)\cos^2\delta_0$$
$$I_{D0} = \cos\delta_0 I_{d0} + \sin\delta_0 I_{q0}$$
$$I_{Q0} = -\sin\delta_0 I_{d0} + \cos\delta_0 I_{q0}$$

B.2 State Space Model of the Turbine - Generator Mechanical System

The six mass representation of the turbogenerator shaft system is modeled in Fig. B.1 , where M represents the moment of inertia , K the spring constant ,

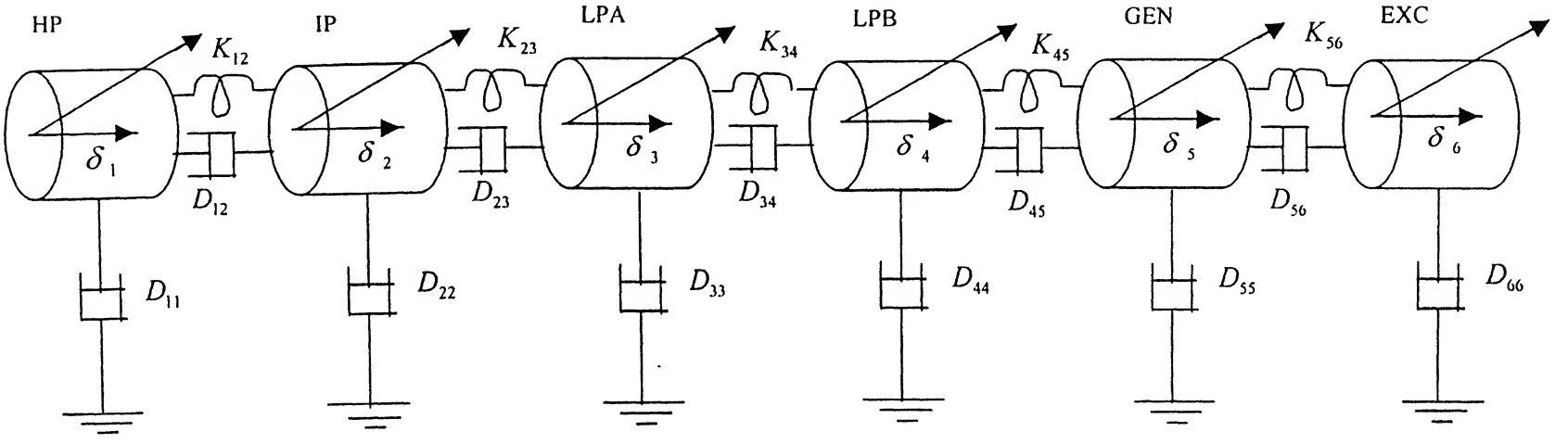

FIG . B.1 SIX MASS MODEL OF A TURBO GENERATOR SHAFT

D is the damping coefficient and δ represents the angular position of concerned mass . T_{mi} is the mechanical torque input corresponding to i th mass while T_e is the electrical torque on the generator. Equations relating the angular position and velocity of various masses are given as

$$
\begin{aligned}
&M_1\ddot{\delta}_1 + (D_{11} + D_{12})\dot{\delta}_1 - D_{12}\dot{\delta}_2 + K_{12}\delta_1 - K_{12}\delta_2 = T_{m1} \\
&M_2\ddot{\delta}_2 - D_{12}\dot{\delta}_1 + (D_{12} + D_{22} + D_{23})\dot{\delta}_2 - D_{23}\dot{\delta}_3 - K_{12}\delta_1 \\
&+ (K_{12} + K_{23})\delta_2 - K_{23}\delta_3 = T_{m2} \\
&M_3\ddot{\delta}_3 - D_{23}\dot{\delta}_2 + (D_{23} + D_{33} + D_{34})\dot{\delta}_3 - D_{34}\dot{\delta}_4 - K_{23}\delta_2 \\
&+ (K_{23} + K_{34})\delta_3 - K_{34}\delta_4 = T_{m3} \\
&M_4\ddot{\delta}_4 - D_{34}\delta_3 + (D_{34} + D_{44} + D_{45})\dot{\delta}_4 - D_{45}\dot{\delta}_5 - K_{34}\delta_3 \\
&+ (K_{34} + K_{45})\delta_4 - K_{45}\delta_5 = T_{m4} \\
&M_5\ddot{\delta}_5 - D_{45}\dot{\delta}_4 + (D_{45} + D_{55} + D_{56})\dot{\delta}_5 - D_{56}\dot{\delta}_6 - K_{45}\delta_4 \\
&+ (K_{45} + K_{56})\delta_5 - K_{56}\delta_6 = -T_e \\
&M_6\ddot{\delta}_6 - D_{56}\dot{\delta}_5 + (D_{56} + D_{66})\dot{\delta}_6 - K_{56}\delta_5 + K_{56}\delta_6 = 0
\end{aligned}
\tag{B.8}
$$

Linearizing eqns. (B.8) and writing in state space form as

$$\dot{x}_M = A_M x_M + B_M u_M \tag{B.9}$$

where

$$x_M = [\Delta\delta_1 \quad \Delta\delta_2 \quad \Delta\delta_3 \quad \Delta\delta_4 \quad \Delta\delta_5 \quad \Delta\delta_6 \quad \Delta\dot{\delta}_1 \quad \Delta\dot{\delta}_2 \quad \Delta\dot{\delta}_3 \quad \Delta\dot{\delta}_4 \quad \Delta\dot{\delta}_5 \quad \Delta\dot{\delta}_6]^T$$

$$u_M = [\Delta T_{m1} \quad \Delta T_{m2} \quad \Delta T_{m3} \quad \Delta T_{m4} \quad -\Delta T_e]$$

$$A_M = \begin{bmatrix} 0 & I \\ A_{M1} & A_{M2} \end{bmatrix}$$

I is an identity matrix of dimension (6,6) .

The nonzero elements of A_{M1} are defined by

$$A_{M1}(1,1) = -\frac{K_{12}}{M_1}$$

$$A_{M1}(1,2) = \frac{K_{12}}{M_1}$$

$$A_{M1}(2,1) = \frac{K_{12}}{M_2}$$

$$A_{M1}(2,2) = -\frac{(K_{12} + K_{23})}{M_2}$$

$$A_{M1}(2,3) = \frac{K_{23}}{M_2}$$

$$A_{M1}(3,2) = \frac{K_{23}}{M_3}$$

$$A_{M1}(3,3) = -\frac{(K_{23} + K_{34})}{M_3}$$

$$A_{M1}(3,4) = \frac{K_{34}}{M_3}$$

$$A_{M1}(4,4) = -\frac{(K_{34} + K_{45})}{M_4}$$

$$A_{M1}(4,5) = \frac{K_{45}}{M_4}$$

$$A_{M1}(5,4) = \frac{K_{45}}{M_5}$$

$$A_{M1}(5,5) = -\frac{(K_{45} + K_{56})}{M_5}$$

$$A_{M1}(5,6) = \frac{K_{56}}{M_5}$$

$$A_{M1}(6,5) = \frac{K_{56}}{M_6}$$

$$A_{M1}(6,6) = -\frac{K_{56}}{M_6}$$

The nonzero elements of A_{M2} are given as

$$A_{M2}(1,1) = -\frac{(D_{11} + D_{12})}{M_1}$$

$$A_{M2}(1,2) = \frac{D_{12}}{M_1}$$

$$A_{M2}(2,1) = \frac{D_{12}}{M_2}$$

$$A_{M2}(2,2) = -\frac{(D_{12} + D_{22} + D_{23})}{M_2}$$

$$A_{M2}(2,3) = \frac{D_{23}}{M_2}$$

$$A_{M2}(3,2) = \frac{D_{23}}{M_3}$$

$$A_{M2}(3,3) = -\frac{(D_{23} + D_{33} + D_{34})}{M_3}$$

$$A_{M2}(3,4) = \frac{D_{34}}{M_3}$$

$$A_{M2}(4,3) = \frac{D_{34}}{M_4}$$

$$A_{M2}(4,4) = -\frac{(D_{34} + D_{44} + D_{45})}{M_4}$$

$$A_{M2}(4,5) = \frac{D_{45}}{M_4}$$

$$A_{M2}(5,4) = \frac{D_{45}}{M_5}$$

$$A_{M2}(5,5) = -\frac{(D_{45} + D_{55} + D_{56})}{M_5}$$

$$A_{M2}(5,6) = \frac{D_{56}}{M_5}$$

$$A_{M2}(6,5) = \frac{D_{56}}{M_6}$$

$$A_{M2}(6,6) = -\frac{D_{66}}{M_6}$$

Since self damping and mutual damping between the masses is assumed to be zero , for IEEE First Benchmark System . Matrix A_{M2} becomes a zero matrix .

$$\therefore \quad A_M = \begin{bmatrix} 0 & I \\ A_{M1} & 0 \end{bmatrix}$$

Since the governor system involves large time constants , it is ignored in the present analysis . Thus ,

$$\Delta T_{m1} = \Delta T_{m2} = \Delta T_{m3} = \Delta T_{m4} = 0 \tag{B.10}$$

The electromagnetic torque T_e acting on the generator rotor , as given in [6] , is expressed by

$$T_e = -x_d^{"}(i_d I_q - i_q I_d) \tag{B.11}$$

The currents i_d , i_q and I_d, I_q are transformed to D - Q reference frame using the relationship given in eqn. (2.7) . It is noted that , though eqn . (2.7) is written specifically for transforming i_d , i_q to D -Q axis quantities , the same relation also applies for the transformation of I_d, I_q to corresponding currents in D - Q frame of reference as

$$\begin{aligned} T_e = -x_d^{"}[&(\cos\delta\, i_D - \sin\delta\, i_Q)(\sin\delta\, I_D + \cos\delta\, I_Q) \\ &-(\sin\delta\, i_D + \cos\delta\, i_Q)(\cos\delta\, I_D - \sin\delta\, I_Q)] \end{aligned} \tag{B.12}$$

Alternatively , $T_e = -x_d^{"}(i_D I_Q - i_Q I_D)$ (B.13)

linearizing above eqn . we get ,

$$\Delta T_e = -x_d^{"}[\Delta i_D I_{Q0} + i_{D0}\Delta I_Q - \Delta i_Q I_{D0} - i_{Q0}\Delta I_D] \tag{B.14}$$

Substituting eqns . (B.10 - B.14) in eqn . (B.9) results in

$$\dot{x}_M = A_M x_M + B_{M1} u_{M1} + B_{M2} u_{M2} \tag{B.15}$$

where

$$u_{M1} = \begin{bmatrix} \Delta I_D & \Delta I_Q \end{bmatrix}^t \quad , \quad u_{M2} = \begin{bmatrix} \Delta i_D & \Delta i_Q \end{bmatrix}^t$$

The **nonzero** elements of matrices B_{M1} and B_{M2} are given by

$$B_{M1}(11,1) = -\frac{x_d^{"} i_{Q0}}{M5}$$

$$B_{M1}(11,2) = \frac{x_d^{"} i_{D0}}{M5}$$

$$B_{M2}(11,1) = \frac{x_d^{"} I_{Q0}}{M5}$$

$$B_{M2}(11,2) = -\frac{x_d^{"} I_{D0}}{M5}$$

The output equation of the mechanical system is given by

$$y_M = C_M x_M \tag{B.16}$$

where

$$y_M = \begin{bmatrix} \Delta\delta_5 & \Delta\dot{\delta}_5 \end{bmatrix}$$

The **nonzero** elements of C_M are given by

$$C_M(1,5) = 1.0$$

$$C_M(2,11) = 1.0$$

It may be noted that

$$\Delta\delta = \Delta\delta_5 \tag{B.17}$$

$$\Delta\omega = \Delta\delta_5$$

where $\Delta\delta$ and $\Delta\omega$ are the incremental changes in generator rotor angle and angular speed respectively.

B.3 Network

The nonzero elements of the matrices utilized in eqn. (2.19) are given below

$$S_1(1,1) = -\frac{R_A}{L_A} \qquad S_1(1,2) = -\frac{1}{L_A} \qquad S_1(2,1) = \frac{1}{C}$$

$$S_2(1,1) = -\frac{L_d''}{L_A} \qquad S_3(1,1) = \frac{1}{L_A}$$

The different matrices in the state equation of the network given by eqn (2.22) are defined as follows

$$A_N = \begin{bmatrix} S_1 & -\omega_0 I \\ \omega_0 I & S_1 \end{bmatrix} \qquad B_{N1} = \begin{bmatrix} 0 & \omega_0 S_2 \\ -\omega_0 S_2 & 0 \end{bmatrix}$$

$$B_{N2} = \begin{bmatrix} S_2 & 0 \\ 0 & S_2 \end{bmatrix}$$

The output equation for the network model is written as

$$y_N = C_N x_N \tag{B.18}$$

where $y_N = [\Delta i_D \quad \Delta i_Q]'$

The nonzero elements of C_N are defined by

$C_N\ (1,1) = C_N\ (2,3) = 1.0$

B.4 Interconnection of Various Subsystems

The various vectors and matrices are defined as follows

$$x_T = [x_R \quad x_M \quad x_N]'$$
$$u_T = [u_{R1} \quad u_{R2} \quad u_{M1} \quad u_{M2} \quad u_{N1} \quad u_{N2}]'$$
$$y_T = [y_{R1} \quad y_{R2} \quad y_M \quad y_N]'$$

$$F_T = \begin{bmatrix} 0 & 0 & I & 0 \\ 0 & 0 & 0 & I \\ I & 0 & 0 & 0 \\ 0 & 0 & 0 & I \\ I & 0 & 0 & 0 \\ 0 & I & 0 & 0 \end{bmatrix} \qquad A_T = \begin{bmatrix} A_R & 0 & 0 \\ 0 & A_M & 0 \\ 0 & 0 & A_N \end{bmatrix}$$

$$B_T = \begin{bmatrix} B_{R1} & B_{R2} & 0 & 0 & 0 & 0 \\ 0 & 0 & B_{M1} & B_{M2} & 0 & 0 \\ 0 & 0 & 0 & 0 & B_{N1} & B_{N2} \end{bmatrix}$$

$$C_T = \begin{bmatrix} C_{R1} & 0 & 0 \\ C_{R2} & 0 & 0 \\ 0 & C_M & 0 \\ 0 & 0 & C_N \end{bmatrix} \qquad D_T = \begin{bmatrix} D_{R1} & 0 & 0 & 0 & 0 & 0 \\ D_{R2} & D_{R3} & 0 & 0 & 0 & 0 \\ 0 & 0 & 0 & 0 & 0 & 0 \\ 0 & 0 & 0 & 0 & 0 & 0 \end{bmatrix}$$

APPENDIX C

DETAILS OF SYSTEM MODEL DESCRIBED IN CHAPTER 3

C.1 Network Model

The nonzero elements of matrices S_1 , S_2 , S_3 and S_4 described for the network in eqns . (3.6) , (3.7) are defined as

$$S_1(1,1) = -\frac{R_2}{L_B} \quad , \quad S_1(1,3) = \frac{1}{L_B}$$

$$S_1(1,4) = -\frac{1}{L_B} \quad , \quad S_1(2,2) = -\frac{R_A}{L_A}$$

$$S_1(2,3) = \frac{1}{L_A} \quad , \quad S_1(2,5) = \frac{1}{L_A}$$

$$S_1(3,1) = -\frac{1}{C_n} \quad , \quad S_1(3,2) = -\frac{1}{C_n}$$

$$S_1(4,1) = \frac{1}{C_{se2}} \quad , \quad S_1(5,2) = \frac{1}{C_{se1}}$$

$$S_2(3,1) = -\frac{1}{C_n}$$

$$S_3(2,1) = -\frac{L_d''}{L_A}$$

$$S_4(1,1) = -\frac{1}{L_B}$$

The different matrices in the state equation of the network given by eqn . (3.8) are defined as follows :

$$A_N = \begin{bmatrix} S_1 & -\omega_0 I \\ \omega_0 I & S_1 \end{bmatrix} \quad , \quad B_{N1} = \begin{bmatrix} S_2 & 0 \\ 0 & S_2 \end{bmatrix}$$

$$B_{N2} = \begin{bmatrix} 0 & \omega_0 S_3 \\ -\omega_0 S_3 & 0 \end{bmatrix} \quad , \quad B_{N3} = \begin{bmatrix} S_3 & 0 \\ 0 & S_3 \end{bmatrix}$$

The output equations of the network model are given as

(C.1)

$$y_{N1} = C_{N1} x_N \tag{C.2}$$

$$y_{N2} = C_{N2} x_N$$

where $y_{N1} = [\Delta i_D \quad \Delta i_Q]^t$, $y_{N2} = [\Delta v_{3D} \quad \Delta v_{3Q}]^t$

The nonzero elements of matrices $\mathbf{C}_{N1}$ and $\mathbf{C}_{N2}$ are defined by

$$C_{N1}(1,2) = C_{N1}(2,7) = 1.0$$
$$C_{N2}(1,3) = C_{N2}(2,8) = 1.0$$

C.2 Static VAR System

The nonzero elements of the different matrices used in eqn. (3.24) are defined by

$$A_S(1,1) = -\frac{\omega_0}{Q} \quad , \quad A_S(1,2) = -\omega_0 \quad , \quad A_S(1,6) = \omega_0 v_{3D0}$$

$$A_S(2,1) = \omega_0 \quad , \quad A_S(2,2) = -\frac{\omega_0}{Q} \quad , \quad A_S(2,6) = \omega_0 v_{3Q0}$$

$$A_S(3,4) = -1.0$$

$$A_S(4,1) = -\frac{K_D i_{3D0}}{T_M i_{30}} \quad , \quad A_S(4,2) = -\frac{K_D i_{3Q0}}{T_M i_{30}} \quad , A_S(4,4) = -\frac{1}{T_M}$$

$$A_S(5,3) = -\frac{K_I}{T_S} \quad , \quad A_S(5,4) = \frac{K_P}{T_S} \quad , \quad A_S(5,5) = -\frac{1}{T_S}$$

$$A_S(6,5) = \frac{1}{T_D} \quad , \quad A_S(6,6) = -\frac{1}{T_D}$$

$$B_{S1}(1,1) = \omega_0 B_0 \quad , \quad B_{S1}(2,2) = \omega_0 B_0$$

$$B_{S1}(4,1) = \frac{v_{3D0}}{v_{30} T_M} \quad , \quad B_{S1}(4,2) = \frac{v_{3Q0}}{v_{30} T_M}$$

$$B_{S2}(3,1) = 1.0 \quad , \quad B_{S2}(5,1) = -\frac{K_P}{T_S}$$

$$C_{S1}(1,1) = C_{S1}(2,2) = 1.0 \quad , \quad D_S = 0$$

C.3 Interconnection of Various Subsystems

In this case, the various vectors and matrices are defined as follows:

$$x_T = [x_R \quad x_M \quad x_N \quad x_S]'$$
$$u_T = [u_{R1} \quad u_{R2} \quad u_{M1} \quad u_{M2} \quad u_{N1} \quad u_{N2} \quad u_{N3} \quad u_{S1}]'$$
$$y_T = [y_{R1} \quad y_{R2} \quad y_M \quad y_{N1} \quad y_{N2} \quad y_S]'$$

$$F_T = \begin{bmatrix} 0 & 0 & I & 0 & 0 & 0 \\ 0 & 0 & 0 & I & 0 & 0 \\ I & 0 & 0 & 0 & 0 & 0 \\ 0 & 0 & 0 & I & 0 & 0 \\ 0 & 0 & 0 & 0 & 0 & I \\ I & 0 & 0 & 0 & 0 & 0 \\ 0 & I & 0 & 0 & 0 & 0 \\ 0 & 0 & 0 & 0 & I & 0 \end{bmatrix} \qquad A_T = \begin{bmatrix} A_R & 0 & 0 & 0 \\ 0 & A_M & 0 & 0 \\ 0 & 0 & A_N & 0 \\ 0 & 0 & 0 & A_S \end{bmatrix}$$

$$B_T = \begin{bmatrix} B_{R1} & B_{R2} & 0 & 0 & 0 & 0 & 0 & 0 \\ 0 & 0 & B_{M1} & B_{M2} & 0 & 0 & 0 & 0 \\ 0 & 0 & 0 & 0 & B_{N1} & B_{N2} & B_{N3} & 0 \\ 0 & 0 & 0 & 0 & 0 & 0 & 0 & B_{S1} \end{bmatrix}$$

$$C_T = \begin{bmatrix} C_{R1} & 0 & 0 & 0 \\ C_{R2} & 0 & 0 & 0 \\ 0 & C_M & 0 & 0 \\ 0 & 0 & C_{N1} & 0 \\ 0 & 0 & C_{N2} & 0 \\ 0 & 0 & 0 & C_S \end{bmatrix}$$

$$D_T = \begin{bmatrix} D_{R1} & 0 & 0 & 0 & 0 & 0 & 0 & 0 \\ D_{R2} & D_{R3} & 0 & 0 & 0 & 0 & 0 & 0 \\ 0 & 0 & 0 & 0 & 0 & 0 & 0 & 0 \\ 0 & 0 & 0 & 0 & 0 & 0 & 0 & 0 \\ 0 & 0 & 0 & 0 & 0 & 0 & 0 & 0 \\ 0 & 0 & 0 & 0 & 0 & 0 & 0 & 0 \end{bmatrix}$$

C.4 Details of Auxiliary Controller Model

C.4.1 Line Current Auxiliary Controller

Eqn. (3.32) can be written as

$$u_C = F_1 x_T \tag{C.3}$$

where $u_C = \Delta i_4$

The nonzero elements of F_1 are given by

$$F_1(1,19) = -\frac{i_{4D0}}{i_{40}} \quad , \quad F_1(1,24) = -\frac{i_{4Q0}}{i_{40}}$$

Eqn. (C.3) can be rewritten in matrix form as

$$u_C = F_{CR} x_R + F_{CM} x_M + F_{CN} x_N + F_{CS} x_S \tag{C.4}$$

where the various matrices are defined as submatrices of F_1

$$[F_{CR} \quad F_{CM} \quad F_{CN} \quad F_{CS}] = F_1$$

It is noted that $F_{CR} = F_{CM} = F_{CS} = 0$

The nonzero elements of F_{CN} are given by

$$F_{CN}(1,2) = F_1(1,19)$$
$$F_{CN}(1,7) = F_1(1,24)$$

The state and output equations of the general auxiliary controller depicted in Fig. 3.8 are written as

$$\dot{x}_C = A_C x_C + B_C u_C \tag{C.5}$$

$$y_C = C_C x_C + D_C u_C \tag{C.6}$$

where $x_C = [z_5]$, $y_C = \Delta v_t$

The nonzero element in each of the matrices A_C , B_C , C_C and D_C are defined as

$$A_C(1,1) = -\frac{1}{T_2}$$

$$B_C(1,1) = \frac{K_B}{T_2}(1 - \frac{T_1}{T_2})$$

$$C_C(1,1) = 1.0$$

$$D_C(1,1) = K_B \frac{T_1}{T_2}$$

C.4.2 Computed Internal Frequency (CIF) Auxiliary Controller

Linearizing eqns. (3.41) , (3.42) and substituting in eqn. (3.44) gives

$$\Delta\delta_1 = F_3 x_T + F_4 \dot{x}_T \tag{C.7}$$

where the nonzero elements of F_3 and F_4 are defined as

$$F_3(1,19) = \omega_0 L_E \frac{e_{D0}}{e_0^2} \quad , \qquad F_3(1,20) = -\frac{e_{Q0}}{e_0^2}$$

$$F_3(1,24) = \omega_0 L_E \frac{e_{Q0}}{e_0^2} \quad , \qquad F_3(1,25) = \frac{e_{D0}}{e_0^2}$$

$$F_4(1,19) = L_L \frac{e_{Q0}}{e_0^2} \quad , \qquad F_4(1,24) = -L_E \frac{e_{D0}}{e_0^2}$$

As the perturbation in SVC reference voltage, ΔV_{ref} , is not considered in the analysis of auxiliary SVC control as presented in chapter 3 , eqn.(3.30) gets modified to

$$\dot{x}_T = A\, x_T + B\, u_{S3} \tag{C.8}$$

where $u_{S3} = \Delta v_t$

Matrices A and B are already defined in chapter 3 .

Substituting eqn. (C.8) in eqn. (C.7) gives

$$\Delta\delta_1 = F_3 x_T + F_4 (A\, x_T + B u_{S3})$$

or

$$\Delta\delta_1 = F_5 x_T \tag{C.9}$$

where

$$F_5 = F_3 + F_4 A \quad , \qquad F_4 B = 0$$

The CIF signal is obtained by differentiating eqn. (C.9)

$$\Delta\omega_1 = F_5 \dot{x}_T \tag{C.10}$$

Resubstituting $\dot{x}_T$ from eqn . (C.8) in eqn . (C.10) results in

$$\Delta\omega_1 = F_5 (A\ x_T + B u_{S3})$$

$$\Delta\omega_1 = F_6 x_T \tag{C.11}$$

where $F_6 = F_5 A$,

The nature of matrices F_5 and B is such that

$$F_5 B = 0$$

Eqn. (C.11) can now be written in expanded form as

$$u_C = F_{CR} x_R + F_{CM} x_M + F_{CN} x_N + F_{CS} x_S \tag{C.12}$$

where $u_C = \Delta\omega_1$

The various matrices are defined as submatrices of F_5 as

$$[F_{CR} \quad F_{CM} \quad F_{CN} \quad F_{CS}] = F_5$$

APPENDIX D

SYSTEM DATA FOR IEEE FIRST SSR BENCHMARK MODEL SYSTEM

D.1 System Base Quantities

Base Voltage = 500 kV
Base MVA = 892.4
Base Frequency = 60 Hz

D.2 Generator Data

Sn = 892.4 MVA
Ra = 0.0 pu

x_d=1.79 pu
x_q=1.71 pu
x_l=0.13 pu

x'_d=0.169 pu
x'_q=0.228 pu

x''_d=0.135 pu
x''_q=0.200 pu

T'_{d0}=4.3 sec.
T'_{q0}=0.85 sec.

T''_{d0}=0.032 sec.
T''_{q0}=0.05 sec.

D.3 Multimass Parameters

Mass	Shaft	Inertia H (sec)	Spring Constant K (pu Torque / rad)	Self Damping D (pu)
HP		0.092897		0.0
	HP - IP		19.303	
IP		0.155589		0.0
	IP - LPA		34.929	
LPA		0.858670		0.0
	LPA - LPB		52.038	
LPB		0.884215		0.0
	LPB - GEN		70.858	
GEN		0.868495		0.0
	GEN - EXC		2.822	
EXC		0.0342165		0.0

The mutual damping between the masses is assumed to be zero. The steady state mechanical torque is apportioned among the turbine sections HP, IP, LPA and LPB respectively as follows : 30 %, 26 %, 22 % and 22 %. The exciter steady state torque is assumed to be zero.

D.4 Transformer Data (on system base)

$X_T = 0.14\ pu$

D.5 Transmission Line Data

Resistance (R) = 0.02 pu

Inductve Reactance $(X_L) = 0.5\ pu$

Capacitive Reactance $(X_C) = 0.371\ pu$

Fault Reactance $X_F, (L-G) = 0.04\ pu$

D.6 Static Var Compensator

T_M=2.4 ms , T_S=5.0 ms , T_D= 1.667 ms

$K_I = 90$, $K_P = 2.6$, $K_D = 0.03$ pu (1 %)

APPENDIX E

CALCULATION OF INITIAL CONDITIONS

E.1 Generator Initial Conditions

The vector diagram of the overall system is depicted in Fig. E.1 . The generator current I_g is given by

$$I_g = \frac{P_g - jQ_g}{V_g^*} \qquad (E.1)$$

where V_g^* is the conjugate of generator terminal voltage V_g .
The field voltage V_f and rotor angle δ are computed as follows

$$E_{qa} = V_g + I_g(R_a + jx_q) \qquad (E.2)$$

$$\delta = \angle E_{qa} - \pi/2 \qquad (E.3)$$

$$V_f = |E_{qa}| + I_{gd}(x_d - x_q) \qquad (E.4)$$

where I_{gd} is the component of generator current along d axis .
The initial values of other variables are

$$I_f = \frac{V_f}{x_{df}} \qquad (E.5)$$

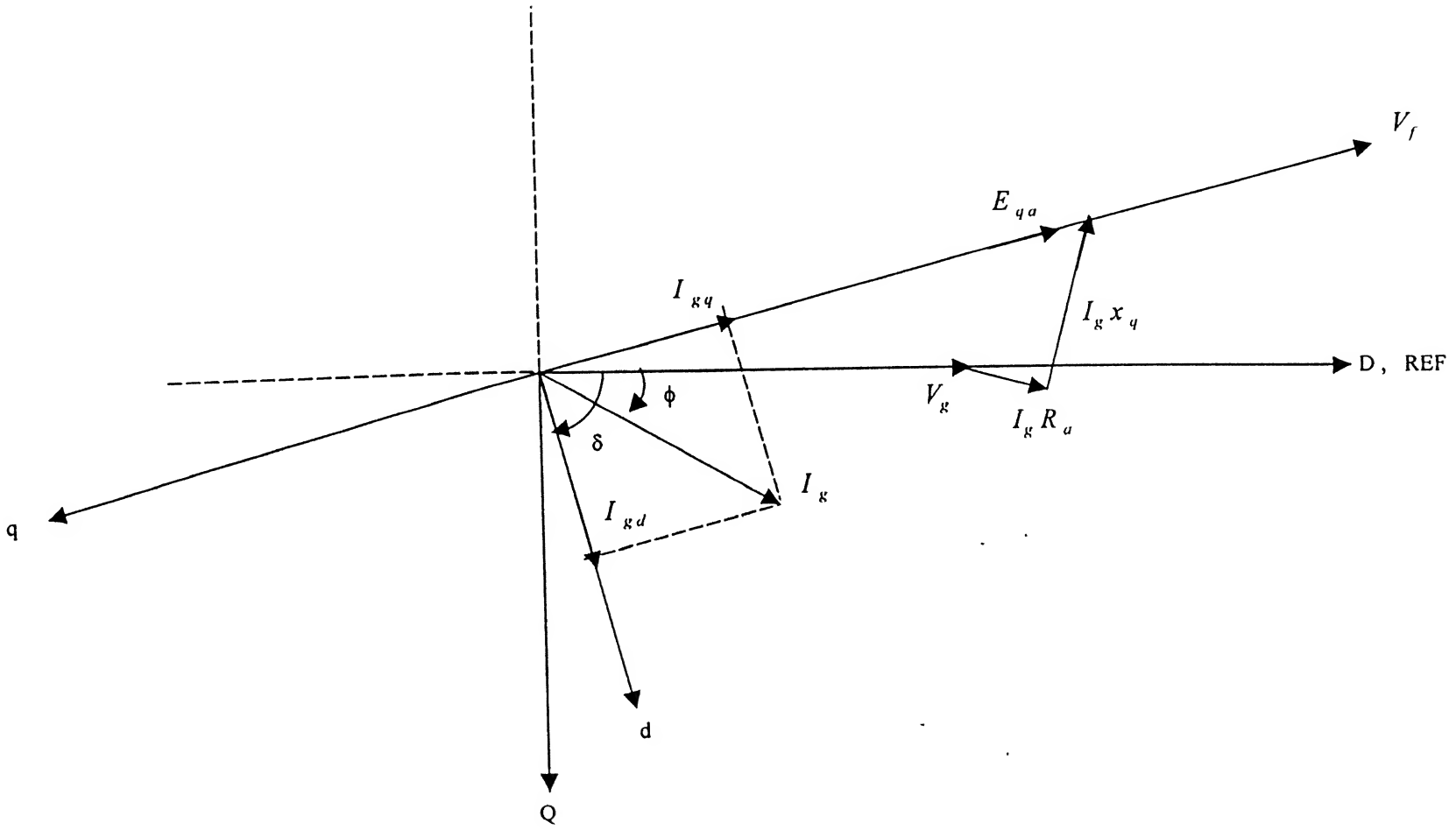

FIG . E .1 VECTOR DIAGRAM OF SYSTEM IN STEADY STATE

$$\Psi_f = x_f I_f + x_{df} I_{gd}$$
$$\Psi_h = x_d I_{gd} + x_{fh} I_f$$
$$\Psi_g = x_{qg} I_{gq} \qquad \text{(E.6)}$$
$$\Psi_k = x_{qk} I_{gq}$$
$$\Psi_c = x_{qc} I_{gq}$$

$$\dot{\delta} = 0$$

where I_{gq} is the q axis component of the generator current.
x_f, x_{df}, x_{fh}, x_{gq} and x_{qk} are defined in Appendix A.

E.2 SVC Initial Conditions

The reactive power generated by SVC fixed capacitor (FC) is given by

$$Q_C = \omega_0 C_{fC} v_{30}^2 \qquad \text{(E.7)}$$

where v_{30} = initial magnitude of SVS bus voltage v_3.

The initial value of TCR susceptance is then computed as

$$B_0 = (Q_C - Q_3)/(v_{30}^2) \qquad \text{(E.8)}$$

where Q_3 is the net reactive power at SVC bus obtained from load flow.

The initial value of TCR current is evaluated as

$$i_{30} = B_0 v_{30} \qquad \text{(E.9)}$$

REFERENCES

[1] Anderson, P. M., Agrawal, B. L., Van Ness, J. E., "Sub-synchronous Resonance in Power Systems", *IEEE Press, New York*, 1990.

[2] IEEE Subsynchronous Resonance Task Force of the Dynamic System Performance Working Group Power System Engineering Committee, "First Benchmark Model for Computer Simulation of Subsynchronous Resonance", *IEEE Transactions on Power Apparatus and systems*, Vol. PAS-96, No. 5, 1977.

[3] P. M. Anderson, A. A. Fouad, "Power System Control and Stability" *Iowa State University Press, Iowa*, 1977.

[4] T. J. E. Miller, "Reactive Power Control in Electric Systems", *John wiley and Sons, New York*, 1982.

[5] P. Kundur, "Power System Stability and Control", *New York : McGraw Hill*, 1994.

[6] R. S. Ramshaw, K. R. Padiyar, "Generalized System Model for Slipring Machines", *IEE Proceedings*, Vol. 120, No. 6, June 1973.

[7] K. R. Padiyar and R. S. Ramshaw, "Dynamic Analysis of Multi-machine Power Systems", *IEEE Trans. on PAS*, Vol. PAS-91, pp. 526-535, Mar./Apr. 1972.

[8] R. K. Varma, "Control of Static VAR Systems for improvement of dynamic stability and damping of torsional oscillations", *Ph. D. Thesis, IIT Kanpur*, April, 1988.

[9] J. Senthil, "Simulation of Transients in Synchronous Generators and HVDC Links and Study of Torsional Interactions", *Ph. D. Thesis, IIT Kanpur*, August, 1990.

[10] G. J. Joos and B. T. Ooi, "Torsional Interactions between Synchronous Generators and Long Transmission Lines", *IEEE Trans. on Power Systems*, Vol. PWRS-2, pp. 17-24, Feb. 1987.

[11] R. L. Hauth, S. A. Miske and F. Nozari, "The Role and Benefits of Static VAR Systems in High Voltage Power System Applications", *IEEE Trans. on PAS*-101, pp. 3761-3770, Oct. 1982.

[12] A. A. Fouad and K. T. Khu, " Subsynchronous Resonance Zones in the IEEE 'Benchmark ' Power System ", *IEEE Trans. on PAS*, Vol. PAS-97, pp. 754-762, May/June 1978.

[13] T. Ohyama, K. Yamashita, T. Maeda, H. Suzuki and S. Mine, " Effective Application of Static VAR Compensators to Damp Oscillations ", *IEEE Trans. on PAS*, Vol. PAS-104, pp. 1405-1410, June 1985.

[14] A. E. Hammad and M. EI-Sadek, "Application of a Thyristor Controlled VAR Compensator for Damping Subsynchronous Oscillations in Power Systems", *IEEE Trans. on PAS*, Vol. PAS –103, pp. 198-212, Jan. 1984.

[15] K. R. Padıyar and R. K. Varma, "Damping Torque Analysis of Static VAR System Controllers", *IEEE Transactions on Power Apparatus and Systems*, Vol.6, No. 2, May 1991.

[16] IEEE-CIGRE " FACTS Overview " and " FACTS Applications "

[17] Stevenson, W. D., Elements of Power System Analysis, 4th edn., MC Graw Hill, New York, 1982.

[18] B. R. Gupta, "Power System Analysis and Design", a. h. wheeler & co., private limited, Edn. 1985.

[19] M.P. Bahrman, E.V. Larsen, R.J. Piwko and H.S. Patel, "Experience with HVDC-Turbine-Generator Torsional Interaction at square Butte", IEEE Trans. on PAS, Vol. PAS-99, pp. 966-975, May/June 1980.

[20] N.G. Hingorani, S. Nilsson, M.P. Bahrman, J. Reeve, E.V. Larsen and R.J. Piwko, "Analysis of Subsynchronous Frequency Interactions Involving HVDC Transmission Systems", 1980 IEEE International Conference on Overvoltages and Compensation on Integrated AC-DC Systems, Winnipeg, Manitoba, July 1980.

[21] IEEE SSR Working Group, "Terms Definitions and Symbols for Subsynchronous Oscillations", IEEE Trans. on PAS, Vol. PAS-104, pp. 1326-1333, June 1985.

[22] K. R. Padiyar and R. K. Varma, "Static Var System Auxiliary Controllers for damping of Torsional Oscillations", International Journal of Electric Power and Energy Systems, Vol. 12, No.4, pp. 271-286, Oct. 1990.

[23] K. R. Padiyar, R. K. Varma, S. Gupta and M. kumar, " A novel static var system control for damping subsynchronous oscillations", NPSC 94.